INVESTIGATION OF THE INFLAMMATORY PATHWAYS IN SPONTANEOUSLY DIFFERENTIATING CACO-2 CELLS

A THESIS SUBMITTED TO
THE GRADUATE SCHOOL OF NATURAL AND APPLIED SCIENCES
OF
MIDDLE EAST TECHNICAL UNIVERSITY
BY

ERHAN ASTARCI

IN PARTIAL FULFILLMENT OF THE REQUIREMENTS
FOR
THE DEGREE OF DOCTOR OF PHILOSOPHY
IN
BIOCHEMISTRY

JULY 2011

Approval of the thesis:

INVESTIGATION OF THE INFLAMMATORY PATHWAYS IN SPONTANEOUSLY DIFFERENTIATING CACO-2 CELLS

submitted by **ERHAN ASTARCI** in partial fulfillment of the requirements for the degree of **Doctor of Philosophy in Biochemistry Department, Middle East Technical University**

Prof. Dr. Canan Özgen
Dean, Graduate School of **Natural and Applied Sciences** _____

Prof. Dr. Candan Gürakan
Head of Department, **Biochemistry** _____

Assist. Prof. Dr. Sreeparna Banerjee
Supervisor, **Biology Department, METU** _____

Assoc. Prof. Dr. Nursen Çoruh
Co-supervisor, **Chemistry Department, METU** _____

Examining Committee Members:

Prof. Dr. Mahinur S. Akkaya
Chemistry, METU _____

Assist. Prof. Dr. Sreeparna Banerjee
Biology, METU _____

Assoc. Prof. Dr. Çetin Kocaefe
Medical Biology, Hacettepe University _____

Assoc. Prof. Dr. Mayda Gürsel
Biology, METU _____

Assist. Prof. Dr. Ayşe Elif Erson Bensan
Biology, METU _____

Date: 29.07.2011 _____

I hereby declare that all information in this document has been obtained and presented in accordance with academic rules and ethical conduct. I also declare that, as required by these rules and conduct, I have fully cited and referenced all material and results that are not original to this work.

Name, Last Name: ERHAN ASTARCI

Signature:

ABSTRACT

INVESTIGATION OF THE INFLAMMATORY PATHWAYS IN SPONTANEOUSLY DIFFERENTIATING CACO-2 CELLS

Astarcı, Erhan

Ph.D., Department of Biochemistry

Supervisor: Assist. Prof.Dr. Sreeparna Banerjee

Co-Supervisor: Assoc. Prof. Dr. Nursen Çoruh

July 2011, 227 Pages

Intestinal epithelial differentiation entails the formation of highly specialized cells with specific absorptive, secretory, digestive and immune functions. Cell-cell and cell-microenvironment interactions appear to be crucial in determining the outcome of the differentiation process. Using the Caco-2 cell line that can undergo spontaneous differentiation when grown past confluency, we observed a loss of *VCAM1* (vascular cell adhesion molecule-1) expression while *ICAM1* (intercellular cell adhesion molecule-1) expression was seen to be stable in the course of differentiation. Protein kinase C theta (PKCθ) acted downstream of PKCα to inactivate Inhibitor of kappa B (IκB) and activate NF-κB in the undifferentiated cells and this axis was inhibited in the differentiated cells. The increase in *ICAM1* expression in the differentiated cells was due to a transcriptional upregulation by

C/EBPβ. The protein expressions of both ICAM-1 and VCAM-1, however, were found to decrease in the course of differentiation, with both proteins getting post-translationally degraded in the lysosome. Functionally, a decrease in adhesion to HUVEC cells was observed in the differentiated Caco-2 cells. Thus, the regulation of ICAM-1 and VCAM-1, although both NF-κB target genes, appear to be different in the course of epithelial differentiation.

microRNAs are known to regulate many cellular pathways. *miR-146a*, which is known to target NF-κB, was shown to be highly upregulated in differentiated Caco-2 cells. As a predicted target of *miR-146a*, mRNA and protein expression of MMP16 was inversely correlated with *miR-146a* during differentiation of Caco-2 cells. *miR-146a* could bind to the 3'UTR of MMP16 and ectopic expression of *miR-146a* resulted in a decreased mRNA and protein expression of MMP16 in the undifferentiated Caco-2 and HT-29 cells. Functionally, decreased gelatinase activity determined by gelatin zymography and reduced invasion and migration through Transwells was observed.

In the final part of the thesis, the inhibition of NF-κB via PPARγ in 15-Lipoxygenase-1 (15LOX1) expressing cells was investigated. The expression of 15LOX1, a member of the inflammatory arachidonate cascade, could lower phosphorylation of IκBα and NF-κB DNA binding activity which was reversed with a 15LOX1 inhibitor. This inhibition was mediated by phospho-PPARγ, which in turn was phosphorylated by ERK1/2.

Keywords: Spontaneous Differentiation, NF-κB, C/EBPβ, colon cancer, cell adhesion

ÖZ

SPONTANE FARKLILAŞAN CACO-2 HÜCRELERİNDE İNFLAMASYON YOLAKLARININ ARAŞTIRILMASI

Astarcı, Erhan

Doktora., Biyokimya Bölümü

Tez Yöneticisi: Y. Doç. Dr. Sreeparna Banerjee

Ortak Tez Yöneticisi: Doç. Dr. Nursen Çoruh

Temmuz 2011, 227 Sayfa

Barsak epitel farklılaşması, çok özel olarak sindirim, sekresyon ve immün görevleri olan özelleşmiş hücrelerin oluşumunu gerektirmektedir. Bu farklılaşma sırasındaki hücre-hücre ve hücre-mikroçevre etkileşimleri farklılaşma sürecinin değerlendirilmesinde kritik gözükmektedir. Birbirleri ile tamamen birleştikten sonra spontane olarak farklılaşmaya giden Caco-2 hücre hattını kullanarak, *VCAM1* (vascular cell adhesion molecule-1) ifadesinde azalma görürken *ICAM1* (intercellular cell adhesion molecule-1) ifadesinin farklılaşma süresinde stabil kaldığını gözledik. Farklılaşmamış hücrelerde Protein Kinaz alfa (PKCα) tarafından active edilen PKCθ nın İnhibitör Kappa B (IκB) ve böylelikle Nükleer Faktör Kappa B (NF-κB) aktivasyonuna neden olduğunu ve bu eksenin farklılaşmış hücrelerde inhibe olduğunu gözledik. *ICAM1* ifadesinin farklılaşmış hücrelerde stabil kalmasının nedeni transkripsiyonel olarak C/EBPβ tarafından artmasından

kaynaklanmakta idi. Buna karşın farklılaşma sırasında hem ICAM-1 hemde VCAM-1 protein seviyelerinin azaldığını ve dahası post-translasyonel olarak lizozomlarda yıkıldıkları bulunmuştur. Fonksiyonel olarak farklılaşan Caco-2 hücrelerinin HUVEC hücrelerine adezyonunda azalma gözlenmiştir. Böylece her ikiside NF-κB hedef geni olduğu halde ICAM-1 ve VCAM-1 in farklılaşma sırasında birbirlerinden farklı düzenlendikleri gözükmektedir.

MikroRNA ların birçok hücresel yolağı düzenledikleri bilinmektedir. NF-κB'yi hedeflediği bilinen *miR-146a* ifadesinin Caco-2 farklılaşması sırasında arttığı gösterilmiştir. Belirlenmiş hedef genlerinden MMP16 mRNA ve protein ifadesinin ise farklılaşma sırasında *miR-146a* ifadesi ile ters orantılı olarak azaldığı görülmüştür. *miR-146a MMP16* 3' UTR kısmına bağlanabilmiş ve ektopik ifadesi farklılaşmamış Caco-2 ve HT-29 hücrelerinde MMP16 mRNA ve protein ifadesinde azalmaya neden olmuştur. Fonksiyonel olarak jelâtin zimogram ile belirlenen jelatinaz aktvitesinde azalmaya ve buna ek olarak invazyon ve migrasyonda azalmaya neden olmuştur.

Tezin son kısmında,15-Lipoksigenaz-1(15LOX1) ifade eden hücrelerde NF-κB inhibisyonunun PPARγ aracılıklı olduğu araştırılmıştırArakidonat arkının bir üyesi olan 15LOX1 ifadesi IκBα fosforilasyonunu ve NF-kB DNA bağlanma aktivitesini azaltmış ve bu durum 15LOX1 inhibitörü ile geriye çevrilebilmiştir. Bu inhibisyonun ERK1/2 fosforilasyonuna bağlı PPARγ fosforilasyonu aracılıklı olduğu bulunmuştur.

Anahtar Kelimeler: Spontane Farklılaşma, NF-κB, C/EBPβ, kolon kanseri, hücre adezyonu.

IN MEMORY

OF

ZİYA AYDINOĞLU

ACKNOWLEDGEMENT

I wish to express my sincere thanks to Assist. Prof. Dr. Sreeparna Banerjee for her valuable guidance, supervision and understanding throughout the research. She made this study possible by accepting and encouraging me in all stages of PhD work.

My very special thanks should be devoted to Assoc. Prof. Dr. Çetin Kocaefe, for his extraordinary support and criticism throughout my study

I wish to extend my thanks to Assist. Prof.Dr.Ayşe Elif Erson Bensan for her invaluable help and support during my study.

My special thanks are due to Ayşegül Sapmaz, for her invaluable support in cloning experiments and discussion.

Love and thanks should go to my laboratory friends, especially Mumine Küçükdemir for her challenging support, patience and help during my study.

I want to express my deepest gratitude to my family, my parents İlhan-Nazan Astarcı for meaning everything to me.

My passed away uncle Ziya Aydınoğlu deserves the best appreciation who had always been with me, and I will hopefully meet him again…

TABLE OF CONTENTS

ABSTRACT iv
ÖZ vi
DEDICATION viii
ACKNOWLEDGEMENT ix
TABLE OF CONTENTS x
LIST OF TABLES xiv
LIST OF FIGURES xv
INTRODUCTION 1
1.1 Intestinal Cell Differentiation 1
1.2 Models for epithelial differentiation 4
1.2.1 The Caco-2 Cell Line 4
1.3 Transcription Factors Involved in Differentiation 6
1.4 Epithelial Differentiation and microRNAs 7
1.5 Inflammation and Colon Cancer 10
1.5.1 Effect of Intestinal Flora on Inflammation and Differentiation 11
1.6 Nuclear Factor Kappa B 12
1.6.1 Regulation of Nuclear Factor Kappa B 13
1.6.2 NF-κB Target Genes in Inflammation 17
1.7 Matrix Metalloproteinases and Cancer 23
1.8 Aim of the Study 25
MATERIALS AND METHODS 26
2.1 Cell Culture 26
2.1.1 Spontaneous Differentiation of Caco-2 cells 27
2.1.2 Treatment of Caco-2 Cells 28
2.2 Alkaline Phosphatase Activity 28
2.3 RNA Isolation 29
2.3.1 RNA Measurement 29
2.3.2 DNAse I Treatment of RNA Samples 30
2.4 cDNA Synthesis 30
2.5 Protein Extraction 31
2.5.1 Total Protein Extraction 31
2.5.2 Nuclear and Cytoplasmic Protein Extraction 31

2.6 Reverse Transcriptase - PCR Studies....32
2.6.1 Real Time PCR Studies....34
2.7 Western Blot Studies....35
2.8 Electrophoretic Mobility Shift Assay (EMSA)....36
2.9 Chromatin Immunoprecipitation (ChIP) Studies....38
2.10 NF-κB Activity Assay....42
2.11 Protein Kinase C (PKC) Activity Assay....43
2.12 Adhesion Properties of Spontaneously Differentiating Caco-2 Cells....44
2.13 Tumor-Endothelium Adhesion Assay....45
2.14 Gelatin Zymography....46
2.15 Matrigel Invasion Assays....47
2.16 Reporter Gene Assays....48
2.17 Vectors Used in This Study....50
RESULTS AND DISCUSSION....52
3.1 Confirmation of Spontaneous Differentiation in Caco-2 Cells....52
3.1.1 Alkaline Phosphatase Activity....52
3.1.2 Sucrase-Isomaltase Gene Expression during Differentiation of Caco-2 cells....54
3.1.3 Expression of p21 During Differentiation of Caco-2 cells....55
3.2 VCAM-1 and ICAM-1 Expression in Spontaneously Differentiating Caco-2 cells....57
3.3 Transcriptional regulation of *ICAM1* and *VCAM1*....61
3.3.1 NF-κB Activity in Differentiating Caco-2 Cells....61
3.3.2 Role of PKC in the Activation of NF-κB in Caco-2 cells....81
3.3.2 Protein Kinase C α is the PKC Isoform that Activates NF-κB....84
3.3.3 Protein Kinase C θ acts Downstream of PKCα to Activate NF-κB....87
3.4 C/EBPβ in Spontaneous Differentiation....93
3.4.1 Expression of *C/EBPβ* during Spontaneous Differentiation of Caco-2 Cells....94
3.4.2 DNA Binding Activity of C/EBPβ in Spontaneously Differentiating Caco-2 Cells....95
3.5 Post Transcriptional and Post Translational Regulation of *ICAM1* and *VCAM1*....103
3.5.1 Post Transcriptional MicroRNA mediated Regulation of *ICAM1* Expression in Differentiating Caco-2 Cells....103
3.6 Post-Translational Protein Degradation Mechanisms of ICAM-1 and VCAM-1 in Spontaneously Differentiating Caco-2 Cells....105

3.7 Functional Significance of the Loss of ICAM-1 and VCAM-1 Proteins in the Differentiated Caco-2 Cells. 112
MicroRNA 146a and Matrix Metalloproteinase-16 118
3.9.1 *miR-146a* Expression in Spontaneously Differentiating Caco-2 Cells 120
3.9.2 MMP16 Expression during Spontaneous Differentiation of Caco-2 Cells 123
3.9.3 3' UTR Analysis *MMP16* Gene in Spontaneously Differentiating Caco-2 Cells 126
3.9.4 Overexpression of *MiR-146a* in Caco-2 Cells 128
CONCLUSIONS 153
REFERENCES 160
APPENDICES 170
Appendix A: Vector Maps 170
A.1 pMIR-Report™ Luciferase Plasmid (Promega, USA) 170
A.2 pGL3™ Basic Plasmid (Promega, USA) 171
A.3 Psuper.Gfp/Neo Plasmid (OligoEngine, USA) 172
A.4 pSV-β-Galactosidase Control Vector (Promega, USA) 173
Appendix B: Buffers And Solutions 174
B.1 Chromatin Immunoprecipitation Buffers 174
B.1.2 SDS-PAGE Buffers 175
B.1.3 Western Blotting Buffers 176
Appendix C: Cloning Studies 178
C.1 Cloning of *ICAM1* 3' UTR Region in p-MIR-REPORT Luciferase Vector 178
C.2 Cloning of The *ICAM1* 3' UTR Region Second Half (1.2) 185
C.3 Cloning of *MMP16* 3' UTR Region in p-MIR-REPORT Vector 190
C.4 Cloning of NF-κB Binding Site In PGL3 Vector 195
C.5 Cloning of *C/EBPβ* in PGL3 Vector 200
C.6 Cloning of *miR-146a* in P-SUPER Vector 202
Appendix D: Site Directed Mutagenesis (SDM) Studies 204
D.1 Site Directed Mutagenesis of the *miR-146a* Binding Site of *MMP16* 3' UTR Region 204
D.2 Site Directed Mutagenesis of *miR146a* in P-Super Vector 205
Appendix E: Extraction of DNA From Agarose Gels 206
Appendix F: Transformation Protocol 207
Appendix G: RNA Isolation Protocol 208
Appendix H: Dnase I Treatment 209
Appendix I: cDNA Synthesis Protocol 210

Appendix J: Plasmid Isolation Protocol 211
Appendix K: Cytoselect Standard Curve 212
Appendix L: PKC Activity Standard Curve 213
Appendix M: Protein Degradation Pathway Inhibitors 214
Appendix N: Synthetic Oigos Used as Casettes 215
Appendix O: Quantitative PCR Standards 216
O.1 Standard and Amplification Curves for NF-κB on *ICAM1* Promoter 216
O.2 Standard and Amplification Curves for NF-κB on *VCAM1* Promoter 220
O.3 Standard and Amplification Curves for C/EBPβ in *ICAM1* Promoter 223
Appendix P: RNA Quality for Taqman MicroRNA Assays 225
P.1 RNA Measurement 225
P.2 Absorbance Spectra of the RNA Samples 225
P.3 Agarose Gel Analysis of the RNA Samples 226
Appendix R: Curriculum Vitae 227

LIST OF TABLES

Table 2.1 PCR Primers Used for Gene Expression Studies.....33
Table 2.2 Oligos Used as Probes in EMSA Reactions.....38
Table 2.3 Primers Used in ChIP Studies.....41
Table 5.1 PCR Conditions for *ICAM1* 3' UTR Amplification 179
Table 5.2 Restriction Digestion Conditions for Cloning of *ICAM1* 3' UTR (1.1) Region 180
Table 5.3 Ligation Reaction Conditions for Cloning *ICAM1* 1.1 UTR Region to p-MIR-REPORT Vector.....182
Table 5.4 Colony PCR Conditions for Amplification of *ICAM1* 1.1 UTR Region.183
Table 5.5 PCR Conditions for *ICAM1* (1.2) 3' UTR Amplification.....185
Table 5.6 Ligation Reaction Conditions for Cloning *ICAM1* 1.2 UTR Region to p-MIR-REPORT Vector.....186
Table 5.7 Colony PCR Conditions for Amplification of *ICAM1* 1.1 UTR 187
Table 5.8 PCR Conditions for Amplification of *MMP16* UTR Region 190
Table 5.9 Restriction Digestion Reaction of *MMP16* UTR and p-MIR-REPORT Vector.....191
Table 5.10 Ligation Conditions of *MMP16* UTR and p-MIR-REPORT Vector.....192
Table 5.11 PCR Conditions for Amplification of NF-κB Binding Site.....195
Table 5.12 PCR conditions for Amplification of NF-κB Element from PGL3 Plasmids 196
Table 5. 13 PCR Conditions for Amplification of *pre-miR-146a*.....202
Table 5.14 PCR Conditions of SDM for *miR-146a* Binding Site of *MMP16* 3' UTR 204
Table 5.15 PCR Conditions for SDM of *miR-146a* Binding Site.....205
Table 5.16 Reaction Parameters of NF-κB Element Amplification 218
Table 5.17 Reaction Parameters of NF-κB Element Amplification 221
Table 5.18 Nanodrop Values for RNAs.....225

LIST OF FIGURES

Figure 1.1 Structure of the Adult Small Intestine 2
Figure 1.2 MicroRNA Regulation 9
Figure 1.3 Pathways for Activation of NF-κB 15
Figure 3.1: Alkaline Phosphatase Enzymatic Activity During Differentiation of Caco-2 Cells 53
Figure 3.2: *Sucrase-Isomaltase* Expression in Spontaneously Differentiating Caco-2 Cells. 54
Figure 3.3: *p21* Expression During Spontaneous Differentiation of Caco-2 Cells 56
Figure 3.4 *VCAM1* Expression in Spontaneously Differentiating Caco-2 Cells 58
Figure 3.5 *ICAM1* Expression in Spontaneously Differentiating Caco-2 Cells 58
Figure 3.6: ICAM-1 Protein During Spontaneous Differentiation of Caco-2 Cells 59
Figure 3.7: VCAM-1 Protein During Spontaneous Differentiation of Caco-2 Cells 60
Figure 3.8: NF-κB p65 Nuclear Translocation in Spontaneously Differentiating Caco-2 Cells 62
Figure 3.9: NF-κB p50 Nuclear Translocation in Spontaneously Differentiating Caco-2 Cells 63
Figure 3.10: IκBα and phospho-IκBα Proteins in Spontaneously Differentiating Caco-2 Cells 64
Figure 3.11 EMSA of NF-κB in Spontaneously Differentiating Caco-2 Cells 66
Figure 3.12 NF-κB p65 ELISA Showing Reduced p65 DNA Binding *in-vitro* 68
Figure 3.13 NF-κB p50 ELISA Showing Decreased DNA Binding of p50 Protein *in-vitro*. 69
Figure 3.14 Amplification of the NF-κB Element in the *VCAM1* Promoter After ChIP with p65 in Spontaneously Differentiating Caco-2 Cells 71
Figure 3.15 Amplification of the NF-κB Element in the *ICAM1* Promoter after ChIP with p65 in Spontaneously Differentiating Caco-2 Cells 72
Figure 3.16 Real Time Amplification of the NF-κB Element on the *ICAM1* Promoter. 73
Figure 3.17 Real Time Amplification of the NF-κB Element on the *VCAM1* Promoter. 74
Figure 3.18: NF-κB Reporter Gene Assay in Differentiating Caco-2 Cells 76
Figure 3.19: NF-κB Reporter Gene Assay with NF-κB Inhibitors. 77
Figure 3.20: NF-κB DNA Binding Assay with TMB-8 79
Figure 3.21: ICAM-1 and VCAM-1 Proteins of TMB-8 Treated Caco-2 Cells 80
Figure 3.22: PKC Activity Standard Assay. 81
Figure 3.23: PKC Activity in Spontaneously Differentiating Caco-2 Cells. 83
Figure 3.24: Quantitative PKC Activity in Spontaneously Differentiating Caco-2 Cells. 84
Figure 3.25: NF-κB Reporter Gene Assay in Protein Kinase Cα Overexpressed Caco-2 Cells. 86
Figure 3.26: Protein Kinase C Proteins in Spontaneously Differentiation of Caco-2 Cells 88
Figure 3.27: PKCθ acts downstream of PKCα 89
Figure 3.28: PKCα Increases the phosphorylation of IκBα. 90
Figure 3.29: Effect of PKCα on p50 DNA Binding Activity 91
Figure 3.30: Effect of Rottlerin and GÖ 6976 on NF-κB Activity. 92

Figure 3.31: C/EBPβ Expression in Spontaneously Differentiating Caco-2 Cells 94
Figure 3.32: C/EBPβ Protein in Spontaneously Differentiating Caco-2 Cells.. 95
Figure 3.33 C/EBPβ EMSA in Spontaneously Differentiating Caco-2 Cells. 97
Figure 3.34 Amplification of the C/EBPβ and NF-κB/ C/EBPβ Elements in the *ICAM1* Promoter after ChIP with C/EBPβ Antibody in Spontaneously Differentiating Caco-2 Cells. 99
Figure 3.35 Amplification of the C/EBPβ Element in the *ICAM1* Promoter. 100
Figure 3.36 C/EBPβ Reporter Gene Assay in Spontaneously Differentiating Caco-2 Cells.. 101
Figure 3.37 *ICAM1* 3'UTR Activity in Spontaneously Differentiating Caco-2 Cells. 0.....104
Figure 3.38: Effect of Lysosomal Degradation Pathway on the Expression of ICAM-1 Protein. 107
Figure 3.39: Effect Lysosomal Degradation on the Expression of VCAM-1 Protein. 108
Figure 3.40: Effect of Proteasomal Degradation on VCAM-1 Expression During Spontaneous Differentiation of Caco-2 Cells 109
Figure 3.41: Effect of Proteasomal Degradation on ICAM-1 Expression During Spontaneous Differentiation of Caco-2 Cells 110
Figure 3.42: Effect of Calpain Induced Degradation on ICAM-1 and VCAM-1 Expression During Spontaneous Differentiation of Caco-2 Cells 111
Figure 3.43: Adhesion of Differentiating Caco-2 Cells to Fibronectin 114
Figure 3.44: Caco-2 Cell Adhesion to HUVEC Cells as a Function of Differentiation. 116
Figure 3.45 *Pre-miR146a* Expression in Spontaneously Differentiating Caco-2 Cells 120
Figure 3.46 *Pre-miR146b* Expression in Spontaneously Differentiating Caco-2 Cell 121
Figure 3.47: Mature *miR-146a* and *miR-146b* Expression in Spontaneously Differentiating Caco-2 Cells.. 122
Figure 3.48: *MMP16* Expression in Spontaneous Differentiation of Caco-2 Cells. 124
Figure 3.49: MMP16 Protein in Spontaneously Differentiating Caco-2 Cells. 125
Figure 3.50: Bioinformatics Analysis of the Predicted Interactions of *miR-146a* with Their Binding Sites at the 3′UTR of *MMP16* (Targetscan) 126
Figure 3.51: *MMP16* 3'UTR Activity in Spontaneously Differentiating Caco-2 Cells. 127
Figure 3.52: *MMP16* 3' UTR Analysis in *miR146a* Overexpressed Caco-2 Cells..129
Figure 3.53: Forced Expression of *pre-miR-146a* in Undifferentiated Caco-2 Cells. 131
Figure 3.54: Mature *miR-146a* Overexpression in Undifferentiated Caco-2 Cells. 132
Figure 3.55: *MMP16* Expression in *miR-146a* Overexpressed Caco-2 Cells. 133
Figure 3.56: MMP16 Protein Expression in *miR146a* Overexpressing Caco-2 Cells. 134
Figure 3.57: Zymography Analysis of *miR-146a* Overexpressing Caco-2 Cells.....136
Figure 3.58 Confirmation of Overexpression of *pre-miR-146a* in Undifferentiated (Day 0) Confluent HT-29 Cells 138
Figure 3.59 *MMP16* Expression in *miR-146a* Transfected HT-29 Cells. 139

Figure 3.60: Matrigel Invasion Assay of *miR-146a* Overexpressing HT-29 Cells..140
Figure 3.61: Quantitative Analysis of Matrigel Invasion Assays 141
Figure 3.62: Phospho-IκBα in 15-LOX-1 Expressing HT-29 Cells. 144
Figure 3.63: EMSA of Stable (HCT-116) and Transiently (HT-29) 15LOX1 Transfected Cells.....146
Figure 3.64: NF-κB EMSA of 15LOX1 Transfected Cells Treated with PPARγ Inhibitor GW 9662 148
Figure 3.65: 15LOX1 Expression Results in Phosphorylation of ERK1/2 and PPARγ 150
Figure 5.1 pMIR-REPORT Luciferase Vector Map 170
Figure 5.2: pGL3- Basic Vector Map 171
Figure 5.3 pSuper.gfp/neo Plasmid Map 172
Figure 5.4: pSV-β-Galactosidase Plasmid Map 173
Figure 5.5 Gel Analysis of HindIII/SpeI Digested p-MIR-REPORT and *ICAM1* 3'UTR Region.....181
Figure 5.6 Colony PCR for Identification of *ICAM1* 1.1 UTR Region Cloned Plasmids 183
Figure 5.7 Restriction Digestion of *ICAM1* 1.1 UTR Region of p-MIR-REPORT Plasmids from Selected Colonies.....184
Figure 5.8 Colony PCR for Identification of *ICAM1* 1.2 3'UTR Region Cloned Plasmids 188
Figure 5.9 Restriction Digestion of *ICAM1* 1.2 UTR Region of p-MIR-REPORT Plasmids from Selected Colonies.....189
Figure 5.10 PCR Amplification of Selected Colonies for Confirmation of Cloned Inserts 193
Figure 5.11 Restriction Digestion of selected Colonies Accommodating 3' UTR Region of *MMP16*.....194
Figure 5.12: Amplification for NF-κB Binding Site from PGL3 Plasmids with PGL3 Empty Vector Primers.....197
Figure 5.13 *pre-miR-146a* Amplification from Selected p-SUPER Plasmids.....203
Figure 5.14 *ICAM1* Promoter NF-κB Element Amplification Standard Curve.....216
Figure 5.15 *ICAM1* Promoter NF-κB Element Standard Melt Curve.....217
Figure 5.16 *ICAM1* Promoter NF-κB Element Standard Curve. 217
Figure 5.17 Amplification of the NF-κB Element in the *ICAM1* Promoter using αp65 Immunoprecipitated Caco-2 Cells 219
Figure 5.18 Melt curve of the NF-κB Element in the *ICAM1* Promoter using αp65 Immunoprecipitated Caco-2 Cells 219
Figure 5.19 Standard Amplification Curve for the NF-κB Element in the *VCAM1* Promoter.....220
Figure 5.20 Standard Melt Curve for the NF-κB Element in the *VCAM1* Promoter 220
Figure 5.21 Standard Curve for the Amplification of the NF-κB Element in the *VCAM1* Promoter. 221
Figure 5.22 Amplification Melt Curve of the NF-κB Element from *VCAM1* Promoter in the Differentiating Caco-2 Cells 222
Figure 5.23 Amplification of the NF-κB Element in the *VCAM1* Promoter using αp65 Immunoprecipitated Caco-2 Cells 222
Figure 5.24 C/EBPβ Element in the *ICAM1* Promoter Standard Curve 223

Figure 5.25 C/EBPβ Element Amplification Melt Curve 223
Figure 5.26 C/EBPβ Element Amplification Curve 224
Figure 5.27 Absorbance Spectra of the RNA Samples 225
Figure 5.28 Agarose Gel Analysis of the RNA Samples 226

CHAPTER 1

INTRODUCTION

1.1 Intestinal Cell Differentiation

The epithelium of the intestine is composed of a system that undergoes constant regeneration. As the cells migrate from crypts to the distal sites of villi they differentiate progressively and are then released into the lumen. Colon, the distal part of the intestine, is lined with a simple epithelium composed of colonocytes (absorptive cells) and goblet cells. An interaction between the epithelial and mesenchymal tissues is necessary for the epithelial cells to differentiate (Stallmach *et al.,* 1989).

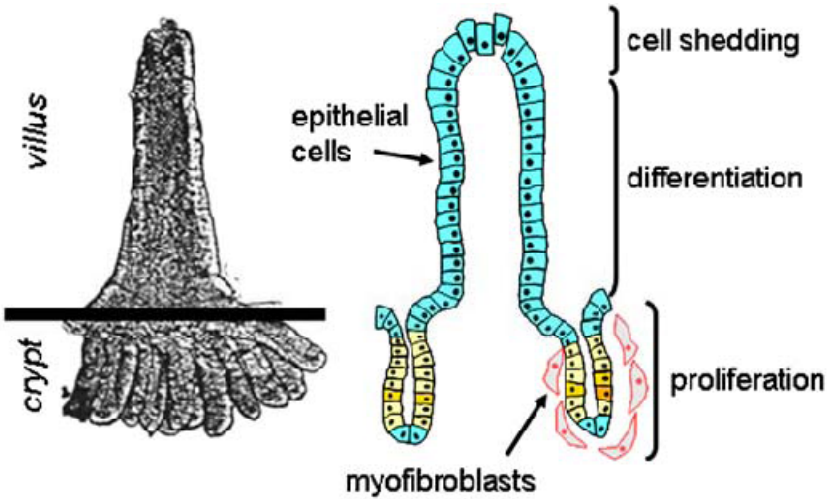

Figure 1.1 Structure of the Adult Small Intestine (Simon-Assmann *et al*., 2007b)

Enterocytes are the main type of cells found in the differentiated intestine, since they are in contact with the cells of the basement membrane. In order to carry out the absorptive and digestive roles, the apical membrane forms a brush border membrane composed of well organized microvilli in which high amounts of hydrolase and transporters are present in order to ensure the absorptive and digestive functions. Hyrolytic enzymes such as sucrase-isomaltase, dipeptidylpeptidase IV, lactase are the most reliable markers of *in vitro* intestinal cell differentiation (Neutra M, 1989).

Although there have been studies that have described the process of formation of polarized cells from undifferentiated (Rousset 1986) cells, the various molecular pathways involved in this phenomenon still remains to be elucidated. Polarization itself is acquired with ordered series of events which involves a variety

of transcription factors that are in contact with the fibroblasts and extracellular matrix (Sancho *et al*., 2004; Teller and Beaulieu, 2001)

Extracellular matrix (ECM) is composed of the interstitial matrix and the basement membrane. Cellular interactions with ECM has a fundamental importance which is required for a variety of biological processes such as development, growth and differentiation. Most of these interactions are mediated via integrins which are known to be expresses family of adhesion molecules. Integrin expression and regulation are important in cell attachment, migration, cell cycle progression and apoptosis.

Terminal differentiation has been regarded as a special type of apoptosis. In apoptosis, cells normally undergo a programmed cell death in which self-destruction takes place. In terms of cellular physiology, there is a genuine way of cell death called terminal differentiation which is needed for the regulation of cell proliferation in tissues such as the epidermis of the skin and the lens. In differentiating cells, there is a pattern of denucleation which is associated with the remaining viable cells. Terminal differentiation is an important process, the lack of which may contribute to the cancer development and the presence in excess may also result in degenerative diseases including Alzheimer's disease (Gagna *et al*., 2001).

Since terminal differentiation is a special type of apoptosis, cease in the cell cycle during the differentiation process is one of the outcomes of differentiation which inevitably requires the inhibition of the highly conserved cyclin-dependent kinases (Cdks), which normally regulate the cell cycle by binding to cyclin proteins. In cell types that can undergo differentiation, these cyclin dependent kinases can be

inhibited by inhibitory proteins which results in an escape from the cell cycle and eventually differentiation. The well known cyclin dependent kinase inhibitors like p21Waf1/Cip1, p27Kip1/Pic2, and p57Kip2, are also known to be activated in some cell types (Caco-2, HT-29) which undergo spontaneous differentiation (Ding *et al*., 2000).

1.2 Models for epithelial differentiation

Jorgen Fogh was the first to establish the colon carcinoma cell line HT-29 that could undergo differentiation in 1977 (Fogh *et al*., 1977). Since then several more cell lines have been established with a variety of different metabolic aspects which made them differ in the degree and type of differentiation and proliferation. It is understood that most of these cell lines do not differentiate under standard culture conditions. However, two cell lines that are capable of undergoing differentiation depending upon the culture conditions are Caco-2 and HT-29. Upon differentiation, they resemble the characteristics of enterocytes and mucus cells.

1.2.1 The Caco-2 Cell Line

Caco-2, a cell line able to undergo differentiation spontaneously, was obtained from a well differentiated tumor (Sambuy *et al.,* 2005). The cells are normally found in an undifferentiated state; however, when they reach the confluency they form monolayers which are composed of polarized cells connected

with tight junctions. Although these cells were derived from adult human colon cancer (Sambuy *et al.,* 2005), when differentiated, they express disaccharidases and peptidases which are enzymes found in the normal small intestinal cells. An increased ability to transport ions and water towards the basolateral membrane also results in the formation of dome like structures in culture which is also used as a morphological marker of spontaneous differentiation (Pinto, 1983). This cell line is therefore widely used as an *in vitro* model for epithelial cell differentiation (Simon-Assmann *et al.,* 2007).

The Caco-2 cell line has been used also to show the relationship between differentiation and interaction with the extracellular matrix proteins. It was shown that when the cells were grown on laminin they displayed significantly higher sucrase activity compared to the cells grown on plastic or collagen type I (Basson *et al*., 1996). The same study also found that laminin-1, but not laminin-2 or laminin-10 triggered intestinal differentiation. Accordingly, sucrase activities were detected to be higher in the cells grown on laminin-1 compared to other substrates. This phenomenon was supported with the higher Caudal Type Homeobox2 CDX-2 nuclear immunoreactivity which is also a known transcription factor involved in differentiation of intestinal cells. In other words its target genes are the genes known as differentiation markers (De Lott *et al.,* 2005).

To further understand the effect of laminin during differentiation a proteomics approach was used with protein samples obtained from differentiated and undifferentiated Caco-2 cells and 60 different proteins were found to be

differentially expressed in differentiated and undifferentiated Caco-2 cells (Turck *et al.,* 2004).Among these Nucleolin usually associated with proliferation was found to be significantly reduced during the differentiation. Besides, its expression was also decreased in the presence of exogenous laminin-1 which mediates cell differentiation as a consequence of polarization (Turck *et al.,* 2006).

In addition, DNA microarray studies let the researchers examine large number of genes during spontaneous differentiation of Caco-2 cells. Feet et. al., have shown 35% of the 601 genes exhibited a differential expression pattern in spontaneous differentiation with a threefold cutoff (Fleet *et al.,,* 2003). cDNA microarray studies conducted by Mariadason *et.al*., also showed that in Caco-2 cell differentiation, 70% of the genes examined were found to be downregulated which were mainly involved in growth arrest and down-regulation of cell cycle (Mariadason *et al.,* 2002)

In another study done with the spotted filter array with 18,149 expressed sequence tags (ESTs) and number of genes were found to be reduced in 7 day Caco-2 cultures (more differentiated) compared to 3 day cultures (less differentiated) (Tadjali *et al.,* 2002).

1.3 Transcription Factors Involved in Differentiation

CCAAT box enhancer binding proteins are family of proteins functioning as transcription factors with six members, all of which share the same leucine zipper domain for DNA dimerization at their C-termini. They have been shown to be

involved in differential regulation of transcription initiation sites and are known to be interacting with the other transcription factors. Differential expression and activity of these transcription factors during cellular proliferation, inflammation and differentiation have been studied. Expression and activity of the C/EBPs are known to be regulated by mitogens, cytokines, hormones, nutrients and toxins (Ramji and Foka, 2002).

One of the interesting features of the C/EBP proteins is their differential expression in terminally differentiated cells which led to the idea of their involvement in the expression of the genes responsible for differentiation (Christy *et al*., 1989). This transcription factor has widely been studied in *in-vitro* differentiation of 3T3-L1 adipoblasts to adipocytes which clarified the putative role of C/EBPβ in terminal differentiation (Cao *et al.,* 1991).

Moreover in fibroblast cells which were allowed to grow continuously, proliferation was seen when cells were stimulated with appropriate hormones and C/EBP activity profiles were found to be correlating with the progress of differentiation (Birkenmeier *et al*., 1989). Furthermore, it was reported that C/EBP proteins interfered with cell proliferation and supported the differentiation of the adipocytes (Umek *et al.,* 1991).

1.4 Epithelial Differentiation and microRNAs

MicroRNAs (miRNAs) are defined as noncoding sequences which are 21-23 nucleotides in length and discovered recently as post transcriptional gene expression

regulators found in wide variety of organisms (Ambros, 2004), (Bartel, 2004), (Zamore and Haley, 2005). They can repress translation or affect the stability of their target mRNA sequences depending on the nature of complementarity (Olsen and Ambros, 1999). Their functions include development (Wightman *et al*., 1993), differentiation (Chen *et al*., 2004), apoptosis (Esau *et al*., 2004) and cell proliferation.

miRNAs are expressed as long precursors called primary miRNA (pri-miRNA) which are shown to be synthesized by RNA polymerase II (Cai *et al*., 2004). After the binding of the polymerase the resulting transcript forms the hairpin loop of the precursor-miRNA (pre-miRNA). After the polyadenylation and splicing product is called primary miRNA (pri-miRNA) (Cai *et al*., 2004).

AS it was shown in Figure 1.2 the double-stranded RNA structure of the pri-miRNA is processed by the enzyme "pasha" which is associating with another enzyme "drosha" for the processing of the pri-miRNA in "microprocessor" complex (Gregory *et al*., 2006). After the microprocessing the resulting miRNA is called precursor-miRNA (pre-miRNA) and they are exported from the nucleus with a shuttle protein "Exportin-5". After entering into the cytoplasm an RNase III enzyme "Dicer" cleaves the pre-miRNA into about 22 bp long two miRNA duplex by interacting with the 3' end of the hairpin structure cutting away the 3' and 5' joining loop (Lelandais-Brière *et al*., 2010). Usually one strand of this complex is interacting with the target mRNA by being incorporated into the RNA-induced silencing complex (RISC).

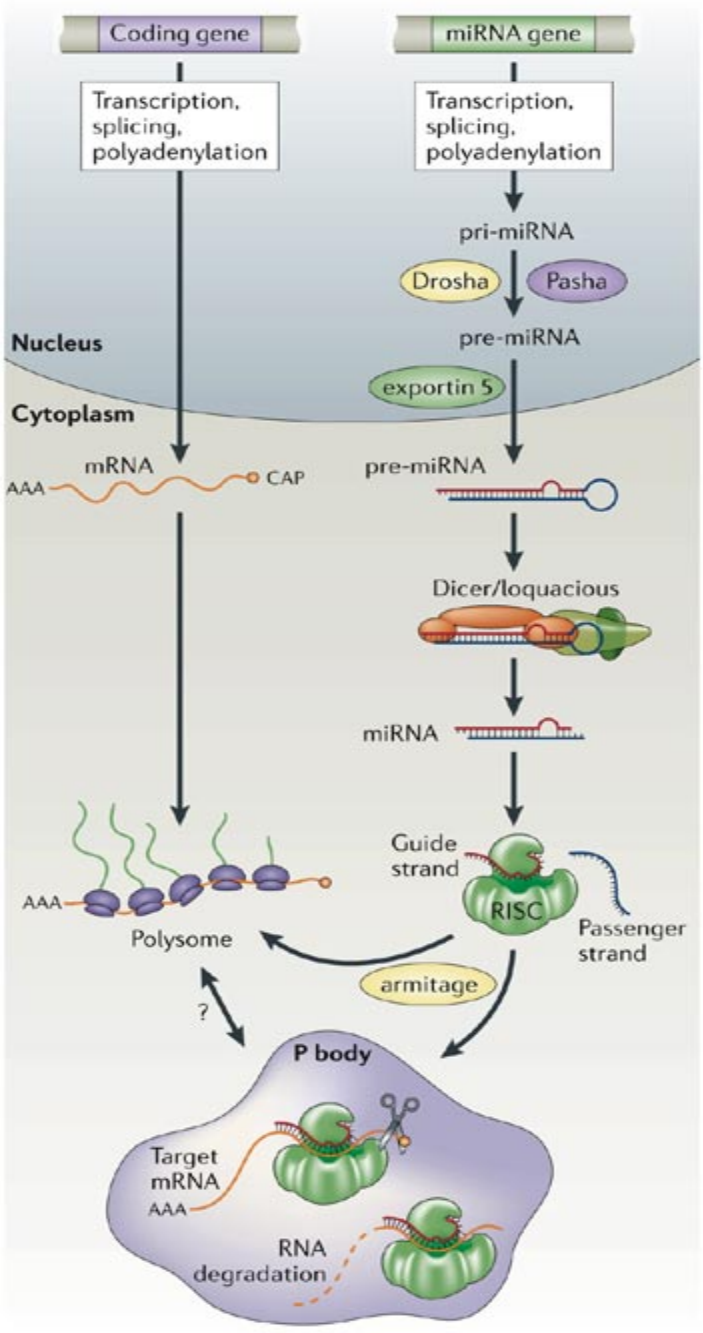

Figure 1.2 MicroRNA Regulation (Kosik, 2006)

Since the Caco-2 cells are a model for intestinal epithelial differentiation, their miRNA profile during differentiation may provide valuable insights about the role miRNAs in epithelial differentiation. In Caco-2 differentiation model a great number

of miRNA expression profiles were found to be either up- or down-regulated. For example, Hino *et al*., have found that during intestinal differentiation miR-194 is one of the up regulated microRNAs involved in differentiation induced by hepatocyte nuclear factor-1α (HNF-1α) which is one of the transcription factors involved in intestinal differentiation (Hino et. al., 2008a). In another study miR-210, miR-338-3p, miR-33a and miR-451 were also found to be increasing in differentiation of Caco-2 cells. *miR-338-3p* and miR-*451* were identified in terms of their function which is their involvement of β1-integrin regulation during differntiation therefore development of cell polarity during differentiation (Tsuchiya *et al.,* 2009).

1.5 Inflammation and Colon Cancer

The development of colon carcinogenesis is a cascaded series events and most of the colorectal cancer related has been reported in signal transduction pathway genes (Vogelstein and Kinzler, 2004). One such pathway in the inflammatory and immune mediated diseases as well as in cell cycle and progression and is considered as a lynchpin of inflammatory cancers is the nuclear factor kappa B (NF-κB) pathway (Coussens and Werb, 2002). Colorectal cancer is considered as an inflammatory cancer since chronic inflammation is one of the factors that activates NF-κB and contributes to the progression of cell proliferation (Karin *et al.,* 2006). In inflammation, the first response is the extravasation of leukocytes including, eosinophils, neutrophils and monocytes to the sites of damage. Neutrophils provide extracellular matrix material which serves as a scaffolding unit on which endothelial cells and fibroblasts can proliferate and migrate. These

processes involve the activation of number of adhesion molecules including the selectin family which in turn activates the release of cytokines triggering integrins. Following this, an integrin mediated immobilization of neutrophils on vascular endothelium can be sustained. This adhesion also requires vascular cell-adhesion molecule-1 (VCAM-1) for adhesion of neutrophils to vascular endothelium and transmigration through the endothelium to sites of injury which is then mediated by the matrix metalloproteinases (MMPs) (Coussens and Werb, 2002).

The development of chronic inflammatory diseases is defined by the pattern of chemokines and cytokines released. The pro-inflammatory cytokine tumor necrosis factor-α (TNF-α) is one of the major factors controlling the populations of inflammatory cells and number of other inflammatory processes. The important concept is the extent of inflammation which is self-limiting for some processes such as wound healing. On the other hand its dysregulation can lead to pathogenesis, contributing to neoplastic progression (Coussens and Werb, 2002).

Since the inflamed colon is accompanied constitutively with the inflammatory cells, reactive oxygen and nitrogen species produced by these cells affect the genes important in carcinogenic pathway including p53, genes involved in DNA mismatch and excision repair genes (Hofseth *et al.,* 2003; Gasche *et al.,* 2001). In addition, activated NF-κB and cyclooxygenases, in response to inflammation, activates nitric oxide and prostanoids which have pro-inflammatory and carcinogenic effects (Yamamoto and Gaynor 2001).

1.5.1 Effect of Intestinal Flora on Inflammation and Differentiation

Gut flora which is mainly composed of bacteria performs inevitable functions in the colon such as modulating the immune system production of the vitamin K and

biotin and fermentation of the unused substrates for energy (Guarner and Malagelada, 2003).

Among these substrates, dietary fiber plays an important role which is yielding short chain fatty acids (SCFA) after microbial attack. Butyrate is one of the major SCFA which has a been shown to inhibit the cell proliferation and stimulate the differentiation of colon cancer cells (Kruh, 1982). One mechanism by which butyrate leads to the differentiation is the modulation of the gene expression via inhibiting histone deacetylases resulting in the changes in the acetylation patterns of the histones which is associated with the activation of gene transcription (Mariadason *et al*., 2002).

However , in some conditions some bacterial species may cause disease by producing infection resulting in inflammation and increase the risk of cancer (Guarner and Malagelada, 2003). Especially gram negative bacteria cell wall component lipopolysaccharide (LPS) contributes to the activation of constitutive inflammation by interacting with the TLR4 receptors which results in the activation of the nuclear Factor Kappa B (NF-κB) (Doyle and O'Neill, 2006).

1.6 Nuclear Factor Kappa B

The Nuclear Factor kappa B (NF-κB) is a transcription factor involved in responding to a wide array of biological stimuli including cytokines, free radicals, oxidized lipoproteins, bacterial infection, etc. It is known to be involved in regulation of immune responses and inflammation and recently its connection with

oncogenesis has been shown. NF-κB target genes are known to regulate proliferation, apoptosis and migration therefore its one of the major factors contributing to the progression of cancer (M Karin, 2006). Abnormal and constitutive NF-κB activation has been shown in many human cancers. NF-κB is therefore rightfully considered as the lynchpin of inflammatory cancers (Dolcet *et al*., 2005).

1.6.1 Regulation of Nuclear Factor Kappa B

NF-κB proteins include five different transcription factor genes which are: NF-κB1 (p50/p105), NF-κB2 (p52/p100), RelA (p65), c-Rel and RelB. The common feature of these proteins is a common Rel Homology Domain (RHD) which is responsible for DNA binding and activation and regulating the interaction with inhibitors. NF-κB proteins RelA, c-Rel and RelB contain a transactivation domain and they are synthesized in their active form. NF-κB1 (p105/p50) and NF-κB2 (p100/p52) are synthesized as precursor forms containing C-terminal ankyrin repeats which are proteolyzed to form mature p50 and p52 proteins which lack transactivation domain but have DNA binding domain (Karin and Ben-Neriah, 2000).

In normal cells, NF-κB proteins are mainly found in the cytoplasm in their inactive state and they interact with the Inhibitors of NF-κB (IκBs) and this interaction sustains the transcriptionally inactive state of NF-κB. Inactivation of NF-κB by IκBs maintained by the interaction of ankyrin repeats found in IκB proteins with RDH domains of NF-κB proteins. IκBs are composed of three members IkBα,

IkBβ, and IkBγ, all of which have two conserved serine residue and are phosphorylated by IκB kinases (IKKs). This phosphorlyation serves as a degradation signal for the IκBs by proteasomal degradation (Karin and Ben-Neriah, 2000).

IKK complex is formed by two catalytic (IKKα, IKKβ) and one regulatory subunit (IKKγ).

There is wide variety of signaling molecules involved in NF-κB activation including growth factors, cytokines, and tyrosine kinases. In addition Ras/MAPK and PI3K/Akt can also activate NF-κB. As shown in Fig.1, there are alternative pathways which have been proposed for NF-κB activation. In classical (canonical) NF-κB pathways, p50 protein together with dimers of RelA or c-rel are sequestered in the cytoplasm by IκB protein (Ghosh and Karin, 2002). Pro-inflammatory cytokines and viral infections are the major activators of this pathway. For activation, the IKKβ subunit phosphorylates the IκB protein, which is the signal for IκB protein to undergo proteasomal degradation. After this degradation NF-κB protein can have access to the nucleus where it executes its function as a transcription factor.

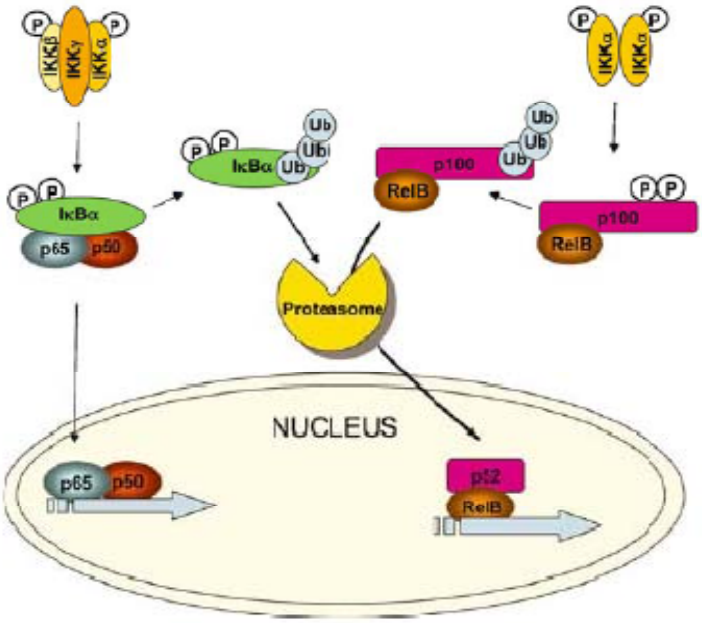

Figure 1.3 Pathways for Activation of NF-κB (Dolcet *et al*., 2005)

Dimers such as RelA-p50, c-Rel-p50 and RelB-p52 are the most commonly produced dimers, however, homodimers such as p50-p50, p52-p52 or heterodimers such as c-Rel-RelA, c-Rel-c-Rel may also be produced and each of the dimers has distinct roles. In normal cells, NF-κB activity should be strictly regulated and activated only after the appropriate stimuli thereby activating its target genes. Following execution of its function it should become to its inactive state. Therefore NF-κB activity is a transient process which is inducible. In tumorigenic cells, abnormal regulation of NF-κB results in hindered control. For instance it may lose its regulation therefore may become constitutively active. This activation may lead to abnormal expression of its target genes involved in control of apoptosis, adhesion, migration and cell cycle control. As all of the events mentioned before do take place in the progression of cancer there is a strong correlation between progression of cancer and NF-κB regulation (Dolcet *et al*., 2005).

NF-κB contributes to the progression of the cell cycle via regulating the genes controlling the cell cycle such as Cyclin D1 (Guttridge *et al*., 1999), D2 (Hinz *et al*., 1999), D3 (Hinz *et al*., 2001) and Cyclin E (Hsia *et al*., 2002).

Uncontrolled and constitutive activation of NF-κB has been implicated in a wide range of outcomes including immune diseases and cancer as it controls many genes in inflammatory response and apoptosis (Ghosh *et al*., 1998).

Dysregulation of the NF-κB pathway is frequently associated with colorectal cancer. This pathway is a known inducer of cell proliferation via regulating the phosphoinositide 3-kinase (PI3-K)- and genes involved in regulation of cell cycle like Cyclin D1, c-myc, cyclin dependent kinase (Shen and Tergaonkar, 2009). Suppression of apoptosis by NF-κB is mediated by the inhibition of the antioxidant enzymes and c-jun-N-terminal kinase (c-JNK) cascade (Papa *et al*., 2006).

Additionally, NF-κB driven up-regulation of its target genes vascular endothelial growth factor (VEGF), cyclooxygenase-2 (COX-2), interleukin (IL)-6, cell adhesion molecules (ICAM-1, VCAM-1) and matrix metalloproteinases (MMPs) facilitate angiogenesis and invasiveness which contribute to the progression to a metastatic phenotype (Bassères and Baldwin, 2006), (Chen and Castranova, 2007). In addition, anti-apoptotic target genes such as Bcl-2 and Bcl-xL are induced by the constitutive action of NF-κB and contributes to the loss of apoptosis, one of the hallmarks of cancer (Chen and Castranova, 2007). Thus, the data obtained so far suggest that NF-κB is a strong contributor of inflammatory cancers.

Contribution of the NF-κB pathway to CRC can be explained by two different pathways that are activated. First, the activation of the anti-apoptotic genes prevents the apoptotic elimination of the preneoplastic cells. Second, expression of key inflammatory cytokines such as IL-1β, TNF-α, IL-6 and IL-8 increases the inflammatory signals and serves as growth factors for the premalignant cells (Karin, 2006). In colorectal carcinogenesis, NF-κB activation takes place in both tumor cells and the surrounding stromal cells (Karin, 2006).

1.6.2 NF-κB Target Genes in Inflammation

Inflammation can be mediated not only by the classical immune cells like B and T lymphocytes, macrophages, dendritic cells etc. but also non immune cells such as mucosal cells (Fiocchi, 1998). One of the major events that occur during inflammation is leukocyte recruitment from the blood to the site of inflammation. This process involves a cascade of events starting from the capture, rolling, firm adhesion and the transmigration of the leukocytes through the vascular endothelium and further migration into the inflamed tissue (Muller 2002). During inflammation, mucosal cells release chemokines which control the influx of immune cells via cell adhesion molecules (CAMs), many of which are NF-κB target genes (Granger and Kubes, 1994). CAMs that mediate leukocyte recruitment are selectins, integrins and adhesion molecules.

Selectins

Selectins, which comprise three different groups E-, L- and P-, are receptors with adhesive property expressed on endothelial cells (E-), leukocytes (L-) and platelets (P-). E-selectin is expressed at basal levels in unstimulated cells mediating

neutrophil adhesion and can be up regulated with pro-inflammatory cytokines which triggers NF-κB activity (Yoshida and Gimbrone, 1997). L-selectin is naturally found on leukocytes and among cytokines only tumor necrosis factor α (TNFα) that can induce its expression (Khan *et al*., 2003). P-selectin is expressed on platelets and thrombin, lipopolysaccharide (LPS) and TNFα are the known inducers (Cambien and Wagner, 2004). These receptors bind to sialyl Lewis x motifs on the leukocytes and mediate relatively weak interaction with the endothelial cells, giving rise to the characteristic 'rolling' of leukocytes. (Foxall *et al.,* 1992)

Integrins

Integrins are mainly found on leukocytes and expressed in a constitutive manner. Main function of the integrins is mediating adhesion between the cells and matrix proteins, cellular receptors and other ligands (Hood & Cheresh 2002).

In inflammation interaction between the integrins and Cell Adhesion Molecules (CAMs) of the Ig superfamily is particularly important since some the CAMs are known to be up regulated by inflammatory cytokines (Carlos & Harlan 1994; Trushin *et al.,* 2003)

In the primary inflammatory response, leukocyte recruitment is mediated by interaction between the lymphocyte function antigen 1 (LFA-1) and the intercellular adhesion molecules ICAM-1 and ICAM-2, which is important for leukocyte adhesion to the endothelium (Hogg *et al.,* 2002) which is one of the main events of the normal adaptive immune response to inflammation (Warnock *et al.,* 1998).

Integrins expressed on lymphocytes and monocytes mediate the rolling with endothelial vascular cell adhesion molecule-1 (VCAM-1) depending on the nature of

the activator in order to extravasate to the site of the inflammation in inflamed tissue (Berlin *et al.,* 1995).

Immunoglobulin superfamily (IGSF) proteins

Immunoglobulin (Ig) superfamily of proteins involves a wide variety of molecules with multiple Ig-like domains including Intercellular Cell Adhesion Molecule (ICAM)-1, ICAM-2, Vascular Cell Adhesion Molecule (VCAM)-1 and Platelet-Endothelial Cell Adhesion Molecule (PECAM-1). ICAM-1 is mainly expressed in endothelial cells and activated upon inflammation in order to increase the recruitment of leukocytes to the area inflammation (Staunton *et al*., 1989). On the other hand, in the epithelial cells, ICAM-1 mediates the formation of a barrier against bacterial invasion (Song *et al*., 2010). In addition, ICAM-2 which is a truncated form of ICAM-1 (Nortamo *et al*., 1991), is involved in cellular migration to non-inflamed tissues (Briscoe *et al*., 1992). VCAM-1 is mostly expressed in the endothelium upon activation, most commonly via NF-κB, and might be very low in endothelial cells which are resting (Briscoe *et al*., 1992).

So far, cellular, animal and human studies have shown that inflamed tissues have much more expression of the adhesion molecules including E-selectin, ICAM-1, ICAM-2, and VCAM-1 (Malizia *et al*., 1991), (Koizumi *et al*., 1992), (Binion *et al*., 1998), (Salmi *et al*., 1994). Extravasation of leukocytes to the epithelium is driven by interactions between adhesion molecules expressed on epithelial cells and leukocytes (Zen and Parkos, 2003).

ICAM-1

ICAM-1, which is transcriptionally regulated by NF-κB, JAK/STAT, MAP Kinase and PKC, has been implicated in cancer as it mediates the binding of transformed epithelial cells to endothelial cells (Jobin *et al.,* 1998). This binding, in turn, favors overproduction of ICAM-1 which eventually leads to the recruitment of cells of the immune system such as macrophages and neutrophils. As a result of this, degranulation of neutrophils occur releasing elastases which degrade the endovascular and endolymphatic barriers. This phenomenon may make ICAM-1 expression as a determinant for the metastatic potential of cells (Roebuck and Finnegan, 1999).

In the intestinal epithelial cells (IEC), ICAM-1 is expressed at low basal levels under normal conditions (Dippold *et al*., 1993). During intestinal inflammation, ICAM-1 expression is increased through an NF-κB dependent pathway (Maaser *et al*., 2001). In stressed or stimulated epithelial cells, ICAM-1 is expressed in a strictly polarized manner with expression exclusively at the apical surface (Parkos *et al*., 1996). This increased expression was associated with the binding of transmigrated neutrophils to the apical surface of IEC (Vainer, 2005). Biopsies taken during an acute episode of intestinal inflammation showed an increased number of infiltrating neutrophils, which correlated with an up-regulation of ICAM-1 expression in IEC (Vainer *et al*., 2006a). In addition, ICAM-1 expression in the submucosal and muscle layers was also reported to increase in patients with Crohn's disease in proportion to the degree of inflammation (Bernstein *et al*., 1996).

These data suggest that ICAM-1 is a strong sign of inflammation and responsible from sustaining of it.

Matrix Metalloproteinases

In the last 25 years experimental evidences suggest the involvement of proteases in cancer. Proteases involved in cancer dissemination are cysteine, aspartic, metalloproteinases and matrix metalloproteinases (MMPs) and in the invasive process MMPs have a major role. Although the mechanism is not understood completely, connective tissue degradation is accompanied by the MMPs secreted from the tumor cells (Zucker, 1988). MMPs may also serve to activate other MMPs which are associated with a start of a cascade in which efficient degradation of the matrix is observed until it reaches to the cell surface (Zucker *et al*., 2000).

MMP protein family has more than 25 members, all of which share a functional domain homology with inevitable zinc dependency. These enzymes were first shown to have extracellular matrix (ECM) degradation ability (Inuzuka *et al*., 2000). The basic structure of an MMP consists of the following domains:

1) Signal Peptide for secretion of the MMP
2) Prodomain preventing the accession of the substrates to the zinc containing active site of MMP
3) Catalytic site containing Zinc
4) Hemopexin domain providing specificity by interacting with the substrates
5) Hinge region connecting the catalytic domain to hemopexin domain.

The membrane type MMPs have an additional transmembrane domain which is composed of 20 amino acids and a cytoplasmic domain seen in (MT1,2,3 and 5) or glycosylphosphatidyl inositol linkage (MT4 and 6) which links them to cell surface. There are 2 major motifs that are common in MMP proteins. VAAHExGHxxGxxH occupies the catalytic domain of all MMPs containing three histidines for coordination with Zinc. and PRCGxPD motif of the prodomain conferring the latency to the proenzyme (Birkedal-Hansen, 1995).

Generally in vivo activity of the MMPs is tightly regulated. They can be found at low levels and their transcriptions are regulated positively or negatively by growth factors, Tumor Necrosis Factor alpha (TNFα), interleukins etc.

Some of these factors can be activated or inactivated by MMPs in a feedback manner. After transcription MMPs activity may be dependent on the latency conferring polypeptide located in the N-terminal end to a major extent. Precisely, the activation of a particular MMP following its secretion is associated with the degree of the exposure of the active site which is hidden by the prodomain.

Additionally, some MMPs such as MMP9 and MMP1 proforms can be activated by MMP-3. Further regulation of the MMPs are achieved by endogenous inhibitors, auto degradation and selective endocytosis (Barmina *et al*., 1999).

Tissue inhibitors of MMPs (TIMP) are a family of 4 inhibitors sharing homology (TIMP-1, -2, -3, and -4) (Zucker *et al*., 2000). Generally, the concentrations of TIMPS are high with respect to the MMPs in extracellular fluids thereby restricting their activity. Opposing their usual roles, TIMP-2 induces MMP2 by enhancing MT-MMP1 by forming a complex. TIMP transcription is also

controlled by similar cytokines and growth factors controlling MMP expression (Sato *et al*., 1994).

1.7 Matrix Metalloproteinases and Cancer

MMPs are known to be able to cleave almost all ECM components such as proteoglycans, collagens, fibronectin, vitronectin, laminin, and enactin. In cancer, most of the attention has been brought to type IV collagen degradation by MMP2 and MMP9 since it is a major component of basement membranes. In addition many non-ECM proteins have also been shown to be degraded by MMPs making it difficult to evaluate the physiologically important substrates. For instance, MMPs induce the release of growth factor proteins from the cell surface which enhances proliferation. In contrast, activation of TGF beta by MMPs can decrease proliferation. MT1-MMP and MMP-1 enzymes have been found to enhance cell migration. MMP2 and -9 have been shown to cleave collagen type IV and expose a cryptic site displaying affinity to avb 3 integrins thus leading to increased angiogenesis (Kajita *et al*., 2001). Also another opposite example can be MMP12 which is able to cleave plasminogen and generates angiostatin which is a powerful inhibitor of angiogenesis. In conclusion, these examples can be regarded as opposing roles of MMPs in cancer, angiogenesis and tumor formation or prevention.

MMPs have been implicated in colorectal cancer and may be required for invasion and metastasis. Transformations of several adenomatous polyps to an invasive colon cancer have been shown to be corresponding with MMPs.

(reference?) MMP-1, -2, -3, -7, -9, -12, -13, and MT1-MMP are the MMPs which have been extensively studied in colorectal cancer.

Immunohistochemical studies have suggested that MMP-1 was not expressed in benign adenomas; however, expression was observed in invasive cancers and was found to be proportional to the invasiveness of the cancer being studied (Shiozawa *et al*., 2000).

ProMMP-2 is unique in terms of being expressed in the normal tissue. Therefore it has been regarded as a housekeeping gene which has been shown to be required for normal cellular processes. The role of MMP-2 in colorectal cancer was described by Poulsom *et al.,,* in 1992. Subsequently, it was found that 10 out of 12 samples had MMP-2 expression and no MMPs were detected in the normal or nonmalignant areas (Poulsom *et al*., 1992).

MMP-3 has also been studied in colorectal cancers and was shown to be corresponding with the MMP-9 expression. It has also been claimed that uPA is expressed in correlation with the MMPs which activates plasminogen to plasmin. Then plasmin activation of proMMP-3 results in activation of pro MMP9 giving MMP9, which results in colorectal cancer progression (Inuzuka *et al*., 2000).

MMP9 involvement in colorectal cancer is currently under debate. Overexpression of MMP-9 is associated with metastasis in colorectal cancer and Dukes' staging (Zeng *et al*., 1996). Elevated levels of MMP-9 in colorectal cancer have been attributed to the inflammatory responses of the tissues surrounding the neoplasms instead of direct involvement in tumor progression (Lund *et al*., 1999).

1.8 Aim of the Study

Since the spontaneous differentiation of Caco-2 cells is associated with the cease in the proliferation, NF-κB mediated inflammatory signals might be altered in the course of differentiation process. The aim of the current study is to understand the changes in the NF-κB activity including its two target genes *ICAM1* and *VCAM1* during differentiation of Caco-2 cells and regulation of the NF-κB target genes ICAM-1 and VCAM-1 and also MMP16 regulation via *miR-146a* in the course of spontaneous differentiation.

In addition regulation of *miR-146a* which is one of the microRNAs targeting NF-κB is to be determined with a selected target gene *MMP16.*

Finally, 15-LOX-1 in NF-κB regulation and its crosstalk with PPARγ is also one the aims of the current study.

CHAPTER 2

MATERIALS AND METHODS

2.1 Cell Culture

Caco-2 cells were grown in monolayers in either tissue culture flasks or plates. HCT 116 colon carcinoma cells were grown in RPMI 1640 cell culture medium containing 10% Fetal Bovine Serum (FBS) and 1% Penicillin and Streptomycin at 37°C supplied with 5% CO_2.

Caco-2 cells were grown according to ATCC guidelines in Eagle's Minimum Essential Medium (MEM) containing, 2 mM L-glutamine, 0.1 mM nonessential amino acids, 1.5 g/L sodium bicarbonate, 1mM sodium pyruvate, 20% FBS and 1% Penicillin-Streptomycin

In order to remove the metabolic by products, the cells were washed with a 1X solution of Phosphate Buffered Saline (PBS) before changing the culture medium.

Cells were stored in frozen form in the vapor phase of liquid nitrogen in freezing medium composed of complete culture medium containing 5% Dimethylsulfoxide (DMSO). Before freezing, the cells were first harvested from the

cell culture environment by means of trypsinization which was achieved by adding enough trypsin after having removed all the culture medium and washed with 1X cold PBS twice. Subsequently trypsin activity was terminated by the addition of cell culture medium and then cells were pelleted by centrifugation at 1000 x g for 10 min. After the supernatant was removed, the cells were suspended in culture medium containing 7.5% DMSO ad kept at -80°C overnight in an isopropanol bath in order to ensure a gradual decrease in temperature and then transferred to the liquid nitrogen tank until needed.

To culture cells from the frozen state, first they were thawed at 37°C in a water bath, and transferred to T25 tissue culture flasks containing at least 5 ml of the corresponding cell culture medium. After the attachment of the cells, the culture medium was replenished with fresh medium immediately.

2.1.1 Spontaneous Differentiation of Caco-2 cells

Caco-2 cells are known to undergo spontaneous differentiation upon reaching the in vitro confluency (Simon-Assmann *et al.,* 2007). For that purpose Caco-2 cells were seeded in 6-well cell culture plates and medium was changed three times a week. The day on which cells reached 100% confluency was counted as day 1 and cells were left to grow for 30 days. In regular time intervals cells were collected and either protein or RNA was isolated from the cells as described elsewhere.

2.1.2 Treatment of Caco-2 Cells

Caco-2 cells were treated with NF-κB inhibitors (SN 50: 50µg/ml, TMB-8: 100-250µM, N-Acetyl-cysteine: 10-30µM, ;Pyrollidine dithiocarbamate PDTC: 50-100µM). Lipopolysaccharide (LPS) was treated in a concentration of 100 µg/ml. PKCα inhibitor GÖ 6976 and –θ inhibitor Rottlerin were used in concentrations of 3 µM. All treatments were done in serum free refreshed culture media on the days mentioned.

Proteasomal inhibitor MG 132 was used in a concentration of 10µM. Concentrations of lysosomal inhibitors were; Pepstatin A : 1µg/ml, Leupeptin: 100µM, trans-Epoxysuccinyl-L-leucylamido(4-guanidino)butane E64: 10µM. Calpain inhibitor I (ALLN) was used in concentration of 100µM

2.2 Alkaline Phosphatase Activity

Alkaline Phosphatase is known to be expressed in the brush border membranes after the differentiation of intestinal cells (Mariadason *et al.,* 2002). Alkaline phosphatase activity was therefore measured as a marker of differentiation in post-confluent Caco-2 cells. For that purpose protein extracts were prepared from the Caco-2 cells by using Cell Lysis Buffer (Stratagene) according to manufacturer's instructions. Phosphatase inhibitors were omitted from the extraction buffer owing to potential interference with the alkaline phosphatase activity. Twenty µg of protein was added to the substrate p-nitrophenyl phosphate (Sigma) in 96-well plates and then incubated at 37°C for 30 min. The reactions were stopped by the addition of

150µl 3N NaOH and enzymatic activity was measured spectrophotometrically at 405 nm and relative activities were obtained by using the cell lysis buffer as blank.

2.3 RNA Isolation

For Polymerase Chain Reaction (PCR) experiments, total RNA was isolated from the cultured cells. First the culture medium was removed from culture dish and the cells were washed with ice cold PBS twice. Then Trypsin/EDTA solution 0, 05% / 0, 02% (w/v) enough to cover the entire dish was added to the culture dish and cells were incubated at 37°C for 5-15 minutes in a CO_2 incubator. Afterwards complete medium containing serum was added to the culture dish in order to inactivate the trypsin. The total number of cells were counted and transferred to 15 ml centrifuge tubes and centrifuged for 5 min at 300 x g at room temperature (25°C) to pellet the cells. Subsequently the supernatant was removed and pelleted cells were used for RNA isolation by using spin filter based RNEasy Mini Kit (Qiagen) according to the manufacturer's instructions (Appendix G). The obtained RNA was stored at -80°C freezer until use.

2.3.1 RNA Measurement

The amount of total RNA obtained from cells was measured spectrophotometrically at 260 nm in a quartz cuvette (Warburg and Christian., 1942). First, the spectrophotometer was set to zero by using RNAse free distilled was as a blank. Then absorbance at both 260 and 280 nm wavelengths were recorded and OD

260 nm/ OD 280 nm ratio of 1.7 and above was considered as acceptable values for the downstream applications of the RNA.

2.3.2 DNAse I Treatment of RNA Samples

DNAse I treatment of RNA samples was also performed in order to remove genomic DNA contamination from the RNA. For that purpose each ug of RNA obtained from samples was treated with RNAse Free DNAse I Enzyme (Fermentas) in the presence of RNAse inhibitor (Ribolock RNase inhibitor, Fermentas) according to the manufacturer's instructions. After the DNAse I treatment the enzyme was heat inactivated at 65°C for 10 min in the presence of EDTA to prevent the hydrolysis of RNA in heat treatment. The resulting RNA free of DNA was directly used for the cDNA synthesis.

2.4 cDNA Synthesis

cDNA was synthesized from 1 μg DNAse I treated RNA in the presence of RNAse inhibitor using oligo dT primers in with a cDNA synthesis kit according to the manufacturer's instructions (Revert Aid cDNA Synthesis Kit, Fermentas) (Appendix I).

2.5 Protein Extraction

2.5.1 Total Protein Extraction

Total protein extraction was performed by using 1X Cell Lysis Buffer (CLB) (Stratagene, USA) containing 1X EDTA free protease inhibitor cocktail (Roche), 1 mM sodium orthovanadate and 1mM sodium fluoride according to the manufacturer's instructions. For total protein isolation, first the culture media was removed from the tissue culture dishes/flasks in which cells were being grown. Then the cells were washed with ice-cold PBS with 1X protease inhibitor cocktail twice and following by 400 µl CLB. Subsequently cells were incubated at room temperature for 15 min by gently rocking the plates/dishes in 3 minute intervals. The cells were then scraped from the surface of the tissue culture plate/dish with the aid of a sterile cell scraper (Greiner), transferred to microcentrifuge tubes and vortexed for 15 seconds at the highest speed. The samples were then centrifuged for 2 min at 14000 x g at 4 °C and supernatants containing cellular protein extracts were taken and immediately stored at -80°C until use.

2.5.2 Nuclear and Cytoplasmic Protein Extraction

For isolation of nuclear and cytoplasmic proteins, the cells were washed twice with ice cold PBS and resuspended in 1ml of Buffer A containing 20 mM HEPES pH 7.9, 10 mM KCl, 0.1 mM EDTA, 1mM DTT, 1.5 mM MgCl2, 1X Protease inhibitors (Roche) and incubated on ice for 30 min. The cells were vortexed for 15 seconds at high speed, followed by the addition of 0. 25% NP40 (Applichem),

and cells were incubated on ice for another 5 min and vortexed for 5 s. Supernatants were obtained after centrifugation at 12000 x g for 1 min at 4˚C. The remaining nuclear pellet was washed with 200µl of Buffer A in order to remove all cytoplasmic proteins and centrifuged. The pellet were resuspended in 200µl of Buffer B containing 20 mM HEPES, 10 mM KCl, 0.1 mM EDTA, 1mM DTT, 1.5 mM $MgCl_2$, 0.5 M NaCl, 25% glycerol and incubated on ice for 30 min. The lysate was centrifuged for 10 min at 12 000 x g at 4˚C. The supernatant was considered as the nuclear fraction

2.6 Reverse Transcriptase - PCR Studies

PCR reactions were performed in thermal cycler (Applied Biosystems) using a reaction mixture containing 3µl of 10X buffer, 0.2mM of each dNTP, 2.5mM $MgCl_2$, 0.5 µM forward and reverse primer pairs, , 1U Taq DNA polymerase (Fermentas) and 3µl cDNA (100ng/µl) in a total reaction mixture made up to 30µl with PCR grade water. Primers used in this study were mentioned in Table 2.1

Table 2.1 PCR Primers Used for Gene Expression Studies

Number	Primer	Sequence	TM C°	Gene Name	Accession Number	Amplicon Length	Application
1	VCAM1_259_Fwd	ATGACATGCTTGAGCCAGGG	59.4	VCAM-1	NM_001078.2	259	VCAM-1 Expression
	VCAM1_259_Rev	GTGTCTCCTTCTTTGACACT	55.3				
2	Sucrase_isomaltase_Fwd	CAAATGGCCAAACACCAATG	55.3	SI	NM_001041.3	159	SucraseIsomaltase Expression
	Sucrase_isomaltase_Rev	CCACCACTCTGCTGTGGAAG	61.4				
3	EA_MMP16_Fwd	GCTGACCCAAGGAAAAATGA	55.30	MMP16	NM_022564.3	270	MMP16 Expression
	EA_MMP16_Rev	CACAAAATTCCCGTCGCTAT	55.30				
4	hsa_miR146a_Fwd	CCGATGTGTATCCTCAGCTTTGA	60.60	MIR146A	NR_029701.1	99	MiR146a Expression
	hsa_miR146a_Rev	ACGATGACAGAGAGATATCCCAGCTG	62.70				
5	miR_146b_Fwd	CCTGGCACTGAGAACTGAATTCC	62.40	MIR146B	NR_030169.1	73	miR 146b Expression
	miR146b_Rev	CCGGGCACCAGAACTGAGTCCAC	67.80				
6	238GAPDHFwd	CGACCACTTTGTCAAGCTCA	57.30	GAPDH	NM_002046.3	238	GAPDH Expression
	238GAPDHRev	CCCCTCTTCAAGGGGTCTAC	61.40				
7	STp21forward	ATGAAATTCACCCCCTTTCC	58.35	p21, Cip1	NM_078467.1	173	p21 Expression
	STp21reverse	CCCTAGGCTGTGCTCACTTC	64.50				
8	RF_ICAM_FRWD	CAGGGAATATGCCCAAGCTA	60.40	ICAM-1	NM_000201.2	244	ICAM-1 Expression
	RF_ICAM_REV	TGAACCATGATTGCACCACT	58.35				
9	SB111	GGTGAAGGTCGGAGTCAACG	57.90	GAPDH	NM_002046.3	496	GAPDH Expression
	SB112	CAAAGTTGTCATGGATGACC	51.49				
10	CEBP_Fwd	GACAAGCACAGCGACGAGTA	59.4	CEBPB	NM 005194.2	157	CEBPB Expression
	CEPB_REv	AGCTGCTCCACCTTCTTCTG	59.4				

For duplex PCR reactions, 0.05- 0.5 µM control primer (GAPDH) was added to the PCR mix for co amplification of the GAPDH gene. Ten µl of the reaction products were run in 1-2% agarose gels depending upon the size of the expected product. Band intensities were measured with the ImageJ (http://rsbweb.nih.gov/ij/) program, ratios of band intensities against their corresponding GAPDH band was calculated and fold change data were obtained.

2.6.1 Real Time PCR Studies

In order to determine the expression of the genes of interest, quantitative PCR (qPCR) was used. For that purpose RNA samples from cells were prepared as described before, subsequently cDNA was prepared from 2µg of RNA following DNAse I treatment qPCR reactions were performed in 10µl reaction volumes containing 10 µl 2X Fast Start SYBR Green Mastermix, 0.5 µM forward and reverse primers and 2 µl cDNA prepared from 2µg DNAse I treated RNA. In order to determine the fold change in the target gene expression, the housekeeping gene GAPDH primers were amplified in separate tubes. A standard curve was constructed by using different amounts of cDNAs and the delta Ct values were calculated. The fold change was calculated by delta delta Ct method (Pfaffl, 2001).

In addition, expression levels of the mature form of the intended microRNAs (miRNAs) were also determined via qPCR. For that purpose RNA samples from cells were prepared as described before, subsequently cDNA was prepared from 30 ng of RNA with TaqMan MicroRNA Reverse Transcription Kit (Applied Biosystems, Foster City, USA) according to the instructions of the kit following DNAse I treatment qPCR reactions were performed in 20µl reaction volumes

containing 10 µl 2X TaqMan Universal PCR Mastermix, 1µl of 20X Real time Primer-Probe mixture, 1.33 µl cDNA and 7.67 µl water. In order to determine the fold change in the target gene expression, the housekeeping gene RNU6B reactions were conducted in separate tubes. A standard curve was constructed by using different amounts of cDNAs and the delta Ct values were calculated. The fold change was calculated by delta delta Ct method (Pfaffl, 2001).

2.7 Western Blot Studies

Proteins (total, cytoplasmic or nuclear) collected from the cells were boiled in the presence of 1X Laemmli gel loading buffer containing SDS and β-mercaptoethanol as reducing agent at pH 6.8 and kept at -20°C until use. Proteins were separated in a 12% SDS-PAGE gel containing a 4% of stacking gel, under denaturing conditions at 100V for 1 hour and 45 minutes at room temperature.

Proteins in the gel were then transferred to a PVDF membrane (Bio-Rad) which was previously rehydrated in methanol and equilibrated with transfer buffer. Then a sandwich cassette was prepared according to the manufacturer's instructions (Bio-Rad) and proteins were electroblotted on to the PVDF membrane for 1 hour and 45 minutes at 4°C.

After transfer, the membrane was briefly washed with Phosphate Buffered Saline (PBS) or Tris Buffered Saline (TBS) containing 1% Tween-20. Bovine serum albumin (BSA) or skim milk at concentrations varying from 5% to 10% was used in the wash buffer as blocking agents. Unless otherwise stated, the membranes were

blocked for 2 hours at room temperature with gentle and constant agitation and incubated with primary antibody in blocking buffer in dilutions ranging between 1:100-1:1000, overnight at 4°C. The membranes were washed three times for 10 min each with washing buffer and incubated with an appropriate HRP-conjugated secondary antibody in dilution of 1:1500-1:2000 at room temperature for 1 hour with constant agitation. After briefly drying, the membrane was incubated with 3 ml of HRP ECL substrate mixture (1.5 ml hydrogen peroxide and 1.5 ml enhancer) (Pierce) and incubated for 1 min at room temperature. The membranes were wrapped with stretch film and placed in the X-ray cassette and exposed to an X-ray film (KODAK) for 1 to 10 min in a dark room. The films were scanned and quantified if necessary using the ImageJ program. Compositions of western blotting buffers were mentioned in Appendix B.

2.8 Electrophoretic Mobility Shift Assay (EMSA)

Nuclear proteins were extracted from differentiating Caco-2 cells on Day 0 and 10 as described elsewhere. NF-κB and C/EBPβ consensus DNA binding sequences were designed using public databases (http://www.ncbi.nlm.nih.gov/nucleotide/) and obtained commercially (Iontek, Turkey). The stranded oligos containing the consensus sequences for sense and antisense strands were biotinylated at the 3' end of each oligo. For this, 1µM of each oligo was added into the biotinylation reaction mixture containing 25µl ultrapure water, 10µl of 5X terminal transferase reaction buffer, 5µl oligo (1µM), 5µl biotin-11-UTP, 5µl terminal transferase enzyme (2U/µl). After 30 min of incubation at 37°C, the reaction was stopped by the addition of 2.5 µl 0.2M EDTA and the

resulting products were refined by phenol:chloroform extraction. Equal amounts of the oligos were annealed by heating to 95°C and gradually cooling at the rate of 1°C/minute until ambient temperature was achieved. To show specificity, unlabeled strands were hybridized in same manner and used in the binding reactions in concentrations of 200 fold excess.

For binding reactions 10µg of protein was mixed in a 20µl reaction volumes with 2µl 10X binding buffer, 1µl of 50% glycerol, 1µl of 100mM MgCl2 , 1µl of 1µg/µl Poly (dI•dC), 1µl of 1% NP-40, 20mol labeled oligo and ultrapure water. Reaction specificity was confirmed by inclusion of 200 fold molar excess of unlabeled oligos, which will lead to a loss of the gel shift. Additionally, antibodies against the specific nuclear proteins being studied were also included, leading to a supershift of the oligo-protein-antibody complex. For this, all of the components except antibody were added to the reaction mixture and incubated on ice for 10 min and at room temperature for 20 min after which the oligos and antibodies against the protein of interest (1-3µl) were added and incubated for a further 10 min at room temperature. Before loading to the gel 6µl of 4X Loading Dye was added to the reactions.

The products were separated in 8% polyacrylamide gel prepared with TBE at 100 V for 1 h at 4°C and transferred on to a nylon membrane according to the manufacturer's instructions (Biodyne, precut B Nylon membrane, Pierce, USA) by using electro blotting in 0.5X TBE buffer at 4°C. Afterwards, the cut membrane with the DNA side facing downwards was placed on transilluminator and cross linking reaction was carried out for 15 min. The membrane was then blocked using a blocking reagent supplied by the manufacturer. Detection was achieved by means of

Luminol enhanced hydrogen peroxide substrate and signals were collected on X-ray films which were processed in a Kodak X-Ray film developer machine.

The consensus sequences of C/EBPβ and NF-κB used to detect the DNA binding activity of these proteins in differentiating Caco-2 cells have been shown below.

Table 2.2 Oligos Used as Probes in EMSA Reactions

Number	Primer	Sequence	Application
1	NF_kB_sense	AGTTGAGGGGACTTTCCCAGGC	NF-KB consensus sequences
	NF_kB_Antisense	GCCTGGGAAAGTCCCCTCAACT	
2	cebp_SENSE	AGTTGAGGATTGCGCAATCAGGC	CEBPbeta consensus sequences
	cebp_ANTISENSE	GCCTGATTGCGCAATCCTCAACT	

2.9 Chromatin Immunoprecipitation (ChIP) Studies

Chromatin immunoprecipitation studies were carried out in order to determine the binding of C/EBPβ and NF-κB to the ICAM-1 and VCAM-1 gene promoters in the spontaneously differentiating of Caco-2 cells. For this purpose, first primers were designed from the promoter of ICAM-1 within bases 721-961 spanning the proximal NF-κB element, within bases 1081-1201 spanning the NF-κB and C/EBPβ elements, and within bases 901- 1036 spanning a single C/EBPβ element in the ICAM-1 promoter. As control, primers amplifying bases within 121-241 in the ICAM-1 gene promoter were used. For the VCAM-1 promoter, primers amplifying the region between -160-0 spanning the NF-κB binding site in theVCAM-1 were

designed. As controls primers for the upstream of the NF-κB region (bases -2167 and -1967) in the promoter were designed.

The Caco-2 cells were grown until they reached in vitro confluency in T25 flasks. On the 0th and 10th day after reaching 100% confluency, the culture medium was refreshed and 280µl concentrated formaldehyde was added to initiate the crosslinking, incubated at room temperature for 2 min and stopped by adding 1ml of 1M glycine. Cells were washed with PBS twice and then cells were scraped into 1.5ml eppendorf tubes and centrifuged at 13000 x *g* for 1min. The pellets were then frozen in liquid nitrogen and then thawed in buffer C (composition given in the appendix). Thawed cells were incubated on ice for 20 min and centrifuged after which they were resuspended in a breaking buffer and sonicated for 1 minute and 30 seconds in a water bath sonicator (Bandelin, SONOREX, Walldorf, Germany). After this 1ml of Triton buffer was added and 400µl of the sample was taken as the input control. After protein measurement, equal protein amounts were loaded in protein A-agarose containing spin filter based columns (NAb spin columns, Pierce) which were previously equilibrated according to the manufacturer's instructions. Afterwards 6µl of anti-NF-κB p65 antibody or anti-C/EBPβ antibody was added to the column and incubated at 4°C with constant agitation for 1 h. The columns were then washed and samples were eluted with elution buffer (Pierce). Then 400µl of SDS-NaCl-DTT buffer was added and samples were incubated at 65°C, vortexed well and incubated at 65°C overnight to reverse the crosslinking. On the following day, same volume of phenol-chloroform (1:1) was added to the both immunoprecipitated and input control samples, vortexed well and centrifuged at 13000 x *g* for 10 min at 4°C, the aqueous phase was taken from samples and the same extraction procedure was applied. Subsequently, 1/1000 volume 3M sodium acetate was added and after precipitate

was observed, 600 µl ethanol was added to the samples and incubated for 30 min at room temperature. Samples were then centrifuged at 13000 x *g* for 10 min, supernatants were removed and pellets were washed with 70% ethanol. Then samples were dissolved in 40µl of molecular biology grade water after it was ensured that all of the ethanol had evaporated.

PCR was carried out with both immunoprecipitated and control samples both semi quantitatively in an Applied Biosystems PCR machine followed by separation on a 2% agarose gel, and quantitatively on a Corbett Real Time PCR machine using the primers described above. Primers used in ChIP assays are given in Table 2.3.

Table 2.3 Primers Used in ChIP Studies

Number	Primer	Sequence	TM	Gene Name	Accession Number	Amplicon Length (bp)	Application
1	ICAM_1_Far_NF_KBChip_Fwd__	CACTCCCACGGTTAGCGGTCG CCGGGAGGTGC	> 75	637 bp at 3' side: ICAM-1	NT_011295.11	209	NF-κB Element in ICAM-1 promoter
	ICAM_1Far_Nf_kB_Chip_Rev_	GAGACTCCAGGCTGCGAGGG GTCCGAACTC	75.0				
2	ICAM_NF_ANDCEBP_CHP_FWD	GCCGGGAAACGGGAGGCGTG CAGCCCGGGA	> 75	277-bp at 3' side: ICAM-1	NT_011295.11	120	NF-KB / CEBP adjacent elements in ICAM-1 promoter
	ICAM_NF_ANDCEBP_CHP_REV_	CCGGACTGACAGGGTGCCCG GGCCGAGAGG	> 75				
3	ICAM_FARCEBP_CHIP_FWD_	AGGCCTGGGTAAGCTGGAGA CGGACCACTT	72.2	465 bp at 3' side at ICAM-1	NT_011295.11	117	CEBP Element in ICAM-1 promoter
	ICAM_FAR_CEBP_CHIP_REV_	CGCTAAGGTCTTATTAAGTACT TTTAAATA	58.6				
4	ICAM_1_Input_Ctrl_Fwd_	ATAGGAAGGGGCTGCGCGGTCC GGGGACCCT	> 75	12-5 bp at 3' side ICAM-1	NT_011295.11	123	ICAM-1 Upstream primers for control
	ICAM_1_Input_Ctrl_Rev_	GTACTCTTAAGTCTCGGAGCA CCAAGCCGC	70.9				
5	VCAM1_NfKB_Chip_Fwd	ACAGAGAGAGGAGCTTCAGC AGTGAGAGCA	69.5	262 bp at 3' site VCAM-1	NT_032977.9	128	NF-κB Element in VCAM-1 Promoter
	VCAM1_Nf_KB_Reverse_	GTCTGTGCTTTATAAAGGGTC TTGTTGCAG	65.4				
6	_VCAM1_Upstream_Fwd_	GAATTCAAAATGATATTTCAGT CGGGACAAGGCCAAAC	68.4	2254 bp at 3' side VCAM-1	NT_032977.9	250	VCAM-1 Upstream Control
	VCAM1_down_Stream_	TCATTCTGCATTTACTGATTAA TATGCC	59.3				

2.10 NF-κB Activity Assay

NF-κB activity in the spontaneously differentiating Caco-2 cells was also determined using an ELISA Plate format activity assay kit (Combo NF-κB p50/p65 Transcription Factor Assay kit, Cayman, USA). For that purpose, Caco-2 cells were allowed to undergo spontaneous differentiation and nuclear extracts were obtained as described elsewhere.

The nuclear extract, made up to 100µl with the transcription factor binding buffer was applied in the wells of the ELISA plate, sealed and incubated at 4°C overnight without agitation. Then wells were emptied and washed with 200µl 1X wash buffer five times. After the last wash the plate was tapped in order to get rid of the residual washing buffer. In the meantime, 1:100 dilution of the NF-κB (p65 and p50) primary antibody was prepared and 100µl of each antibody was added to the wells except the ones used as blank. The plate was incubated at room temperature for one hour without agitation and same washing procedure was performed as mentioned above. Following this, 1:100 dilution of the anti-goat-HRP conjugated secondary antibody was prepared and 100µl was added to the wells. After 1h incubation at room temperature the plate was washed and 100µl of the developing solution was added to the wells and incubated at room temperature for 45 min with gentle agitation. Then 100 µl of stop solution was added to the wells and absorbance was read at 450 nm.

As controls, 10µl of the competitor double stranded DNA was used in some wells. Wells containing buffer only were used as blanks and 10µl of the positive control sample (provided by the manufacturer) was used as the positive control.

2.11 Protein Kinase C (PKC) Activity Assay

PKC activity was determined using a commercial non-radioactive PKC Assay kit (Pep Tag, Promega, USA) using protein extract from Day 0 and Day 10 differentiated Caco-2 cells in T25 flasks. The cells were scraped with a PKC extraction buffer, vortexed well and lysates were centrifuged for 5 min at 4°C at 14000 x g. The supernatants were removed and passed through DEAE-Cellulose column with a packaging density of 0.9 g/ml (500 µl column volume in spin filters) previously equilibrated with the PKC extraction buffer. The flow through was obtained by brief centrifugation and the columns were washed with same buffer three times. The bound samples were eluted with the extraction buffer containing 200 mM NaCl. After a desalting step using commercially available desalting columns (ZebaSalt, Pierce) according to the manufacturer's instructions, proteins were measured. Protein (2µg) from each sample was subjected to the activity assay reaction which contained 5µl 5X Buffer, 5µl substrate, 5µl sonicated Activator Solution and water up to a final volume of 25µl. The tubes were incubated at 30°C for 1 h and the enzyme was inactivated at 95°C for 2 min and loaded on a 0.8% agarose gel prepared with Tris buffer (pH 8.0) and electrophoresed for 30 min in the same buffer at 100V. In this step, the non-

phosphorylated substrate was expected to run to the cathode while phosphorylated substrate produced as a result of the kinase activity of PKC was expected to run to anode since it would gain negative charge. The same reaction conditions were also prepared with the standard pure enzyme in different concentrations varying from 0 to 10 ng of enzyme in order to obtain a standard curve.

After observing the bands in the gel, quantification of the bands was carried out spectrophotometrically at 570 nm. To do that, first the bands were excised from the gel and incubated at 95°C until they melted and samples occupying a volume less than 250 µl was completed to 250 µl with water. Then 125 µl of each sample was transferred to another tube already containing 75µl Gel Solubilization solution and 50 µl of glacial acetic acid. Then absorbances at 570 nm were obtained by using the tube not containing any enzyme as the blank.

2.12 Adhesion Properties of Spontaneously Differentiating Caco-2 Cells

Cell adhesion molecules such as ICAM-1 and VCAM-1 are capable of doing specific interactions with the extracellular matrix (ECM). For that purpose adhesion assays were performed by using fibronectin as a representative protein from the (ECM). Caco-2 cells were grown for 10 days after reaching the in vitro confluency, counted and collected. On the day of the experiment 96 well plates were coated with 50 µg/µl fibronectin in EMEM complete medium from a 1mg/ml stock. Control wells were not coated. After coating, the plates were

incubated for 1 h at 37˚C, washed twice with washing buffer (0.1% BSA in OPTI-MEM). The plate was then blocked with a blocking buffer containing 1% BSA in OPTI-MEM and incubated at 37˚C for 1 h. After a washing step as described previously, the plate was chilled on ice, brought back to 37˚C and 400000 cells/ml were added in 100µl total volume to each plate and incubated at 37˚C for 2 h. Following this, the plate was washed with PBS in order to remove the cells unbound to the fibronectin matrix, 10µl MTT reagent (Invitrogen, USA) was added to the cells and incubated another 4 h. The formazan crystals formed in the attached cells was dissolved with 100µl SDS in 0.01 N HCl cells. The plate was incubated at 37˚C overnight and read spectrophotometrically at 570 nm.

2.13 Tumor-Endothelium Adhesion Assay

Adhesion of circulating leukocytes and tumor cells to the endothelium for their extravasation into tissues during an inflammatory response and metastasis respectively is influenced by expression of surface molecules such as ICAM-1 and VCAM-1.

In our study, in order to determine the effect of cellular differentiation on their adhesion to human umbilical cord vein endothelial cells (HUVEC) a Cytoselect Tumor Endothelial Cell Adhesion Kit (Cell Biolabs, USA) was used. First, the wells of a 96 well plates were coated with 100µl of gelatin solution and incubated for 60 min at 37ºC in a humidified incubator. Then, 100,000 HUVEC

cells were added to the wells and cultured for 48-72 hours until they formed a monolayer. Following this, Caco-2 cells at 0^{th} or 10^{th} days after reaching confluency were harvested by trypsinization, counted and adjusted to a concentration of 10^6 cells / ml in serum free media and labeled with 500X CytoTracker (2µl/ml) (Cell Biolabs) solution for 60 min at 37ºC in a humidified incubator. Then the cells were centrifuged at 1000 rpm for 2 min, the medium was aspirated and the cells were washed with serum free medium twice. The cells were then resuspended in serum free media at a final concentration of 10^6 cells /ml. In the meantime, the HUVEC cell monolayer in the 96 well plate were washed once with serum free media and 200µl of 0th or 10th day differentiated Caco-2 cells labeled with CytoTracker were added into each well. As controls, 200 µl of the cells were added in HUVEC free empty wells. Then cells were incubated overnight in order to allow the adhesion Caco-2 cells onto HUVEC cells. Next, the medium was aspirated, and the cells were washed 250 µl 1X Wash Buffer three times, treated with 150µl of 1X Lysis Buffer and incubated at room temperature for 5 min. The fluorescence was read with a fluorometer (FMax, Molecular Devices, Sunnyvale, California, US) with a 480nm / 520 nm excitation/emission with 530 nm cutoff.

2.14 Gelatin Zymography

The activity of matrix metalloproteinases in spontaneously differentiating Caco-2 Cells was determined by gelatin zymography. For this, conditioned

medium was collected from the cells and separated SDS polyacrylamide gels impregnated with gelatin under non-reducing and non-denaturing conditions.

Gelatinase activity in 48 h conditioned media collected from Caco-2 cells was detected as described previously (Nakamura *et al*., 1999). Total protein (1mg) from the conditioned media from each sample was separated on a 10% SDS-PAGE containing1mg/ml gelatin under non reducing conditions. Following electrophoresis, the gel was washed and incubated with renaturation buffer containing 2.5% Triton-X-100 at room temperature. The gel was then washed with distilled water and incubated for 16 h at 37°C in a developing buffer (50 m*M* Tris-HCl, pH 7.8, 0.2 *M* NaCl, 5 m*M* $CaCl_2$,1mM $ZnCl_2$ and 0.02% v/v Brij 35) washed with distilled water and stained with a staining solution (0.5% w/v Coomassie Blue R-250, 5% v/v methanol, and 10% v/v acetic acid) for 1 h at room temperature and destained with a destaining solution (10% v/v methanol, 5% v/v acetic acid). Proteins with gelatinase activity were observed as blue bands against blue background.

2.15 Matrigel Invasion Assays

Matrigel assays were performed in order to determine the effect of *miR-146a* overexpression and therefore MMP16 downregulation on invasive properties of HT-29 cells. For that purpose cells were grown in 6 well tissue culture plates and transfected with a *miR-146a* overexpression vector (P_SUPER) along with its empty and mutated counterparts as controls by using 1:3

lipofectamine as transfection agent for 24 hours. In the meantime, first Matrigel (10mg/ml) was diluted to 2mg/ml with cold serum free RPMI 1640 medium and 100µl was added in Boyden chambers and incubated at 37°C for 5 hours for gelation. Then transfected cells were trypsinized and washed three times with RPMI 1640 medium with 1% FBS. After the counting, approximately 100,000 cells were added in 100µl volume in 1% FBS containing RPMI 1640 medium on Transwells containing solidified Matrigel. Bottom part was filled with 600µl RPMI 1640 medium containing 10% FBS and 50µg/ml fibronectin used as chemoattractant. Then plates were put in the incubator and after incubation of 96 hours Transwells were removed and top part containing Matrigel and non-invaded cells were remove gently with the aid of sterile cotton swabs and bottom parts of the Transwells were dipped into the methanol and fixed for 7 minutes. Afterwards excessive methanol was drained and Transwells were dipped into the Giemsa for 2 minutes which is followed by excessive washing with sterile distilled water. Then, the filters in the Boyden chambers with the migrated cells facing upwards were peeled off and mounted on microscope slides with few drops of immersion oil. The filters were covered with cover slips and visualized under light microscope and the invaded cells were counted.

2.16 Reporter Gene Assays

In our study, firefly luciferase based reporter gene assays were performed in order to gain insights about two different purposes; miRNA mediated 3'UTR

regulation of genes of interest, including ICAM-1 and MMP16 and the activity of transcription factors NF-κB and C/EBPβ in the course of spontaneous differentiation. Vectors used for these purposes are listed in the Appendix A.

For all transfections, Lipofectamine and Plus reagents (Invitrogen, USA) were used as transfection agent and enhancer, respectively. For transfections, vectors (0.5 - 1,.μg/well depending upon the well surface area) were diluted with Opti-MEM and PLUS reagent was added in 1:10 μg vector/μl reagent ratio. In a separate tube Lipofectamine reagent was added to Opti-MEM at 10 X μl per μg of vector. The mixtures were then incubated at room temperature for 15 min and incubated another 15 min after they were pooled. In the meantime, the cells to be transfected were washed twice with PBS and the culture medium was replaced with serum and antibiotic free Opti-MEM. The transfection mixtures were added drop-wise to the medium and gently swirled. In addition to the luciferase based reporter vectors, the cells were co-transfected with a pSV-beta-galactosidase vector (Promega, USA) for normalization. In order to determine the luciferase activity, transfected cells were washed with PBS twice and harvested in 200-350μl 1X Cell Lysis Buffer (Promega, USA) for15 min at room temperature. The harvested cells were vortexed for 15s and centrifuged at 4°C at 14000 x g for 2 min. Supernatants were collected and 20 μl of the sample was mixed with 100μl luciferase assay reagent (Roche), and after 8s of integration time, the luminescence values were read with lumiometer (Modulus, Turner Biosystems, USA). For β-galactosidase activities, each protein sample (100μl) was mixed with

same volume of 2X β-galactosidase Assay Buffer (200mM sodium phosphate buffer (pH 7.3), 2mM $MgCl_2$, 100mM β-mercaptoethanol, 1.33mg/ml ONPG) and incubated at 37°C for 1h until faint yellow color was obtained. The reactions were stopped by adding 150 µl of 1M sodium carbonate and the absorbance of samples was read at 410 nm.

2.17 Vectors Used in This Study

For the reporter gene assays, PGL3 (Promega, USA) vectors was used to evaluate the transcriptional activities of NF-κB and C/EBPβ. Also empty vector and mutated counterparts of the vectors were used. Description of vectors in detail was given in Appendix A.

To determine the UTR activities, p-MIR-REPORT (Ambion, USA) vectors were used and intended UTR regions of the candidate genes were also cloned into the same backbone. Mutated and empty vector counterparts were also used as controls. Detailed information was given in Appendix A.

pSV-beta-galactosidase commercial β-galactosidase vector (Promega, USA) was used for normalization in reporter gene assays.

Forced expression of the *microRNA-146a* (*miR-146a*) was sustained with P-SUPER vector (Oligoengine, USA). Mutated and empty vectors were also used as controls. Description of the vectors and preparation were given in Appendix A and C.

All transfections were done with Lipofectamine and Plus reagents (Invitrogen, USA) as transfection agents. Per one microgram of vector 10µl of each transfection agent was used in transfection studies. For that purpose culture media were replaced with fresh serum free OPTI-MEM (Gibco, USA), vectors were prepared in required amounts in same medium along with plus reagent and incubated for 15 minutes at room temperature. Lipofectamine was prepared in a different tube and incubated at room temperature for 15 minutes. Subsequently, two tubes were mixed and required volume from the transfection mix was added drop-wise to the cells.

CHAPTER 3

RESULTS AND DISCUSSION

Section I: ICAM-1 and VCAM-1 Regulation in Dfferentiating Caco-2 Cells.

Caco-2 cells are a well established model to study enterocyte differentiation, with the cells showing characteristic brush border membranes, dome like structure and expression of specific differentiation markers. However, in spite of these cells' widespread use as models for enterocyte differentiation, these are malignant cells with mutated p53, APC, β-catenin and Smad4 (Gayet *et al.,* 2001)

3.1 Confirmation of Spontaneous Differentiation in Caco-2 Cells

3.1.1 Alkaline Phosphatase Activity

During the course of differentiation Caco-2 cells express the phenotypic features of differentiation such as brush border membrane associated hydrolases and alkaline phosphatase. Among these enzymes, alkaline phosphatase is a well known differentiation marker for enterocytes (Chantret *et al*., 1988). For that reason alkaline phosphatase enzymatic activity was measured from total protein

extracts of Caco-2 cells in order to confirm the differentiation after reaching confluency (Figure 3.1), as described in the materials and methods section.

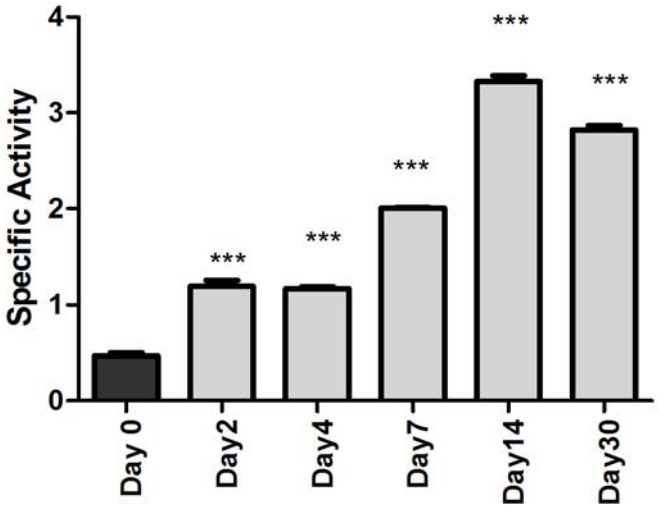

Figure 3.1: Alkaline Phosphatase Enzymatic Activity During Differentiation of Caco-2 Cells. (Day 0- Day 30 indicate days of Caco-2 cells grown after post confluency, protein samples were collected on designated days (without any phosphatase inhibitor). The data are displayed with mean ± standard deviation of three replicates. All differentiated cells (Day 2- Day 30) showed significantly higher ($p<0.0001$) alkaline phosphatase activity compared to undifferentiated confluent Day 0 cells.

As can be observed from Figure 3.1, alkaline phosphatase enzymatic activity was significantly higher in post confluent Caco-2 cells validating the occurrence of spontaneous differentiation. Wang *et. al*., demonstrated that the Caco-2 cells line exhibited decreased expression of differentiation marker after 21

days of post confluent cultures. In our system, a similar pattern was observed in which alkaline phosphatase activity decreased after day 14.

3.1.2 Sucrase-Isomaltase Gene Expression during Differentiation of Caco-2 cells

Further validation of differentiation was carried out by determining the expression levels of selected genes in post confluent Caco-2 cells. Of these, *sucrase-isomaltase* is a well known differentiation marker (Neutra M, 1989). cDNA was prepared from the RNA samples obtained from post confluent Caco-2 cells in different time intervals and RT-PCR was performed (Figure 3.2) as described elsewhere.

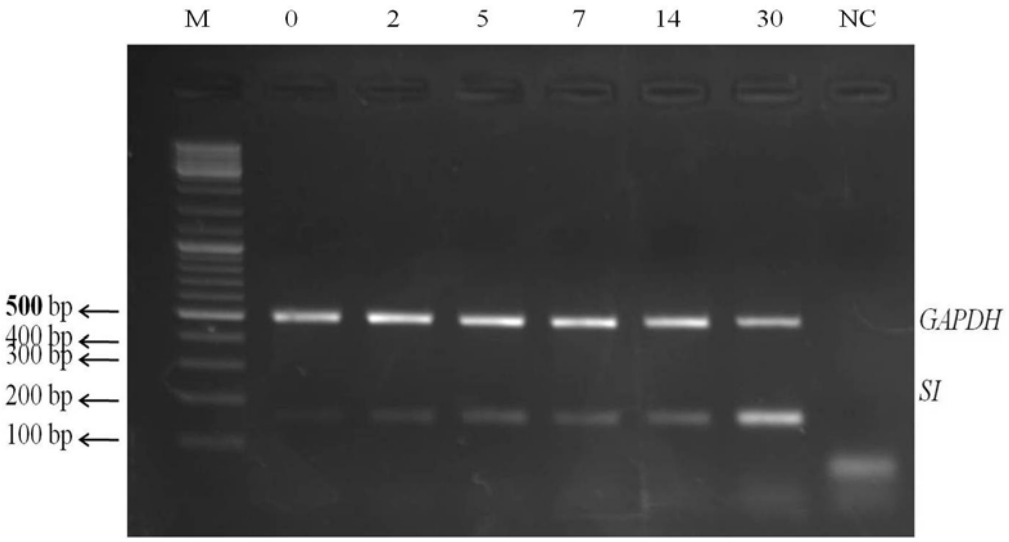

Figure 3.2: *Sucrase-Isomaltase* Expression in Spontaneously Differentiating Caco-2 Cells. Lanes: M: Marker-GeneRuler™ DNA Ladder Mix (Fermentas), 0-30: Days after post confluency, NC: Negative Control. cDNAs were synthesized from 2µg DNAse I treated RNA by using oligo dT primer.

As can be observed from Figure 3.2, Caco-2 cells showed an increase in *sucrase-isomaltase* expression during spontaneous differentiation, which further supports the occurrence of differentiation. Sucrase-isomaltase expression is regulated by a number of different transcription factors including HNF1α, Cdx2 and GATA-4 (Boudreau *et al.,* 2002). Recently it has been shown that the increase in the mRNA expression of *sucrase-isomaltase* genes during intestinal differentiation requires Histone H3 modifications including methylation of the lysine 9 and di-acetlyation of lysine 9/14 after which the binding of CDX-2 to sucrase-isomaltase promoter was shown (T. Suzuki *et al.,* 2008)

3.1.3 Expression of p21 During Differentiation of Caco-2 cells

p21 is known to be a cyclin dependent kinase inhibitor, which is involved in the G1 phase of the cell cycle and is known to inhibit cyclin CDK 2 and 4.

Since Caco-2 cells cease to proliferate during the course of differentiation, *p21* expression in the course of differentiation was monitored by RT-PCR (Figure 3.3).

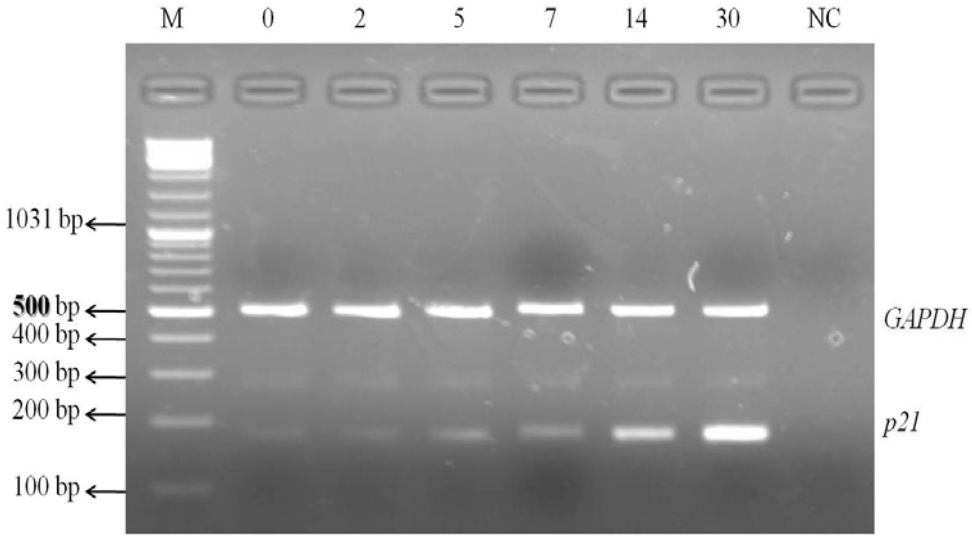

Figure 3.3: *p21* Expression During Spontaneous Differentiation of Caco-2 Cells. Lanes: M: Marker; GeneRuler™ DNA Ladder Mix (Fermentas), 0-30: Days after post confluency, NC: Negative Control. cDNAs were synthesized from 2µg DNAse I treated RNA by using oligo dT primer.

After the RT-PCR analysis, elevated *p21* expression was observed in Caco-2 cells undergoing spontaneous differentiation. p21 which interacts with the D-type cyclins, cyclin E, and Cdk2, causing an irreversible growth arrest (Tian & Quaroni 1999). Although the exact molecular mechanism has not been established yet, p21 induction during differentiation was thought to be under the mediation of Kruppel Like Transcription Factor 4 (KFL4), which was induced by sulforaphane (4-methylsulfinylbutyl isothiocyanate, a dietary compound derived from broccoli) treated Caco-2 cells (Traka *et al.,* 2009).

3.2 VCAM-1 and ICAM-1 Expression in Spontaneously Differentiating Caco-2 cells

Immunoglobin superfamily proteins ICAM-1 and VCAM-1 which are target genes of NF-κB (Xia *et al.,* 2001) are known to be regulated via cytokines and their expression is increased during an inflammatory response (Lawson and Wolf, 2009). Cancer cells not only exhibit abnormalities in CAM expression and cell-to cell interactions, but they also acquire new adhesive properties (Kobayashi *et al*., 2007). In the tumor cell extravasation process, these cells attach to the vascular endothelial cells via integrins mediating the adhesion to ICAM-1 and VCAM-1. In a recent study, colonocytes obtained from patients with bowel and colon neoplasms were seen to have higher ICAM-1 expression (Vainer *et al*., 2006b), which may be involved in tumor adhesion and peritoneal metastasis (Ziprin *et al*., 2003). In addition, VCAM-1 was found to be required for ther interaction of gastric cells with gastric fibroblasts in gastric cancers (Semba *et al*., 2009). The effects of ICAM-1 and VCAM-1 on cell phenotype has being studied in several different cancer types, however, their regulation in spontaneous differentiation of the colon is not entirely known.

We have therefore examined the expression of *VCAM1* and *ICAM1* in spontaneously differentiating Caco-2 cells. For this purpose RNA was isolated from Caco-2 cells collected at predetermined days, converted to cDNA and semiquantitative PCR was carried out (Figures 3.4 and 3.5).

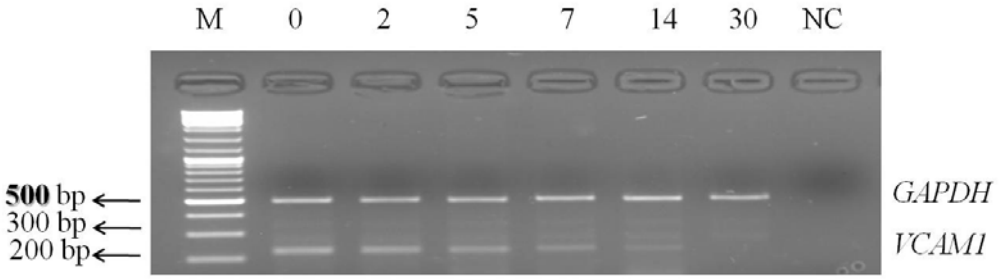

Figure 3.4 *VCAM1* Expression in Spontaneously Differentiating Caco-2 Cells. Lanes: M: Marker; GeneRuler™ DNA Ladder Mix (Fermentas), 0-30: Days after post confluency, NC: Negative Control. cDNAs were synthesized from 2µg DNAse I treated RNA by using oligo dT primer

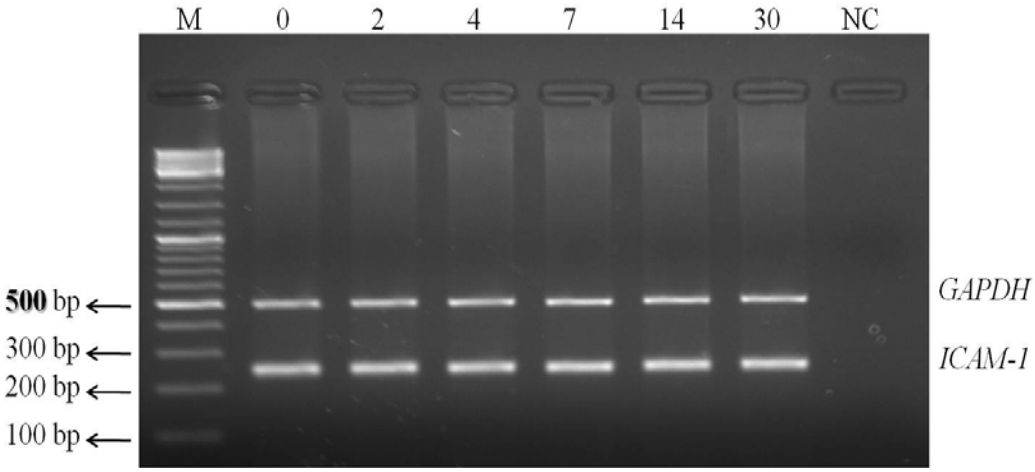

Figure 3.5 *ICAM1* Expression in Spontaneously Differentiating Caco-2 Cells. Lanes: M: Marker; GeneRuler™ DNA Ladder Mix (Fermentas), 0-30: Days after post confluency, NC: Negative Control. cDNAs were synthesized from 2µg DNAse I treated RNA by using oligo dT primer

As shown in Figures 3.4 and 3.5, the expression of *VCAM1* was found to decrease in the course of spontaneous differentiation. However, surprisingly, the expression of *ICAM1*, which is regulated in a similar manner to *VCAM1*, was found to be stable in the course of differentiation.

The protein expression of ICAM-1 and VCAM-1 were next examined by Western blot to determine whether they correlated with their respective transcript levels. Total proteins were extracted from differentiating Caco-2 cells on pre-designated days of differentiation with 1X Cell Lysis Buffer (Stratagene) according to the manufacturer's instruction with the addition of Nonidet-P40 in order to increase the amount of membrane bound protein extraction. Subsequently, the proteins were separated by 12% SDS-PAGE under denaturing conditions and transferred to a PVDF membrane and probed against ICAM-1 and VCAM-1 proteins (Figure 3.6 and 3.7). As loading controls, GAPDH protein was probed on the same membrane after stripping.

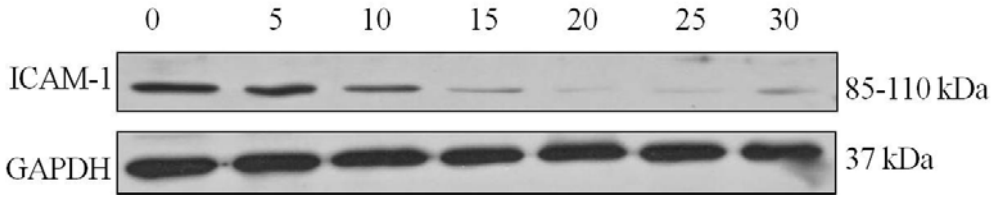

Figure 3.6: ICAM-1 Protein During Spontaneous Differentiation of Caco-2 Cells. Lanes: 0-30: Days after reaching 100% confluency. 80µg of proteins from each sample was loaded and transferred on PVDF membrane at 100V for 1 hour 45 minutes, 5% Skim milk in PBST was used as blocking agent. Antibody Dilutions: Anti-ICAM-1 1:500, Anti-GAPDH 1:1000, Anti-Rabbit-HRP 1:3300; All incubations were carried out at room temperature for 1 hour with gentle agitation in the presence of blocking agent. Proteins were probed against GAPDH as loading control after stripping.

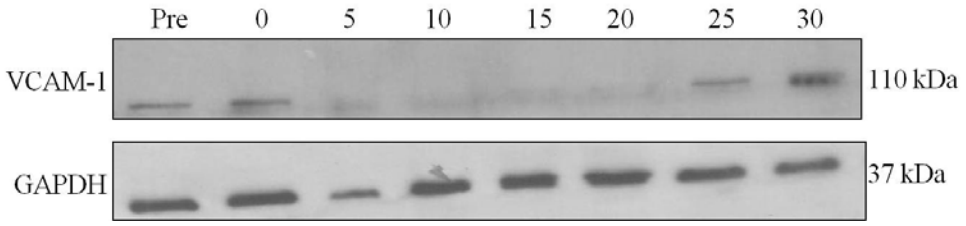

Figure 3.7: VCAM-1 Protein During Spontaneous Differentiation of Caco-2 Cells. Lanes: Pre: Preconfluent; Cells harvested before reaching 100% confluency, 0-30: Days after reaching 100% confluency. 80µg of proteins from each sample was loaded and transferred on PVDF membrane at 100V for 1 hour 45 minutes, 5% Skim milk in PBST was used as blocking agent. Antibody Dilutions: Anti-VCAM-1 1:250, Anti-GAPDH 1:1000, Anti-Rabbit-HRP 1:3300; All incubations were carried out at room temperature for 1 hour with gentle agitation in the presence of blocking agent except Anti-VCAM-1 (overnight at 4°C without agitation) Proteins were probed against GAPDH as loading control after stripping.

The Western blot results for ICAM-1 indicated that the ICAM-1 protein level decreased during the course of spontaneous differentiation of Caco-2 cells (Figure 3.6). This was unexpected, since the *ICAM1* gene expression was stable in the differentiated cells. On the other hand, VCAM-1 protein exhibited a decrease in protein expression up to the 20th day after reaching confluency (Figure 3.7). This correlated with the decreased mRNA expression observed in the differentiated cells (Figure 3.4). The recovery of VCAM-1 expression in the 25th and 30th days of differentiation might be due to the recovery of NF-κB activity on later days of differentiation.

We, therefore, wanted to determine the effect of differentiation in the regulation of these genes at three levels:

1. Transcriptional – involvement of transcription factors

2. Post transcriptional – involvement of microRNAs
3. Post-translational – involvement of protein degradation pathways

3.3 Transcriptional regulation of *ICAM1* and *VCAM1*

The expression of both *ICAM1* and *VCAM1* are regulated by the inflammatory transcription factor NF-κB (Xia *et al.,* 2001). We therefore wanted to determine the transcriptional activation of NF-κB in Caco-2 cells in the course of spontaneous differentiation.

3.3.1 NF-κB Activity in Differentiating Caco-2 Cells

NF-κB is normally held inactive in the cytoplasm by Inhibitor of kappa B (IκB). In the presence of a stimulus, signaling pathways are activated which eventually leads to the phosphorylation of IκB by Inhibitor of kappa B kinase (IKK) causing the former to be ubiquitinated and degraded in the cytoplasm. NF-κB (most commonly formed of the subunits p65 and p50) is then free to enter the nucleus, bind to its consensus sequence and enable the transcription of its target genes (H L Pahl 1999).

Therefore, in the course of spontaneous differentiation of Caco-2 cells, we have looked three different aspects of NF-κB activation:

1. Phosphorylation status of IκB and the nuclear and cytoplasmic distribution of NF-κB using Western blot.

2. DNA binding studies including electrophoretic mobility shift assay (EMSA), an ELISA based colorimetric assay and chromatin immunoprecipitation (ChIP).

3. Transcriptional activity by reporter gene assays.

1. Nuclear translocation of NF-κB

Total and fractionated proteins were extracted from spontaneously differentiating Caco-2 cells and were subjected to Western blot analysis against NF-κB and IκBα proteins (Figures 3.8, 3.9 and 3.10). TopoIIβ and β-actin antibodies were used as both loading and to ensure the lack of cross contamination between nuclear and cytoplasmic proteins.

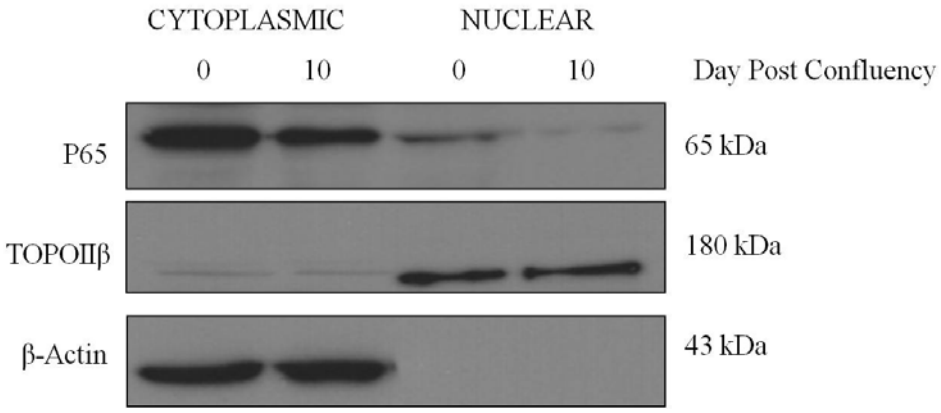

Figure 3.8: NF-κB p65 Nuclear Translocation in Spontaneously Differentiating Caco-2 Cells. Lanes: 0-10: Days after reaching 100% confluency. 80µg of proteins from each sample was loaded and transferred on PVDF membrane at 100V for 1 hour 45 minutes, 10% Skim milk in PBST was used as blocking agent. Antibody Dilutions: Anti-p65 1:250, Anti-β-Actin1:1000, Anti-TopoIIβ 1:200 Anti-Mouse-HRP 1:2000; All primary antibody incubations were carried out at 4°C overnight in the presence of blocking agent except secondary antibody (room temperature 1h with gentle agitation).

As shown in Figure 3.8, a decrease in the nuclear levels of NF-κB p65 protein in Caco-2 cells on the 10th day after reaching confluency can be seen when compared to Day 0 after reaching confluence. Additionally, there also appears to be an overall decrease in the p65 protein levels in the differentiated cells which might be due to the downregulation of NF-κB during differentiation.

When the nuclear and cytoplasmic proteins were probed with an antibody against the p50 protein, a similar decrease in the nuclear translocation of p50 was also observed in the course of spontaneous differentiation (Figure 3.9).

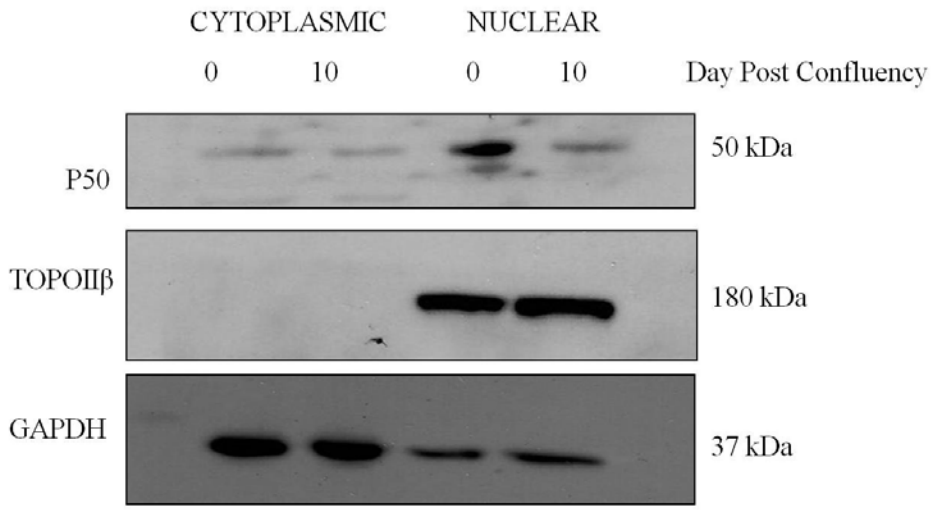

Figure 3.9: NF-κB p50 Nuclear Translocation in Spontaneously Differentiating Caco-2 Cells. Lanes: 0-10: Days after reaching 100% confluency. 80μg of proteins from each sample was loaded and transferred on PVDF membrane at 100V for 1 hour 45 minutes, 10% Skim milk in PBST was used as blocking agent. Antibody Dilutions: Anti-p50 1:500, Anti-GAPDH:1000, Anti-TopoIIβ 1:200 Anti-Mouse-HRP 1:2000, Anti-Rabbit-HRP 1:2000; All primary antibody incubations were carried out at 4°C overnight in the presence of blocking agent except secondary antibodies (room temperature 1h with gentle agitation)

Additionally, we determined the phosphorylation status of the IκBα protein in the cytoplasm from protein extracts obtained from post confluent Day 0 and Day 10 Caco-2 cells (Figure 3.10).

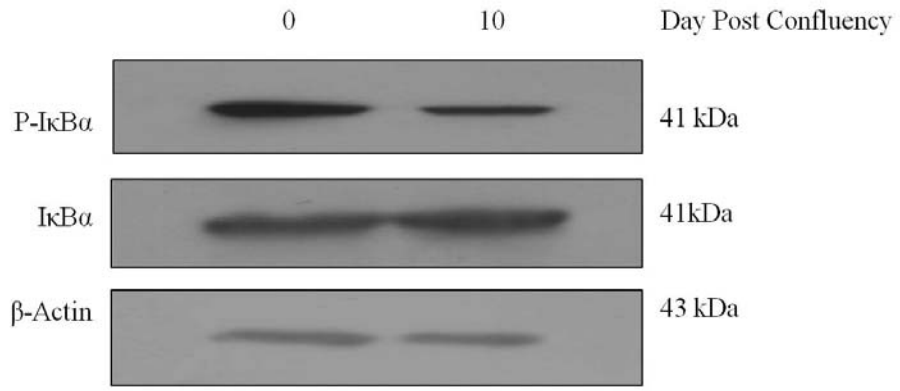

Figure 3.10: IκBα and phospho-IκBα Proteins in Spontaneously Differentiating Caco-2 Cells. Lanes: 0-10: Days of after reaching 100% confluency. 80µg of proteins from each sample was loaded and transferred on PVDF membrane at 100V for 1 hour 45 minutes, 10% Skim milk in PBST was used as blocking agent. Antibody Dilutions: Anti-p-IKBα 1:500, Anti-IKBα 1:500, Anti-β-Actin 1:1000 Anti-Mouse-HRP 1:2000, Anti-Rabbit-HRP 1:2000; All primary antibody incubations were carried out at 4°C overnight in the presence of blocking agent except secondary antibodies (room temperature 1h with gentle agitation).

As seen in Figure 3.10, a decrease in the phosphorylation of IκBα was observed in the Day 10 cells compared to the Day 0 cells. This indicates a decrease in the degradation IκBα, and further confirms the retention of NF-κB in the cytoplasm of the differentiated cells.

Since differentiation of enterocytes is associated with a decrease in the proliferation rate, lesser NF-κB (which has mitogenic properties) nuclear translocation and subsequent activation during the differentiation process might be expected. A possible molecular mechanism underlying this phenomenon might be by the transcriptional activation of cyclin D1 by NF-κB, thereby enhancing the progress of the cell cycle from G1 to S phase (Guttridge *et al.,* 1999).

2. DNA binding ability of NF-κB in differentiating Caco-2 cells

To determine if decreased translocation of NF-κB to the nucleus correlated with decreased DNA binding activity, we performed Electrophoretic Mobility Shift Assays (EMSA)

Electrophoretic mobility shift assay (EMSA)

This assay is based on the principle of differences in mobility of DNA when bound to protein, compared to free DNA. Biotinylated oligonucleotides containing the NF-κB consensus sequence was incubated with nuclear extracts from Day 0 and Day 10 post confluent Caco-2 cells, separated on a polyacrylamide gel, transferred to a nylon membrane and photographed as indicated in Materials and Methods (Figure 3.11).

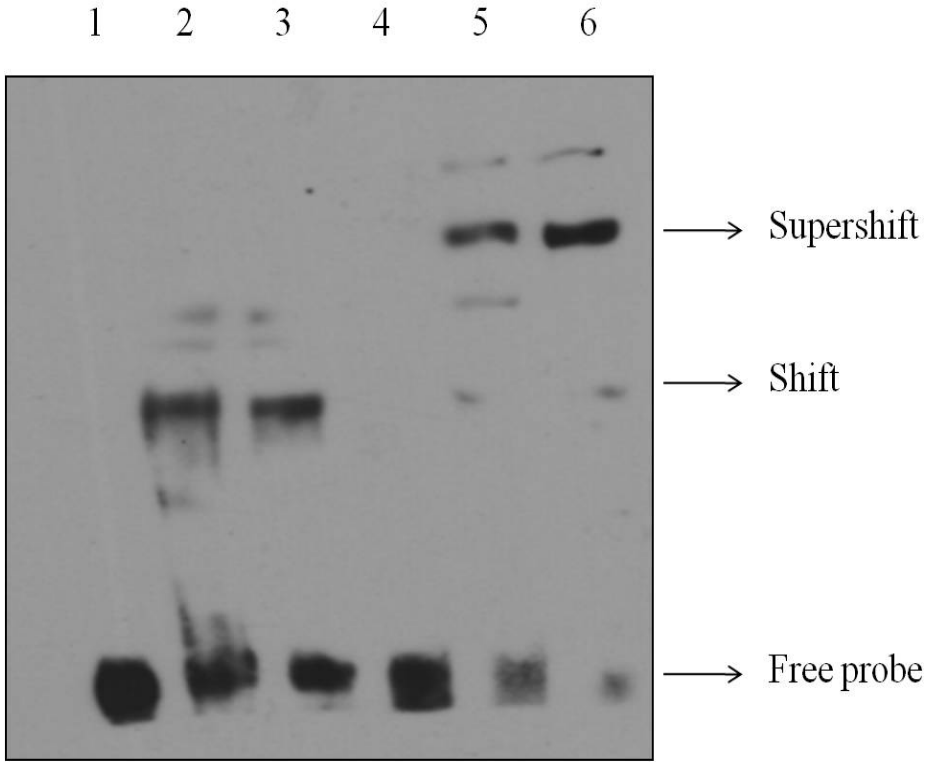

Figure 3.11 EMSA of NF-κB in Spontaneously Differentiating Caco-2 Cells. (Lanes: 1: Free probe, 2: Day 0, 3: Day10, 4: Day 0 + cold probe, 5: Day0 + αp65, 6: Day 0 + αp50). For all binding reactions 5µg of the nuclear extracts obtained from designated days were used. Binding reactions were prepared and incubated on ice for 10 minutes and at room temperature for 20 min after which the oligos and antibodies against the protein of interest (1-3µl) were added and incubated for a further 10 min at room temperature. Samples were separated in 8% polyacrylamide gel prepared with TBE transferred on to a nylon membrane (Biodyne, precut B Nylon membrane, Pierce, USA) for 45 minutes at 4°C. After crosslinking membranes were treated according to the instructions of the manufacturer.

The data indicated a decrease in DNA binding of NF-κB from Day 0 to Day 10 post confluent Caco-2 cells. Control reactions included incubation with a 200 fold excess of 'cold' unlabeled probe (lane 4) showing a decrease in the shifted signal. Additionally, incubation of the complex with antibodies against

p50 and p65 resulted in a super shift of the protein, DNA, antibody complex, further confirming the specificity of the reaction.

DNA binding ELISA assay

DNA binding activity of NF-κB was further confirmed with the help of an ELISA based NF-κB human p50/p65 combo transcription factor assay kit (Cayman, USA). For this, nuclear extracts obtained from Day 0 and Day 10 confluent Caco-2 cells were applied onto wells of a 96 well that was pre-coated with oligonucleotides containing the NF-κB consensus sequence. After the application of the protein sample (10µl, 5µg), the wells were incubated with the p50 or p65 antibody (provided in the kit). After the incubation periods and washing steps, reagents to develop the HRP signal were added and plates were read at 570 nm. To confirm the specificity of the reaction, the NF-κB inhibitor SN50 was also used (50µg/ml) on 0 day confluent cells (Figure 3.12). As controls, blanks were prepared without any added protein samples. In some wells antibodies against p50 and p65 were added in the absence of protein samples as a control for non-specific binding. Pure NF-κB proteins, provided in the kit, were used as positive controls. The final DNA binding capacity of NF-κB in the course of differentiation of Caco-2 cells was determined on the basis of the standard curve.

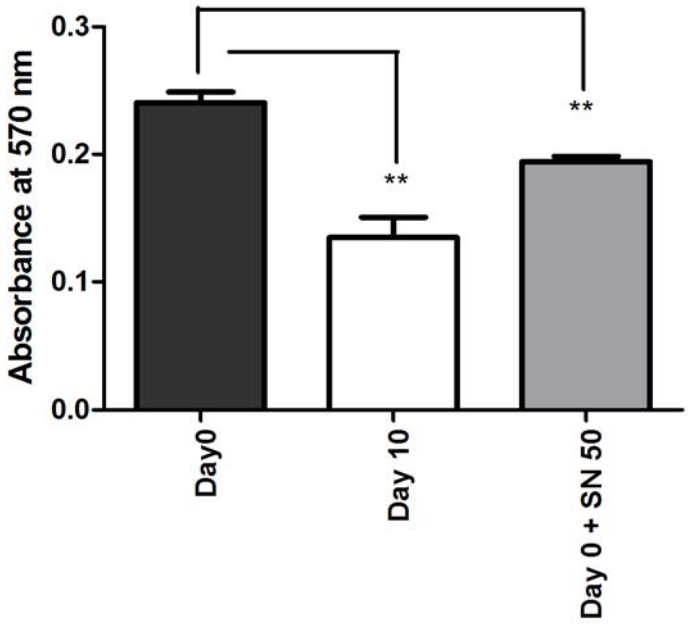

Figure 3.12 NF-κB p65 ELISA Showing Reduced p65 DNA Binding *in-vitro*. (Day 0- Day 10 indicate days of Caco-2 cells grown after post confluency, nuclear protein samples were collected on designated days. Day 0 confluent cells were treated with SN 50 as NF-κB inhibitor (50µg/ml) for 24 hours. 5µg of protein was used for the assay. The data are displayed with mean ± standard deviation of three replicates. Differentiated Day 10 cells showed significantly lower p65 DNA binding activity ($p = 0.0043$) compared to Day 0 (black bar). SN 50 (gray bar) treatment showed significant decrease in p65 DNA binding activity ($p= 0.0085$) compared to untreated Day 0 cells.

As can be observed from Figure 3.12, p65 DNA binding activity decreased significantly (**$p<0.05$) in the differentiated Caco-2 cells. Treatment of the confluent undifferentiated cells with SN50 also significantly reduced the NF-κB DNA binding activity (** $p<0.05$), further testing the specificity of the reaction.

Same experiment performed for the p50 protein as well (Figure 3.13) exhibited a similar pattern to p65.

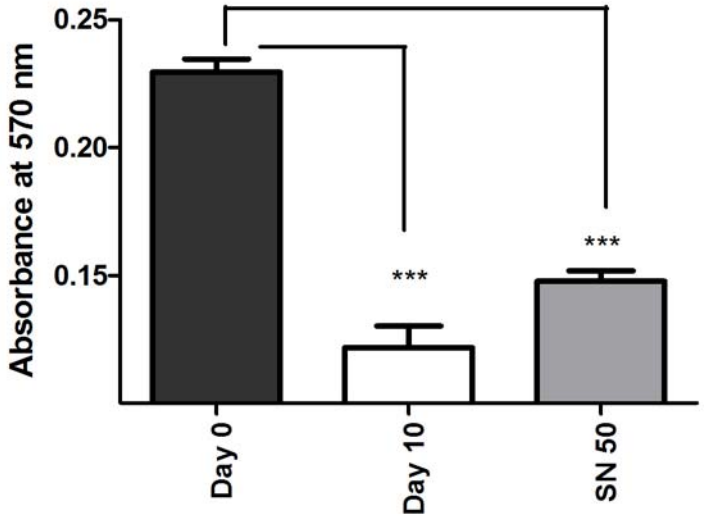

Figure 3.13 NF-κB p50 ELISA Showing Decreased DNA Binding of p50 Protein *in-vitro*. Day 0- Day 10 indicate days of Caco-2 cells grown after post confluency, nuclear protein samples were collected on designated days. Day 0 confluent cells were treated with SN50 as NF-κB inhibitor (50µg/ml) for 24 hours. 5µg of protein was used for the assay. The data are displayed with mean ± standard deviation of four replicates. Differentiated Day 10 cells (white bar) showed significantly lower p50 DNA binding activity ($p < 0.0001$), compared to Day 0 (black bar). SN 50 treatment (gray bar) showed significant decrease in 50 DNA binding activity ($p < 0.0001$), compared to untreated Day 0 cells (black bar).

The DNA binding of the p50 protein was also significantly (***$p < 0.001$) reduced from Day 0 to Day 10 day in post confluent Caco-2 cells (Figure 3.13). Overall, the EMSA and ELISA data indicate that NF-κB p65 and p50 proteins obtained from 0 day confluent Caco-2 cells had reduced DNA binding *in-vitro* compared to the samples obtained from 10 day confluent cells.

Chromatin Immunoprecipitation (ChIP) Assay

In order to gain detailed information about the recruitment of NF-κB to the promoter of *ICAM1* and *VCAM1*, chromatin immunoprecipitation (ChIP) assays were performed. In this assay, the promoter regions are expected to be immunoprecipitated only when the intended transcription factor is available and binding to the target consensus sequence in the promoter being investigated. The *ICAM1* promoter has NF-κB binding sites within bases 821-831 and 1161-1171, where 1386th base is the translation initiation site (Roebuck & Finnegan 1999). The VCAM-1 promoter has an NF-κB binding sites located at -77 and -63 of the promoter (Iademarco *et al.,* 1992). Post confluent Caco-2 cells were grown for 0 or 10 days and genomic DNA was immunoprecipitated by using an NF-κB p65 (Santa Cruz, USA) antibody as described in Materials and Methods. Additionally, for each ChIP experiment, 100µl from each sample were taken before the addition of the antibodies and labeled as "input" control. They were used as positive controls for the amplification reactions.

The precipitated DNA was subjected to PCR amplification with the primers designed to amplify the intended NF-κB elements in the promoters of *ICAM1* and *VCAM1*. Primers were also designed to amplify the upstream regions (without any transcription factor binding sites) of each promoter to evaluate the specificity of the immunoprecipitation reaction (Figure 3.14 and Figure 3.15)

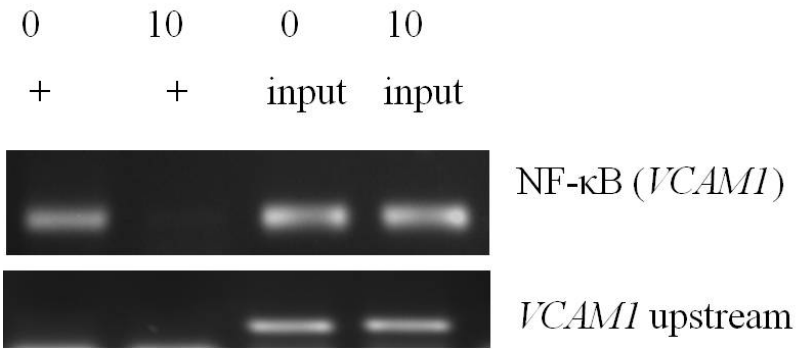

Figure 3.14 Amplification of the NF-κB Element in the *VCAM1* Promoter After ChIP with p65 in Spontaneously Differentiating Caco-2 Cells (+: NF-κB p65 antibody). For each assay, a total of 100% confluent cells were fixed, sonicated and after an aliquot (input control) was taken, equal protein amount containing samples were incubated with p65 antibody at 4°C for 1 hour with gentle agitation in protein A-agarose containing spin filter columns (NAb spin columns, Pierce).

PCR was carried out with both immunoprecipitated and control samples semiquantitatively in an Applied Biosystems PCR machine followed by separation on a 2% agarose gel, and quantitatively on a Corbett Real Time PCR machine using the primers described in the Materials and Methods Section.

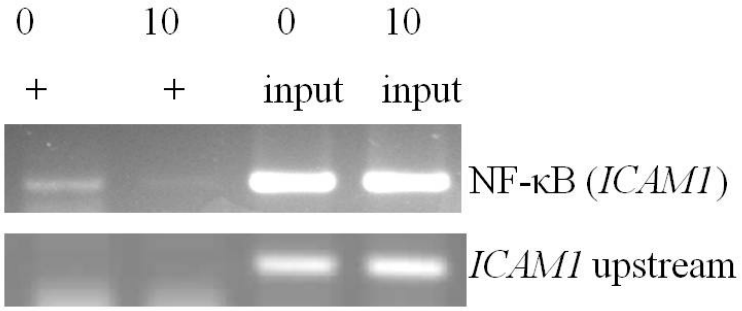

Figure 3.15 Amplification of the NF-κB Element in the *ICAM1* Promoter after ChIP with p65 in Spontaneously Differentiating Caco-2 Cells (+: NF-κB p65 antibody) For each assay, a total of 100% confluent cells were fixed, sonicated and after an aliquot (input control) was taken, equal protein amount containing samples were incubated with p65 antibody at 4°C for 1 hour with gentle agitation in protein A- agarose containing spin filter columns (NAb spin columns, Pierce).

In the samples immunoprecipitated with the NF-κB p65 antibody, it was observed that NF-κB recruitment by *ICAM1* and *VCAM1* promoters were decreasing in differentiated cells (Figures 3.14 and 3.15).

In order to further confirm the phenomenon described above, the precipitated chromatin was amplified by real time PCR using a Fast Start real time PCR mastermix (Roche) kit in a 20µl reaction volume (Figure 3.16 and 3.17).

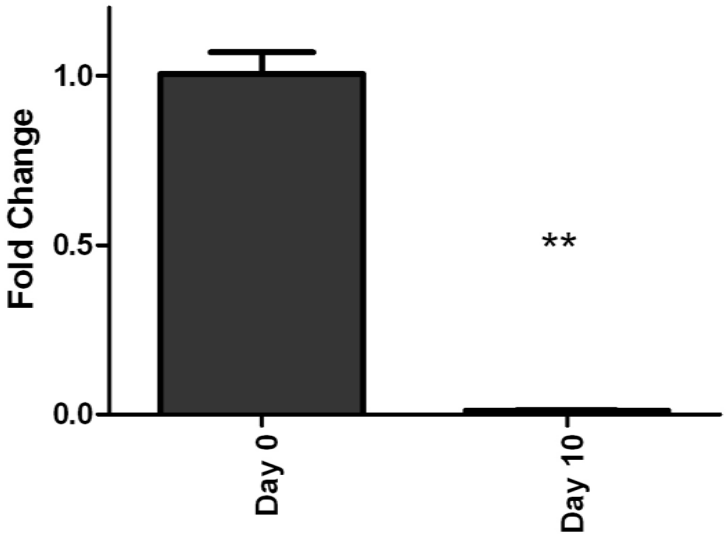

Figure 3.16 Real Time Amplification of the NF-κB Element on the *ICAM1* Promoter. Day 0- Day 10 indicate days of Caco-2 cells grown after post confluency). The data are displayed with mean ± standard deviation of three replicates. Differentiated day 10 cells showed significantly lower NF-κB recruitment ($p = 0.00043$) compared to Day 0 (black bar).

As can be seen from the Figure 3.16, NF-κB recruitment to the *ICAM1* promoter during differentiation of Caco-2 cells was significantly reduced. We next wanted to determine whether a similar effect was seen for the *VCAM1* promoter. For this, first a standard curve was obtained with the different dilutions of the DNA sample obtained from the Day 0 confluent cells subjected to immunoprecipitation with the p65 antibody.

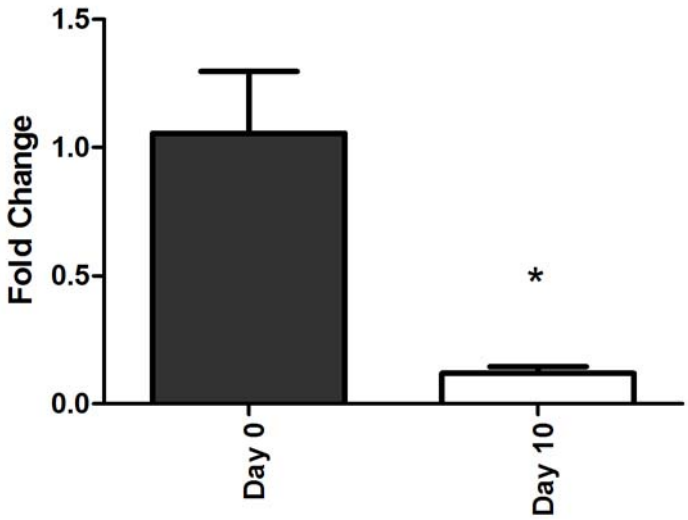

Figure 3.17 Real Time Amplification of the NF-κB Element on the *VCAM1* Promoter. Day 0- Day 10 indicate days of Caco-2 cells grown after post confluency, The data are displayed with mean ± standard deviation of three replicates. Day 10 differentiated cells (white bar) exhibited significantly lower NF-κB recruitment to the *VCAM1* ($p = 0.0179$) compared to the 0 day confluent cells (black bar).

As can be seen from Figure 3.16 and Figure 3.17 NF-κB could bind to the promoters of both *ICAM1* and *VCAM1* in the confluent but undifferentiated Caco-2 cells. However, once the cells were differentiated, NF-κB recruitment to the promoters was found to decrease significantly (* $p< 0.05$). This also corroborates with the decreased DNA binding observed by EMSA and ELISA assays.

3. Transcriptional Activity of NF-κB in Differentiating Caco-2 Cells

Reporter Gene Assays

In order to determine the transcriptional activity of NF-κB during spontaneous differentiation of Caco-2 cells, reporter gene assays were performed with spontaneously differentiating Caco-2 Cells. For that purpose three copies of the NF-κB p65 consensus sites were cloned into the pGL3 vector as described in the Materials and Methods Section. The empty pGL3 vector and vector inserted with a mutated sequence of the NF-κB binding sequence (sequences are shown in Appendix N) were used as controls. The NF-κB vectors, along with a β-gal vector for normalization were co-transfected into the spontaneously differentiating Caco-2 cells on Day 0 and Day 10 after reaching confluency. Although the transfection process via the cationic lipid polymers may induce inflammatory response of the cells (Zhang *et al*., 2007), day 0 and day 10 cells were transfected and harvested at the same time to minimize the transfection agent induce variations. The cells were lysed using a 1X Cell Lysis buffer (Stratagene, USA) and luciferase activity in the protein samples were analyzed in a luminometer. ß-galactosidase activity was used for normalization and the data were reported as Relative Light Units (RLU) (Figure 3.18).

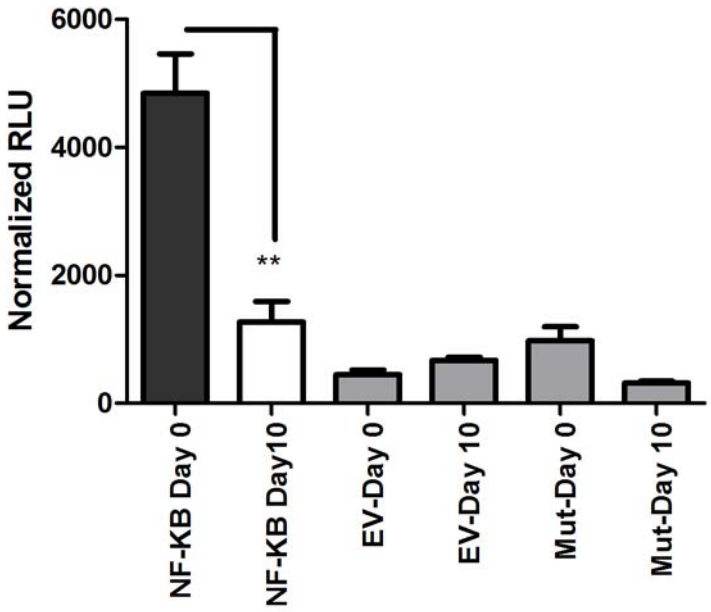

Figure 3.18: NF-κB Reporter Gene Assay in Differentiating Caco-2 Cells. 0 Day (black bar) and 10 day (open gray bar) confluent Caco-2 cells were transfected with NF-κB plasmids (NF-κB), NF-κB mutated plasmids (Mut) or Empty PGL3 reporter vector (EV) 24 hours post-transfection, proteins were extracted with 1X CLB buffer and luciferase activities were measured with 20µl of the extracts. Beta–galactosidase activity was used for normalization. The data are displayed with mean ± standard deviation of three replicates. NF-κB activity of the 10 day confluent (white bar) cells were significantly lower ($p=0.0066$) than day 0 confluent cells (black bar).

As shown in Figure 3.18, NF-κB activity was significantly (** $p< 0.05$) reduced during spontaneous differentiation of Caco-2 cells when compared to the empty vector and mutated vector samples. This corroborates with the decreased nuclear translocation and DNA binding of NF-κB, indicating an overall decrease in NF-κB activity in differentiated Caco-2 cells.

In order to further confirm that the results obtained were specific to NF-κB, confluent undifferentiated Day 0 Caco-2 cells (which have high NF-κB activity) were transfected with the reporter plasmids and necessary controls, treated with a panel of NF-κB inhibitors, and analyzed for transcriptional activity (Figure 3.19).

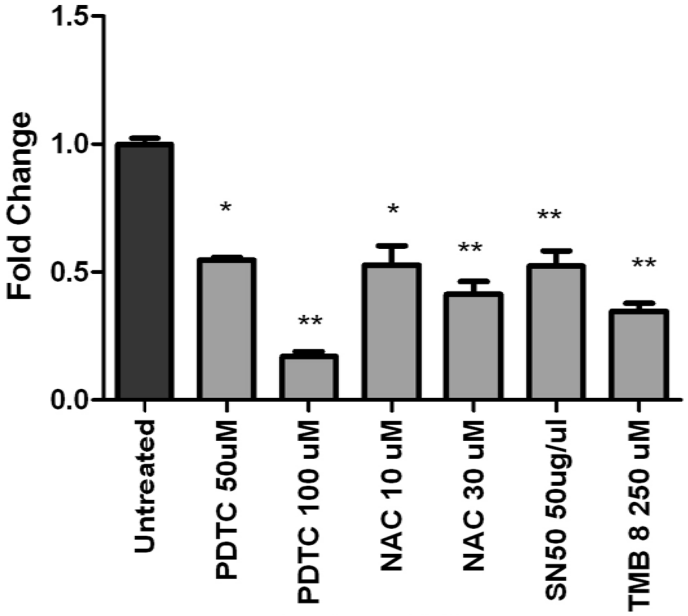

Figure 3.19: NF-κB Reporter Gene Assay with NF-κB Inhibitors. 0 Day (black bar) confluent Caco-2 cells were transfected with NF-κB plasmids (NF-κB), 4 hours post-transfection, transfected cells were treated with inhibitors (grey bars). 18 hours post-treatment cells were harvested with 1X CLB buffer and luciferase activities were measured with 20µl of the extracts. Beta –galactosidase activity was used for normalization. The data are displayed with mean ± standard deviation of three replicates. All treated cells (gray bars) showed significantly lower ($p<0.005$) NF-κB activity compared to undifferentiated confluent Day 0 cells (black bar).

As can be seen from Figure 3.19, incubation of the Caco-2 cells with the inhibitors resulted in a significant inhibition of NF-κB transcriptional activity. Pyrollidine dithiocarbamate (PDTC) showed a dose dependent inhibition of NF-κB between 50-100μM concentrations. The mechanism of action of PDTC has been shown to be through the inhibition of IκBα activation (S. F. Liu *et al.,* 1999). Similarly N-acetyl-cysteine (NAC) is known to inhibit the NF-κB activity by targeting the IκBα and IκBβ (Oka 2000) and it also exhibited a similar down-regulation of NF-κB activity. SN50 is a synthetic peptide, which contains a hydrophobic cell permeable motif with mutated nuclear localization signal on it that binds to NF-κB p50 subunit and prevents the nuclear translocation of different NF-κB homo and heterodimers (Y.-Z. Lin 1995). Of interest, 8-(N, N-diethylamino) - octyl 3,4,5-trimethoxybenzoate (TMB-8), was also found to inhibit NF-κB activity. This chemical chelates the intracellular calcium released from the endoplasmic reticulum, which can activate NF-κB when there is an ER overload in the cell (H. L. Pahl 1996). We next determined whether TMB-8 can affect NF-κB DNA binding or the expression of the NF-κB target genes ICAM-1 and VCAM-1.

The effect of TMB-8 on the DNA binding activity of NF-κB was determined with the NF-κB DNA Binding ELISA kit as described previously. The data indicate that treatment of the confluent but undifferentiated Caco-2 cells (at Day 0) with 250μM TMB-8 resulted in a significant (***$p<0.0001$) decrease in the DNA binding capacity of p65 protein (Figure 3.20)

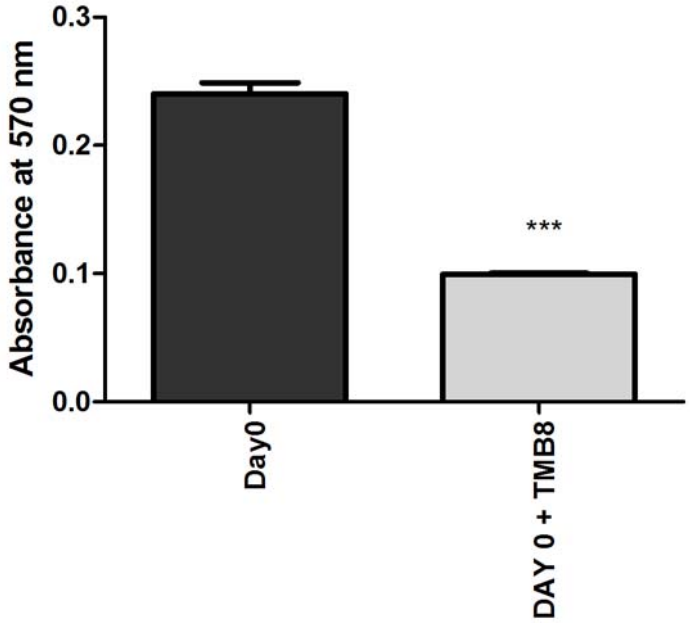

Figure 3.20: NF-κB DNA Binding Assay with TMB-8. Nuclear protein samples were collected on designated days. Day 0 confluent cells were treated with TMB-8 as NF-κB inhibitor (200 μM) for 24 hours. 5μg of protein was used for the assay. The data are displayed with mean ± standard deviation of three replicates. Treated cells (gray bar) showed significantly lower ($p<0.0001$) NF-κB activity compared to untreated cell (black bar).

In order to determine any effect of TMB-8 treatment on the expression of the NF-κB target genes ICAM-1 and VCAM-1, confluent undifferentiated Day 0 Caco-2 cells were treated with different concentrations of TMB-8 (100-200μM) and the cells were collected and processed for protein isolation and Western blot. The data (Figure 3.21) indicate the when the cells were treated with 200μM TMB-8, a decrease in the protein levels of both ICAM-1 and VCAM-1 could be

observed, most likely due to an inhibition of the expression of the genes owing to an inhibition of NF-κB activity.

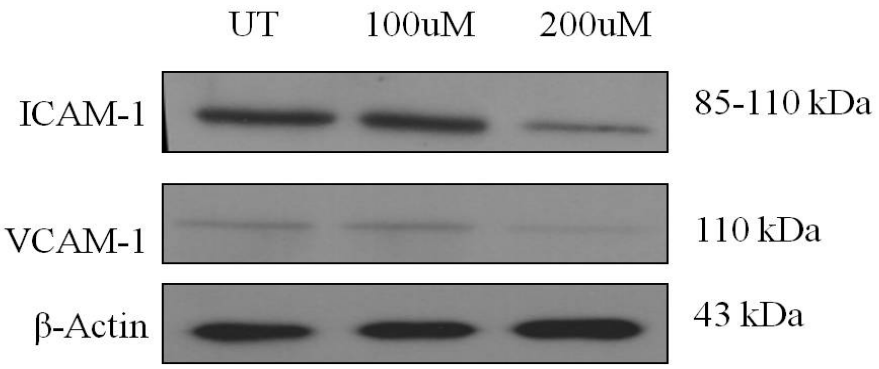

Figure 3.21: ICAM-1 and VCAM-1 Proteins of TMB-8 Treated Caco-2 Cells. (Lanes: UT: Untreated Day 0 Caco-2 cells, 100uM-200uM: Day 0 confluent cells treated with TMB-8 (100-200μM) for 24 hours. 80μg of proteins from each sample was loaded and transferred on PVDF membrane at 100V for 1 hour 45 minutes, 10% Skim milk in PBST was used as blocking agent. Antibody Dilutions: Anti-ICAM-1 1:500, Anti-VCAM-1 1:200, Anti-β-Actin1:1000, Anti-Rabbit-HRP and Anti-Mouse-HRP 1:2000; All primary antibody incubations were carried out at 4°C overnight in the presence of blocking agent except secondary antibodies (room temperature 1h with gentle agitation)

Having established that TMB-8 treatment and the consequent chelation of intracellular Ca^{++} could inhibit NF-κB DNA binding, transcriptional activity and expression of the target genes ICAM-1 and VCAM-1, we hypothesized that the regulation of NF-κB may be mediated by Ca with the possible involvement of a Ca activated protein kinase C (PKC).

3.3.2 Role of PKC in the Activation of NF-κB in Caco-2 cells

We used a nonradioactive Protein kinase C assay (Peptag, Non-Radioactive PKC Activity Assay Kit, Promega, USA) in order to determine whether the process of spontaneous differentiation in Caco-2 cells could affect PKC activity. This assay is a general PKC activity assay and does not distinguish between the different categories of Ca^{++} dependent PKC enzymes. First, the standard enzyme provided in the kit was used to construct a calibration curve (Figure 3.22).

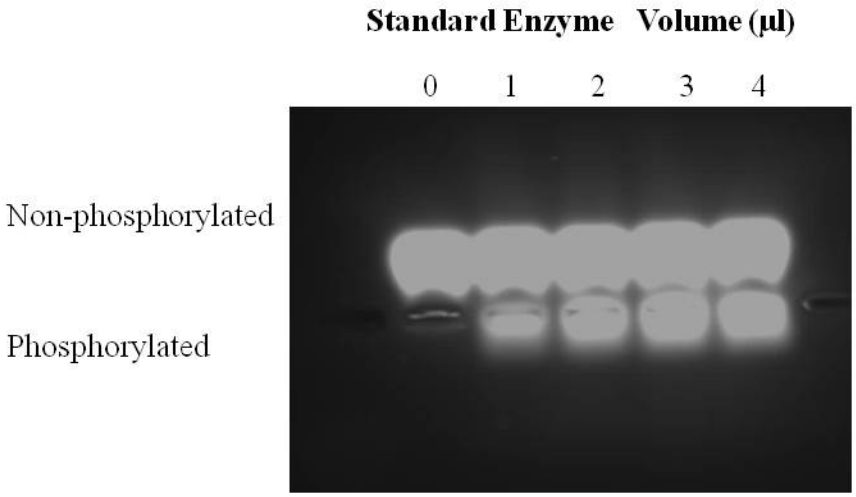

Figure 3.22: PKC Activity Standard Assay. 2 µg of PepTag® C1 Peptide was incubated as described in the standard PKC assay in a final volume of 25µl for 30 minutes at room temperature. The reactions were stopped by heating to 95°C for 10 minutes. The samples were separated on a 0,8% agarose gel at 100V for 15 minutes. Phosphorylated peptide migrated toward the cathode (+), while nonphosphorylated peptide migrated toward the anode (–)

Proteins were extracted from spontaneously differentiating Caco-2 cells with an extraction buffer and incubated with a fluorescent peptide specific for

PKC according to the manufacturer's instructions and as described in Materials and Methods. The reaction mix was run on an agarose gel. Phosphorylation of the peptide would result in a change of the charge, which allows it to be separated on an agarose gel at neutral pH (Figure 3.22) For quantitative analysis, the phosphorylated peptide bands observed in the gel were cut, solubilized and measured spectrophotometrically as described by manufacturer.

Our data indicate that in the differentiated cells, the phosphorylation of the peptide was lower, indicating that PKC is less active when cells undergo differentiation (Figure 3.23, 3.24). Additionally, in order to determine whether PKCα was the specific subtype of PKC that was involved in this activation axis, a PKCα Dominant Negative (DN) vector was transfected in the undifferentiated Day 0 Caco-2 cells. We observed that inhibition of PKCα resulted in a decrease in the phosphorylation of the peptide. Further proof of the activation of PKCα was obtained by transfection the Day 10 differentiated cells with a PKCα overexpressing vector. A recovery in the phosphorylation of the peptide was obtained in the differentiated cells when PKCα was overexpressed further confirming that the kinase activity of PKCα decreases in the course of spontaneous differentiation.

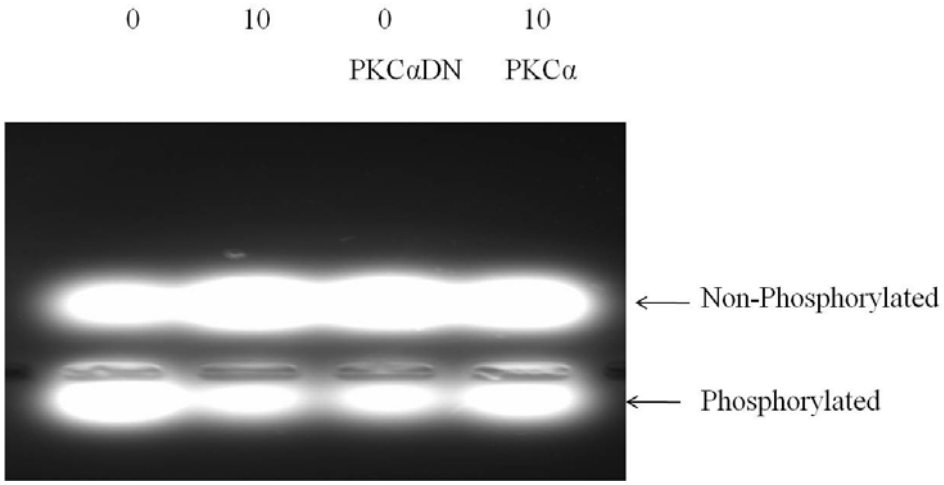

Figure 3.23: PKC Activity in Spontaneously Differentiating Caco-2 Cells. (Lanes: 0-10 indicate day 0 and day 10 postconfluent cells, 0 Day cells were transfected with dominant negative form of PKCα vector (PKCαDN), 10 day confluent cells were transfected with PKCα Overexpression vector (PKCα) for 24 hours. Protein samples were extracted and subjected to enzymatic reaction by using 2 µg of PepTag® C1 Peptide as substrate. Reactions were stopped by heating to 95°C for 10 minutes.The samples were separated on a 0.8% agarose gel at 100V for 15 minutes. Phosphorylated peptide migrated toward the cathode (+), while nonphosphorylated peptide migrated toward the anode (–)

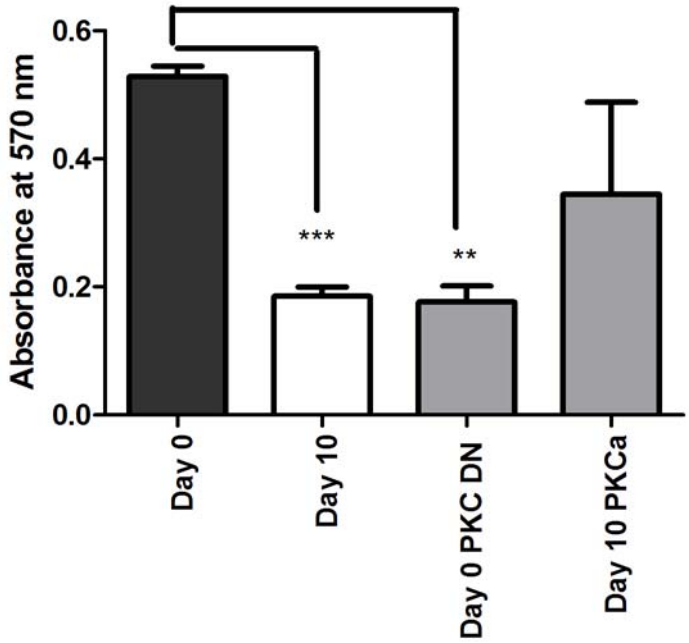

Figure 3.24: Quantitative PKC Activity in Spontaneously Differentiating Caco-2 Cells. (Lanes: 0, 10: Indicates day 0 and day 10 confluent cells, 0 Day cells were transfected with dominant negative form of PKCα vector (PKCαDN), 10 day confluent cells were transfected with PKCα Overexpression vector (PKCα) for 24 hours. Protein samples were and subjected to enzymatic reaction by using 2 µg of PepTag® C1 Peptide as substrate. Reactions were stopped by heating to 95°C for 10 minutes.The samples were separated on a 0.8% agarose gel at 100V for 15 minutes. Phosphorylated peptide migrated toward the cathode (+), while nonphosphorylated peptide migrated toward the anode (–). Phosphorlyated substrates were cut and eluted from agarose gel and measured spectrophotometrically at 570 nm. The data are displayed with mean ± standard deviation of three replicates. Day 10 confluent cells (white bar) showed significantly reduced PKC activity (p=0.0002) compared to day 0 confluent cells (white bar). PKCα DN transfected day 0 Caco-2 cells (first gray bar) also showed significantly lower PKC activity (p=0.0013) compared to untransfected day 0 confluent cells (black bar)

3.3.2 Protein Kinase C α is the PKC Isoform that Activates NF-κB.

In order to further confirm that PKCα was the PKC isoform activating NF-κB reporter gene assays were carried out. Caco-2 cells were grown to

confluency and on Day 0 or Day 10, were transfected with either the NF-κB pGL3 luciferase vector, or its mutated counterpart, or the empty pGL3 vector. At the same time, the cells were co-transfected with a PKCα overexpression vector, or a PKCα dominant negative vector. In addition the beta galactosidase vector was also transfected for normalization. Then extracts were prepared as described in the Materials and Methods section and luciferase values were determined and normalized against beta-galactosidase activities.

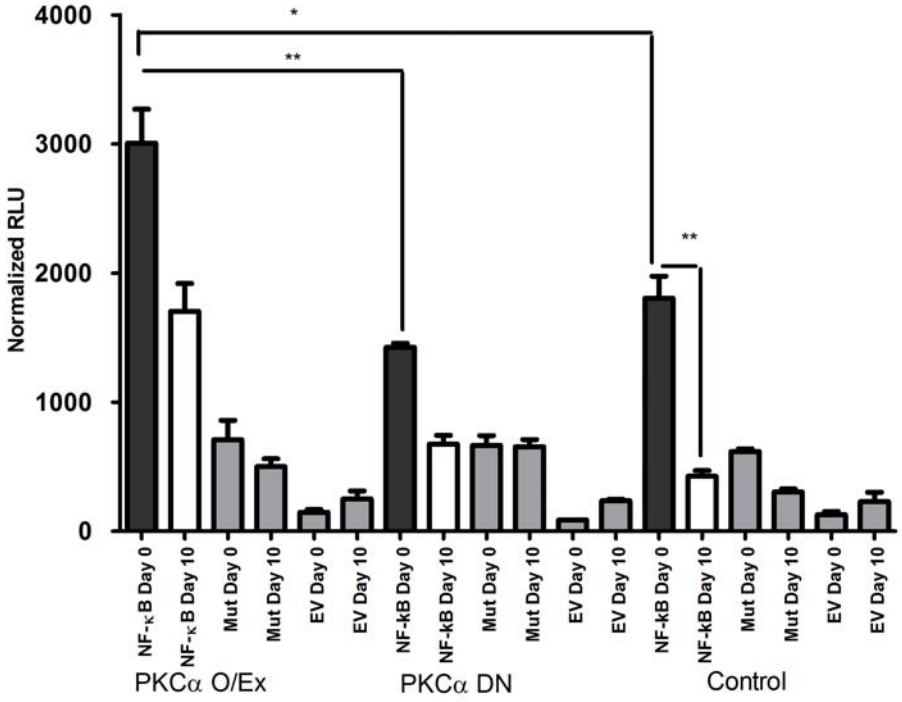

Figure 3.25: NF-κB Reporter Gene Assay in Protein Kinase Cα Overexpressed Caco-2 Cells. 0 Day (black bar) and 10 day (white bar) confluent Caco-2 cells were transfected with NF-κB plasmids (NF-κB), NF-κB mutated plasmids (Mut) or Empty PGL3 vector plasmids (EV) along with PKCα overexpression vector (PKCα O/Ex) or its dominant negative counterpart (PKCα DN). All cells were transfected with pSV-β-Gal vector for normalization. 24 hours posttransfection, cells were harvested with 1X CLB buffer and luciferase activities were measured with 20µl of the extracts. Beta–galactosidase activity was used for normalization. PKCα Overexpression (PKCα O/Ex) showed significantly higher NF-κB activity ($p=0.0039$) compared to control (control).

The data (Figure 3.25) indicate that when PKCα is overexpressed, NF-κB activity is significantly (*$p<0.05$) higher when compared to cells that do not overexpress PKCα (control columns) in both differentiated and undifferentiated cells (Day 10 vs. Day 0). In addition, Caco-2 cells, where PKCα is inhibited by

transfection with the dominant negative vector showed a significantly lower NF-κB transcriptional activity. The effect of PKCα on NF-κB transcriptional activity was not observed in those cells transfected with the vector containing a mutated NF-κB consensus sequence as well as those cells transfected with the empty pGL3 vector. We therefore established that NF-κB transcriptional activity in spontaneously differentiating Caco-2 cells is dependent on PKCα activity.

3.3.3 Protein Kinase C θ acts Downstream of PKCα to Activate NF-κB

PKCα has previously been shown to cross-talk with NF-κB via PKC θ in T lymphocytes (Trushin *et al.,* 2003). In order to determine whether a similar activation axis was contributing towards NF-κB activation in the undifferentiated Caco-2 cells, we determined PKCθ phosphorylation by Western blot. Caco-2 cells were grown and protein extracts were collected on post-confluent Day 0 and Day 10 cells (Figure 3.26).

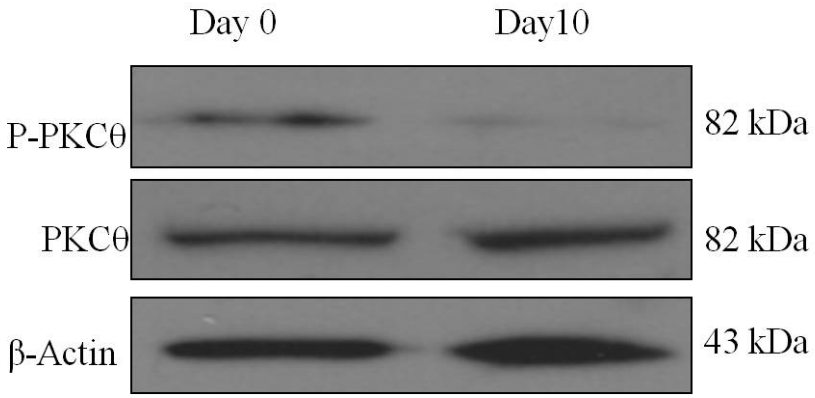

Figure 3.26: Protein Kinase C Proteins in Spontaneously Differentiation of Caco-2 Cells. Lanes: 0-10: Days after reaching 100% confluency. 80µg of proteins from each sample was loaded and transferred on PVDF membrane at 100V for 1 hour 45 minutes, 5% Skim milk in PBST was used as blocking agent. Antibody Dilutions: Anti-P-PKCθ 1:250,Anti-PKCθ 1:500, Anti-β-Actin1:1000, Anti-Mouse-HRP 1:2000; All primary antibody incubations were carried out at 4°C overnight in the presence of blocking agent except secondary antibody (room temperature 1h with gentle agitation)

Western blot analysis (Figure 3.26) revealed that the phosphorylation and thereby the activation of PKCθ was considerably lower in the differentiated cells when compared to the undifferentiated (Day 0) confluent cells. In order to confirm that PKCα acted upstream of PKCθ, Caco-2 cells were transfected with either the PKCα overexpression vector, or the dominant negative vector, proteins were isolated and Western blot analysis was performed against the phosphorylated PKCθ protein (Figure 3.27). Data obtained indicated that when PKCα was overexpressed, a corresponding increase in phosphorylation of PKCθ was observed, which was decreased in the presence of the dominant negative PKCα vector, confirming that PKCα indeed acts upstream of PKCθ.

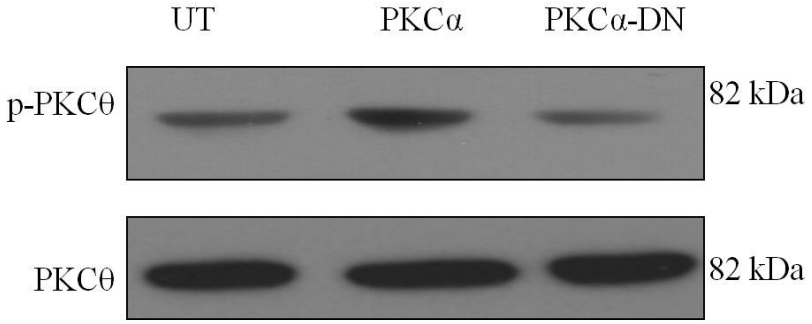

Figure 3.27: PKCθ acts downstream of PKCα. UT: Untransfected confluent undifferentiated (Day 0) Caco-2 cells, PKCα: Day 0 Caco-2 cells transfected with the PKCα overexpression vector, PKCα-DN: Day 0 Caco-2 cells transfected with the dominant negative PKCα vector. 80μg of proteins from each sample was loaded and transferred on PVDF membrane at 100V for 1 hour 45 minutes, 5% Skim milk in PBST was used as blocking agent. Antibody Dilutions: Anti-P-PKCθ 1:250,Anti-PKCθ 1:500, Anti-Mouse-HRP 1:2000; All primary antibody incubations were carried out at 4°C overnight in the presence of blocking agent except secondary antibody (room temperature 1h with gentle agitation)

In order to confirm that the PKCα-PKCθ activation axis also activates NF-κB, we used the same proteins as above to probe for the phosphorylation of IκBα.

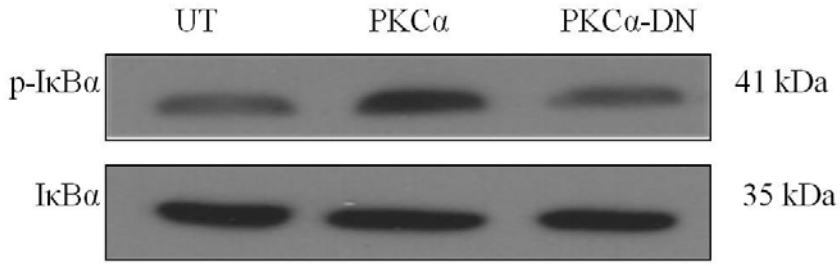

Figure 3.28: PKCα Increases the phosphorylation of IκBα. UT: Untransfected confluent undifferentiated (Day 0) Caco-2 cells, PKCα: Day 0 Caco-2 cells transfected with the PKCα overexpression vector, PKCα-DN: Day 0 Caco-2 cells transfected with the dominant negative PKCα vector. 80μg of proteins from each sample was loaded and transferred on PVDF membrane at 100V for 1 hour 45 minutes, 5% Skim milk in PBST was used as blocking agent. Antibody Dilutions: Anti-P-IκBα 1:250, Anti-IκBα 1:500, Anti-Mouse-HRP 1:2000; All primary antibody incubations were carried out at 4°C overnight in the presence of blocking agent except secondary antibody (room temperature 1h with gentle agitation)

As can be seen from Figure 3.28 PKCα overexpression resulted in increased phosphorylation of IκBα, which would cause its proteasomal degradation, thereby leading to the activation of NF-κB. When the PKCα dominant negative vector was transfected, a decrease in the phosphorylation of IκBα was observed, indicating the inhibition of NF-κB.

Further confirmation of the involvement of PKCα and PKCθ in the activation of NF-κB was obtained by the use of the specific inhibitors: Rottlerin, which inhibits PKCα and GÖ6976, which inhibits PKCθ. Caco-2 cells were

grown until confluency and the undifferentiated cells were treated with 3µM of the inhibitors for 18h and the p65 DNA binding ELISA assay and NF-κB reporter gene assay were performed as elsewhere (Figure 3.29 and Figure 3.30).

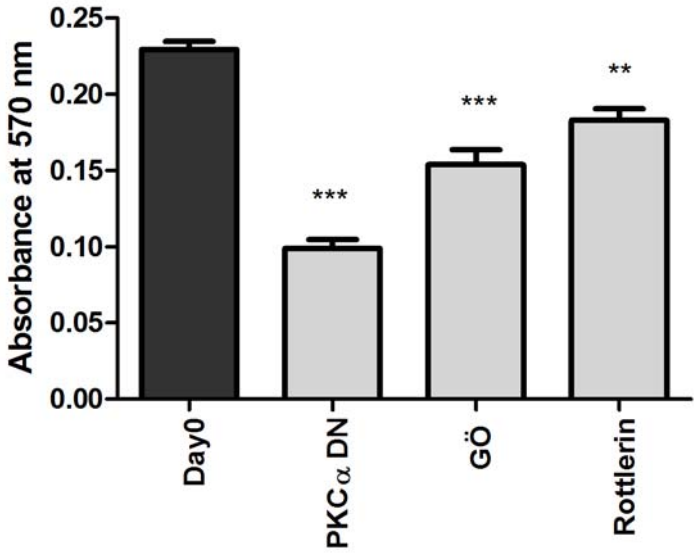

Figure 3.29: Effect of PKCα on p50 DNA Binding Activity (Day 0 indicates days of Caco-2 cells grown after post confluency, PKCα DN: Day 0 confluent cells were transfected with PKCα dominant negative vector. GÖ-Rottlerin: Day 0 Untransfected cells were treated with GÖ (3µM) and Rottlerin (3µM) for 24 hours. Nuclear protein samples were collected on designated days. 5µg of protein was used for the assay. The data are displayed with mean ± standard deviation of three replicates. PKCα-DN Overexpression showed significant decrease (p=0.0001) in p50 DNA binding activity compared to untreated day 0 cells (black bar). Treatment of 0 day confluent cells with GÖ6976 and Rottlerin showed significant decrease (p=0.0005 and p=0.0022, respectively) compared to untreated 0 day confluent Caco-2 cells.

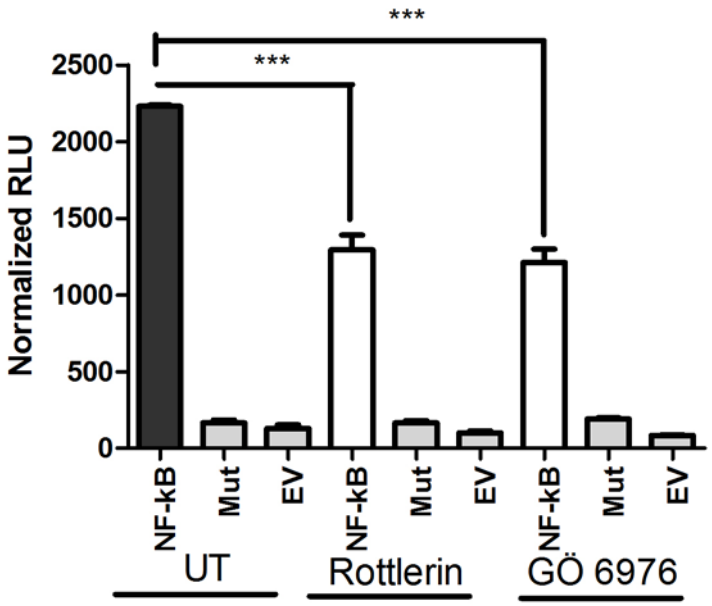

Figure 3.30: Effect of Rottlerin and GÖ 6976 on NF-κB Activity. Day 0 confluent Caco-2 cells were transfected with NF-κB plasmids (NF-κB), NF-κB mutated plasmids (Mut) or Empty Vector Plasmids (EV) along with pSV-β-galactosidase vector. 4 hours posttransfection, transfected cells were treated with either GÖ (3μM) or Rottlerin (3μM) (white bars). 18 hours post-treatment cells were harvested with 1X CLB buffer and luciferase activities were measured with 20μl of the extracts. Beta –galactosidase activity was used for normalization. The data are displayed with mean ± standard deviation of three replicates. Both PKCα and –θ inhibitor treated cells (white bars) showed significantly lower ($p=0.0006$, and $p=0.0003$, respectively) compared to untreated cells (black bar).

The data shown in Figure 3.29 indicate that the DNA binding activity of NF-κB was significantly lower when undifferentiated Caco-2 cells were treated with Rottlerin or GÖ6976 and that this inhibition was comparable to that obtained

when PKCα was specifically inhibited by the PKCα dominant negative vector. Furthermore, the transcriptional activity of NF-κB was also significantly reduced in the presence of both GÖ6976 (**$p<0.001$) and Rottlerin (*$p<0.05$) (Figure 3.30). This inhibition was not observed in cells transfected with the NF-κB luciferase vector containing the mutated consensus sequence, or the empty pGL3 vector (Figure 3.30).

3.4 C/EBPβ in Spontaneous Differentiation

ICAM1 and *VCAM1* are both NF-κB target genes, however, their mRNA expressions did not correlate, with the expression of *VCAM1* decreasing in the course of spontaneous differentiation, while that of *ICAM1* remains stable (Figures 3.4 and 3.5). The *ICAM1* promoter, in addition to the NF-κB binding consensus sequence, also contains C/EBPβ consensus sequences (Roebuck & Finnegan 1999b). It was reported that in HeLa, A549 and EV304 cells, the NF-κB and C/EBPβ both needed to bind to a composite element containing consensus sequences for both transcription factors in order to direct the transcription of *ICAM1* (Catron *et al.,* 1998). Additionally, C/EBPβ was shown to be transcriptionally active during differentiation of adipocytes (Darlington *et al.,* 1998). Therefore we hypothesized that C/EBPβ could be as activated in the course of epithelial differentiation and could drive the expression of *ICAM1*.

3.4.1 Expression of *C/EBPβ* during Spontaneous Differentiation of Caco-2 Cells

In order to understand the possible involvement of *C/EBPβ* in the expression of ICAM-1 in the course of differentiation of Caco-2 cells, first, the

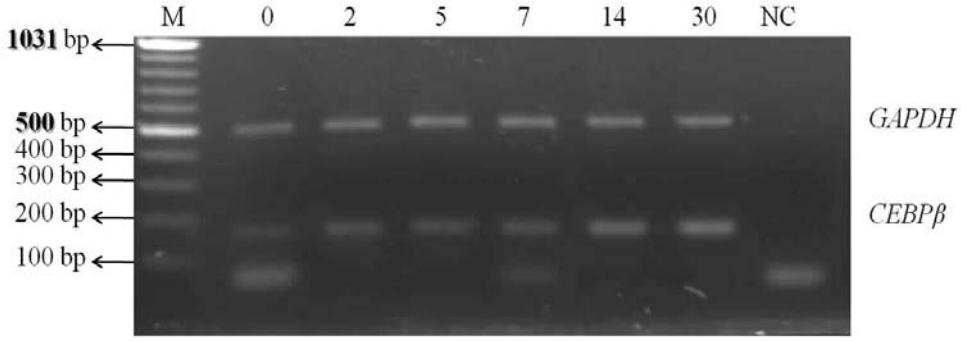

RNA expression of *C/EBPβ* was assessed by PCR (Figure 3.31).

Figure 3.31: C/EBPβ Expression in Spontaneously Differentiating Caco-2 Cells. M: Marker; GeneRuler™ DNA Ladder Mix (Fermentas), 0-30: Days after post confluency, NC: Negative Control. cDNAs were synthesized from 2µg DNAse I treated RNA by using oligo dT primer

C/EBPβ RNA expression analysis (Figure 3.31) revealed a change in the expression of *C/EBPβ* during the course of differentiation of Caco-2 cells. We next wanted to determine the nuclear protein levels of C/EBPβ in order to ascertain the active fraction of the transcription factor in the Caco-2 cells. A Western blot was carried out using nuclear protein extracts from post confluent Day 0 undifferentiated and Day 10 differentiated cells (Figure 3.32).

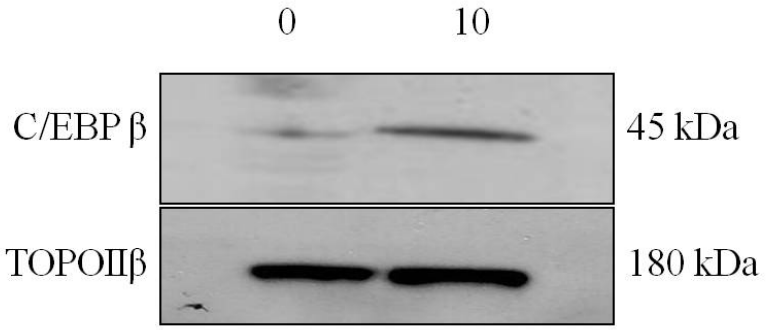

Figure 3.32: C/EBPβ Protein in Spontaneously Differentiating Caco-2 Cells. (Lanes: 0-10:: Days after reaching 100% confluency. 80µg of proteins from each sample was loaded and transferred on PVDF membrane at 100V for 1 hour 45 minutes, 10% Skim milk in PBST was used as blocking agent. Antibody Dilutions: Anti-C/EBPβ 1:500, Anti-TopoIIβ 1:250, Anti-Rabbit-HRP 1:2000, Anti-Mouse-HRP 1:2000; All incubations were carried out at room temperature for 1 hour with gentle agitation in the presence of blocking agent. Proteins were probed against TopoIIβ as nuclear loading control.

The data (Figure 3.32) show that C/EBPβ protein in the nuclear fraction increased during spontaneous differentiation of Caco-2 cells, which indicates that the protein may be transcriptionally more active in the differentiated cells. In order to further support the transcriptional activation of *C/EBPβ* in the spontaneous differentiation DNA binding assays by EMSA and Chromatin Immunoprecipitation (ChIP) and reporter gene assays were carried out.

3.4.2 DNA Binding Activity of C/EBPβ in Spontaneously Differentiating Caco-2 Cells.

Electrophoretic Mobility Shift Assay

In order to determine the DNA binding activity of C/EBPβ, EMSA was carried out. Nuclear extracts (5μg) obtained from differentiating Caco-2 cells (Day 0 and Day 10) were incubated with biotin labeled oligonucleotides containing the consensus C/EBPβ binding sequence and subjected to a gel shift assay as described in the Materials and Methods. Control reactions included competition with 200 fold excess of the non-labeled (cold) probe, and the inclusion of the C/EBPβ antibody resulting in a supershift of the protein-DNA-antibody complex.

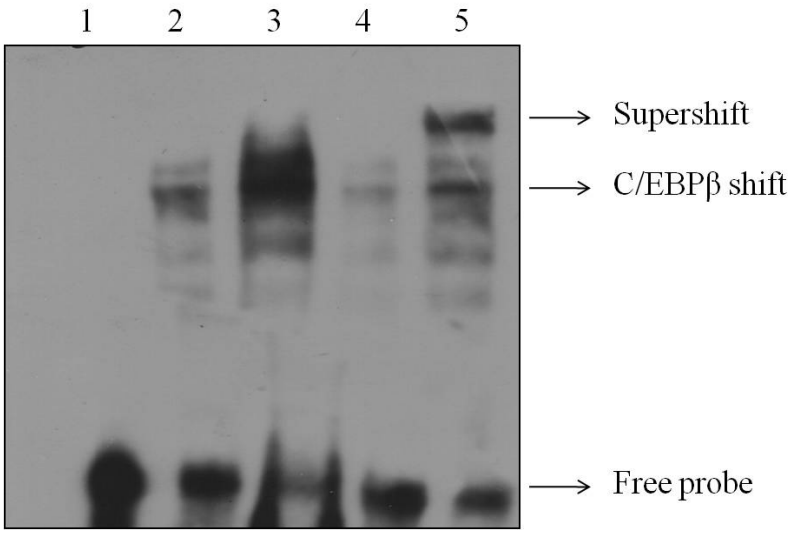

Figure 3.33 C/EBPβ EMSA in Spontaneously Differentiating Caco-2 Cells (Lanes: 1: Free Probe, 2: Day 0 nuclear protein, 3: Day10 nuclear protein, 4: Day 10 nuclear protein and unlabeled (Cold) competitor, 5: Day 10 nuclear protein and C/EBPβ antibody). For all binding reactions 5µg of the nuclear extracts obtained from designated days were used. Binding reactions were prepared and incubated on ice for 10 minutes and at room temperature for 20 min after which the oligos and Anti-C/EBPβ (3µl) antibody was added and incubated for a further 10 min at room temperature. Samples were separated in 8% polyacrylamide gel prepared with TBE transferred on to a nylon membrane (Biodyne, precut B Nylon membrane, Pierce, USA) for 45 minutes at 4°C. After crosslinking, membranes were treated according to the instructions of the manufacturer.

As can be seen from Figure 3.33 the labeled oligonucleotide containing the C/EBPβ consensus sequence was retarded more when incubated with the nuclear proteins from the Day 10 differentiated Caco-2 cells when compared to the undifferentiated Day 0 nuclear extract. The specificity of the reaction was ensured by the loss of signal upon incubation of the Day10 nuclear extract with the cold probe and supershift resulting from the addition of the C/EBPβ antibody.

Chromatin Immunoprecipitation

We had previously established (please see Figure 3.15) that NF-κB recruitment to the promoter of *ICAM1* was reduced in the course of differentiation. We wanted to determine whether there was an increase in the recruitment of C/EBPβ to the promoter of *ICAM1* in order to drive its expression.

Primers were designed to amplify the NF-κB (821-831 before transcription initiation site) and C/EBPβ (969-982 before transcription initiation site) elements. Genomic DNA was isolated from Day 0 and Day 10 confluent Caco-2 cells and processed for ChIP as described previously. In each experiment, 100μl from each sample were taken and labeled as "input" control before addition of the antibodies. They were used as positive controls for the amplification reactions (Figure 3.34).

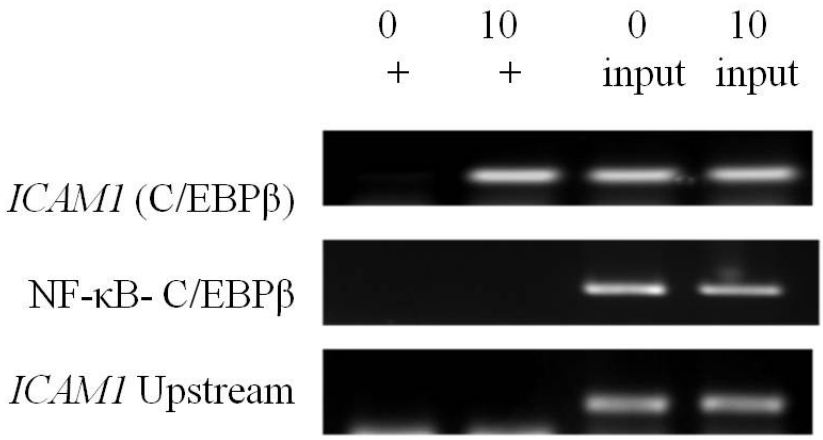

Figure 3.34 Amplification of the C/EBPβ and NF-κB/ C/EBPβ Elements in the *ICAM1* Promoter after ChIP with C/EBPβ Antibody in Spontaneously Differentiating Caco-2 Cells. (+: C/EBPβ antibody). For each assay, a total of 100% confluent cells were fixed with formaldehyde. Pellets were then frozen in liquid nitrogen and thawed in buffer C. After incubation on ice for 20 minutes samples were resuspended in a breaking buffer and sonicated for 2 minutes in a water bath sonicator (Bandelin, SONOREX, Walldorf, Germany). Then 1ml of Triton buffer was added. After removing an aliquot (input control) equal protein amounts containing chromatin were incubated with antibodies against C/EBPβ antibody at 4°C for 1 hour with gentle agitation in protein A- agarose containing spin filter columns (NAb spin columns, Pierce).

As can be seen in Figure 3.34 C/EBPβ was recruited to its consensus sequence in the differentiated Caco-2 cells (Lane 2), but not in the undifferentiated Caco-2 cells (Lane 1). Furthermore, we have observed that the recruitment of C/EBPβ is not to the composite NF-κB – C/EBPβ element. This is in contrast to the data described by Catron *et al* (Catron *et al.,* 1998). However, these authors restricted their *ICAM1* promoter analysis to three specific cell lines: A549, HeLa and EV304. It is possible that recruitment of C/EBPβ to the promoter of *ICAM1* in Caco-2 cells is different from these cell lines.

To further confirm the recruitment of C/EBPβ to the *ICAM1* promoter, the immunoprecipitated C/EBPβ element in from undifferentiated and differentiated Caco-2 cells were also subjected to real time PCR amplification.

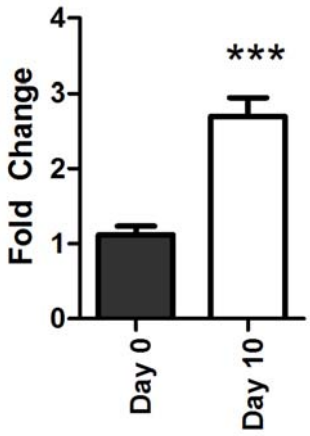

Figure 3.35 Amplification of the C/EBPβ Element in the *ICAM1* Promoter. The data are displayed with mean ± standard deviation of three replicates. Day 10 differentiated cells (white bar) exhibited significantly higher C/EBPβ recruitment to the *ICAM1* ($p<0.0001$) compared to the 0 day confluent cells (black bar).

As it can be seen from the Figure 3.35 recruitment of C/EBPβ to it consensus sequence in the *ICAM1* promoter was increased significantly (***$p<0.0001$) in the differentiated Caco-2 cells when compared to undifferentiated cells. This, most likely, accounts for the stable mRNA expression of ICAM-1 during the course of differentiation.

Reporter Gene assays

We had established that C/EBPβ was recruited to the promoter of *ICAM1* and that its DNA binding activity was higher in the differentiated Caco-2 cells. In order to determine the transcriptional activity of C/EBPβ in spontaneous differentiation of Caco-2 cells, reporter gene assays were carried out. The C/EBPβ consensus sequence from the *ICAM1* promoter was cloned into a luciferase vector (pGL3, Promega) as described previously. As controls, luciferase vectors with mutated C/EBPβ consensus sequence and the empty pGL3 vector were used (Figure 3.36).

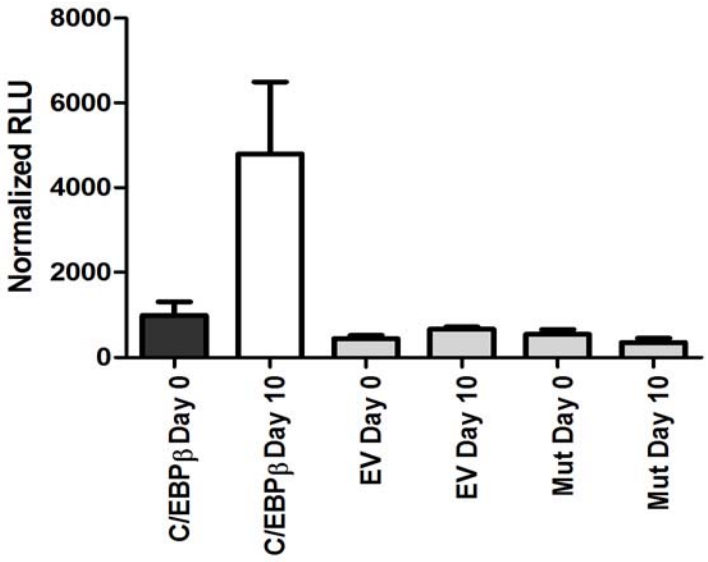

Figure 3.36 C/EBPβ Reporter Gene Assay in Spontaneously Differentiating Caco-2 Cells. 0 Day (black bar) and 10 day (white bar) confluent Caco-2 cells were transfected with C/EBPβ plasmids (C/EBPβ), C/EBPβ mutated plasmids (Mut) or Empty PGL3 reporter vector plasmids (EV) 24 hours posttransfection, proteins were extracted with 1X CLB buffer and luciferase activities were measured with 20µl of the extracts. Beta–galactosidase activity was used for normalization. The data are displayed with mean ± standard deviation of three replicates.

Reporter gene assays (Figure 3.36) revealed that C/EBPβ transcriptional activity increased during differentiation of Caco-2 cells with respect to empty vector and mutated vector counterparts.

With the EMSA, ChIP and reporter gene assays we established the transcriptional upregulation of *ICAM1* in the differentiated Caco-2 cells. This is perhaps not surprising, surprising since C/EBPβ is known to be involved in the process of cellular differentiation. Cao *et. al*, have shown that C/EBPβ activity is required for adipocytes to be converted into 3T3-L1 cells (Cao *et al.,* 1991). It was also shown to be required for lymphocyte differentiation (Lekstrom-Himes & Xanthopoulos 1998). In addition, systemic delivery of C/EBPβ/liposome complex was shown to reduce the proliferation of colon cells in nude mice (Sun *et al.,* 2005). Cells cease to proliferate once they differentiate. It is thus possible that the transcriptional activity of C/EBPβ is necessary to drive the enterocytes into differentiation, an avenue that we are currently studying in the laboratory.

We can thus conclude that *ICAM1* expression is regulated by NF-κB and C/EBPβ, the former being active at the beginning of differentiation while the latter becomes active as the cells undergo differentiation. This keeps the *ICAM1* expression stable through the whole differentiation process (Figure 3.5). On the other hand, *VCAM1* gene, which contains only NF-κB binding sites, (Iademarco *et al.,* 1992) seems more likely to be transcriptionally regulated by NF-κB. Therefore its expression decreases in the course of spontaneous differentiation of Caco-2 cells corresponding with the decrease in NF-κB activity (Figure 3.4).

3.5 Post Transcriptional and Post Translational Regulation of *ICAM1* and *VCAM1*

3.5.1 Post Transcriptional MicroRNA mediated Regulation of *ICAM1* Expression in Differentiating Caco-2 Cells

We have observed that the mRNA expression of *ICAM1* remains steady while the protein expression decreases in the course of differentiation. Since microRNAs are known to regulate gene expression by translational repression of their target genes (D. P. Bartel 2004), we wanted to determine whether *ICAM1* was regulated by microRNAs in the course of spontaneous differentiation.

It was recently shown that miR-221 could regulate *ICAM1* expression during infection by the protozoan *Cryptosporidium parvum* (Gong *et al.,* 2011). On the other hand, *miR-222* and *miR-339* were also found to be down-regulating the ICAM-1 expression in Cytotoxic T Lymphocytes (Ueda *et al.,* 2009). However microRNA regulation of *ICAM1* during differentiation is as of yet unknown.

To establish whether the expression of *ICAM1* was regulated by microRNAs, the *ICAM1* 3'UTR region was cloned in a luciferase based reporter vector (pMIR-REPORT, Ambion). This reporter plasmid works on the principle that when a predicted miRNA target sequence such as the 3'UTR of a target gene is cloned into the vector, the luciferase reporter is subjected to regulation that mimics the miRNA target. A decrease in the luciferase signal would therefore indicate the presence of miRNA based regulation.

The 3'UTR of *ICAM1* was divided into two sections with a 165 bp overlapping region, cloned into the pMIR-REPORT vector and sequenced. The two vectors were then transfected separately into undifferentiated confluent (Day 0) and differentiated (Day 10) Caco-2 cells along with beta-galactosidase reporter vector for normalization. Following 24h or transfection, total protein samples were collected and assayed for luciferase activity and normalized against beta galactosidase activity (Figure 3.37).

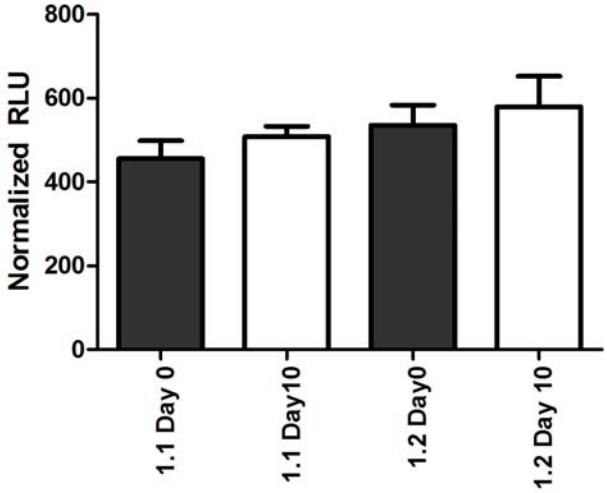

Figure 3.37 *ICAM1* 3'UTR Activity in Spontaneously Differentiating Caco-2 Cells. 0 Day (black bar) and 10 day (white bar) confluent Caco-2 cells were transfected with pMIR-REPORT vector containing first half (1.1)or second half (1.2) of the 3' UTR Region of *ICAM1* gene. 24 hours posttransfection, proteins were extracted with 1X CLB buffer and luciferase activities were measured with 20µl of the extracts. Beta –galactosidase activity was used for normalization. The data are displayed with mean ± standard deviation of three replicates

The data (Figure 3.37) show that there was no significant decrease in the luciferase signal, indicating the lack of miRNA-mediated regulation in either of the halves of the 3'UTR of *ICAM1*. Therefore a reduced translation of ICAM-1

protein due to the binding of a microRNA in the 3'UTR of the ICAM-1 gene is most likely not the reason for its decreased protein levels in the course of differentiation.

3.6 Post-Translational Protein Degradation Mechanisms of ICAM-1 and VCAM-1 in Spontaneously Differentiating Caco-2 Cells

Since the 3'UTR analysis preempted any possible microRNA involvement in the regulation of ICAM-1 protein expression, we therefore investigated the possible protein degradation mechanisms. Proteins can be degraded in cells in lysosomes (de Duve 2005), the proteasome after ubiquitination (Goldberg & Rock 1992) and by calpain mediated protein degradation mechanisms (Ohno *et al.,* 1984.)

It was reported for HMEC-1 cells that after treatment with pyropheophorbide-a methyl ester (PPME), a drug used in photodynamic therapy, the RNA expression of *ICAM1* and *VCAM1* increased with no detectable protein product (Volanti *et al.,* 2004). The authors reported that PPME did not interfere with the translational machinery; rather, the translated proteins were targeted exclusively to lysosomal degradation without the involvement of calpain or proteasomal degradation.

We have hypothesized that the loss of ICAM-1 and VCAM-1 protein levels in the course of differentiation of Caco-2 cells may be due to the activation of a protein degradation pathway. We have treated Day 0 undifferentiated and

Day 10 differentiated confluent cells with specific inhibitors for lysosomal, proteasomal and calpain mediated inhibition and determined whether any of these inhibitors could recover the protein levels of ICAM-1 or VCAM-1 in the differentiated cells.

To determine whether ICAM-1 and VCAM-1 proteins were degraded in the lysosome, the Caco-2 cells were incubated with the lysosomal inhibitors Pepstatin (1μg(ml), Leupeptin (100μM) and E64 (10 μM) for 24 hours before proteins were extracted and subjected to Western blot. To ensure equal protein loading, the same membrane was stripped and reprobed with the GAPDH antibody (Figure 3.38 and Figure 3.39).

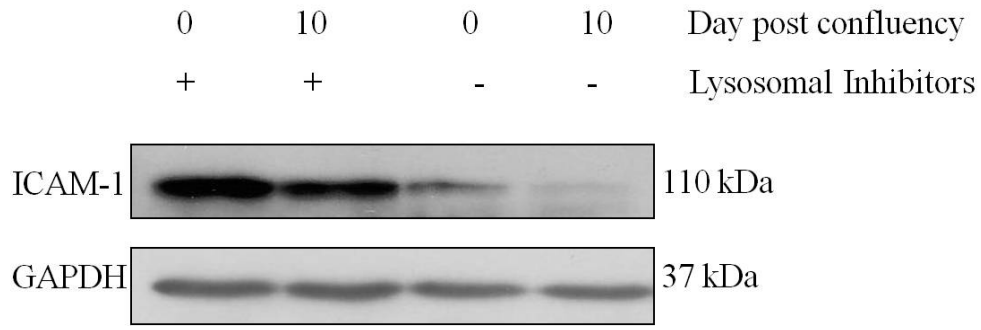

Figure 3.38: Effect of Lysosomal Degradation Pathway on the Expression of ICAM-1 Protein. (Lanes: 0-10 Days after confluency, +: Cells treated with Lysosomal Inhibitors, -: Untreated) Day 0 and Day 10 Caco-2 cells were treated with Pepstatin A (1µg/ml), Leupeptin (100µM) and E64 (10µM) for 24 hours. 80µg of total proteins from each sample was loaded and transferred on PVDF membrane at 100V for 1 hour 45 minutes, 10% Skim milk in PBST was used as blocking agent. Antibody Dilutions: Anti-ICAM-1 1:500, Anti-GAPDH 1:1000, Anti-Rabbit-HRP 1:2000; All primary antibody incubations were carried out at 4°C overnight in the presence of blocking agent except secondary antibodies (room temperature 1h with gentle agitation). GAPDH protein was probed as loading control

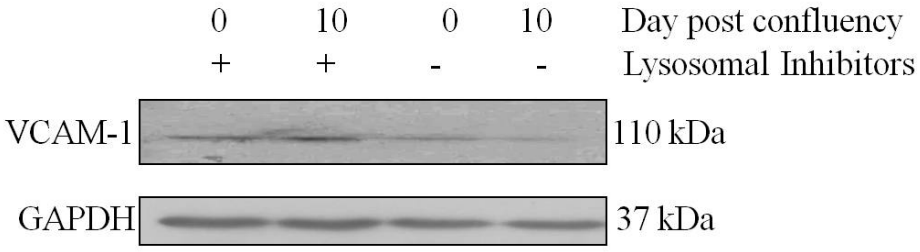

Figure 3.39: Effect Lysosomal Degradation on the Expression of VCAM-1 Protein. (Lanes: 0-10 Days after confluency, +: Cells treated with Lysosomal Inhibitors, -: Untreated) Day 0 and Day 10 Caco-2 cells were treated with Pepstatin A (1µg/ml), Leupeptin (100µM) and E64 (10µM) for 24 hours. 80µg of total proteins from each sample was loaded and transferred on PVDF membrane at 100V for 1 hour 45 minutes, 10% Skim milk in PBST was used as blocking agent. Antibody Dilutions: Anti-VCAM-1 1:250, Anti-GAPDH 1:1000, Anti-Rabbit-HRP 1:2000; All primary antibody incubations were carried out at 4°C overnight in the presence of blocking agent except secondary antibodies (room temperature 1h with gentle agitation). GAPDH protein was probed as loading control.

The data shown in Figure 3.38 and 3.39 reveal that the decreased ICAM-1 and VCAM-1 protein levels in Day 10 (lane 4) could be restored very effectively (lane 2) when the cells were treated with the lysosomal inhibitors. Restoration can also be observed with the undifferentiated (Day 0) cells indicating that lysosomal degradation of ICAM-1 and VCAM-1 is an established degradation mechanism in these cells.

In order to determine the contribution of proteasomal degradation towards the regulation of ICAM-1 and VCAM-1 proteins the Day 0 and Day 10 cells were treated with the proteasomal inhibitor MG-132 (10µM) for 24h. Protein extracts were collected and Western blot analysis was performed. GAPDH protein was also probed to verify the equal loading of samples.

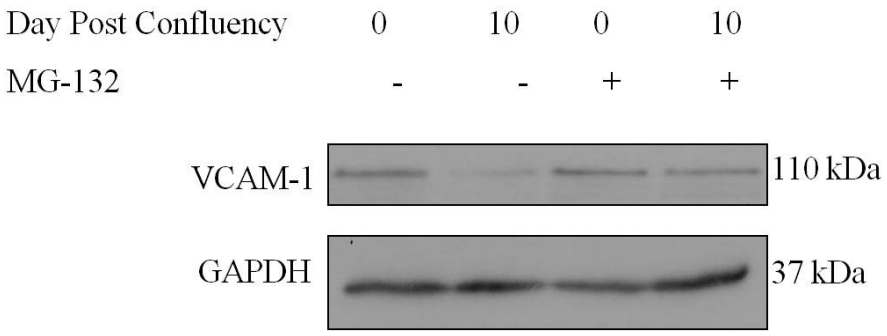

Figure 3.40: Effect of Proteasomal Degradation on VCAM-1 Expression During Spontaneous Differentiation of Caco-2 Cells. (Lanes: 0-10 Days after confluency, +: Cells treated with Proteasomal Inhibitor MG-132, -: Untreated) Day 0 and Day 10 Caco-2 cells were treated with MG-132 (10µM) for 24 hours. 80µg of total proteins from each sample was loaded and transferred on PVDF membrane at 100V for 1 hour 45 minutes, 10% Skim milk in PBST was used as blocking agent. Antibody Dilutions: Anti-VCAM-1 1:250, Anti-GAPDH 1:1000, Anti-Rabbit-HRP 1:2000; All primary antibody incubations were carried out at 4°C overnight in the presence of blocking agent except secondary antibodies (room temperature 1h with gentle agitation). GAPDH protein was probed as loading control

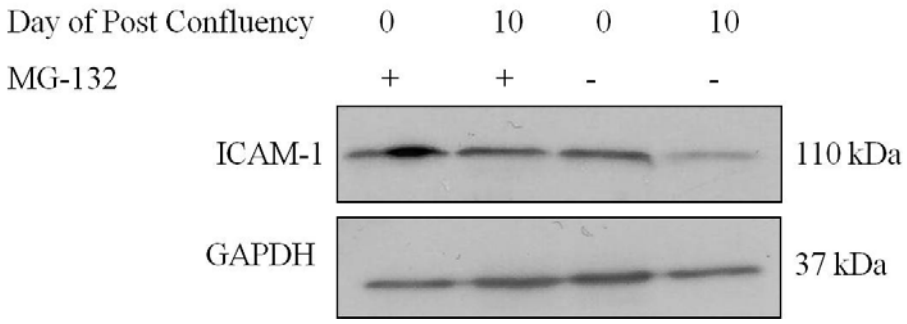

Figure 3.41: Effect of Proteasomal Degradation on ICAM-1 Expression During Spontaneous Differentiation of Caco-2 Cells. Lanes; 0-10: Days after confluency, +: Cells treated with Proteasomal Inhibitor MG-132, -: Untreated) Day 0 and Day 10 Caco-2 cells were treated with MG-132 (10μM) for 24 hours. 80μg of total proteins from each sample was loaded and transferred on PVDF membrane at 100V for 1 hour 45 minutes, 10% Skim milk in PBST was used as blocking agent. Antibody Dilutions: Anti-ICAM-1 1:500, Anti-GAPDH 1:1000, Anti-Rabbit-HRP 1:2000; All primary antibody incubations were carried out at 4°C overnight in the presence of blocking agent except secondary antibodies (room temperature 1h with gentle agitation). GAPDH protein was probed as loading control

As can be seen from Figure 3.40 and 3.41, both VCAM-1 and ICAM-1 proteins levels in the Day 10 differentiated cells could be restored when the proteasomal degradation of the proteins were inhibited. No such restoration could be observed in the undifferentiated cells, indicating that the proteasomal degradation occurs in the differentiated cells only.

Since ICAM-1 and VCAM-1 are membrane proteins, it is likely that the major route for degradation is the lysosome (Sandoval and Bakke, 1994). Additionally, proteasomal inhibitors are also usually NF-κB inhibitors, including MG-132, which has been used in this experiment. Therefore a potential

interference with the NF-κB pathway cannot be discounted. It is possible that the proteasomal inhibitor inhibits other proteins that may indirectly affect the protein levels of ICAM-1 and VCAM-1. Further studies are necessary to confirm this hypothesis.

We next examined whether the Calpain induced degradation pathway degraded ICAM-1 and VCAM-1. For that purpose the Calpain inhibitor I was used 24 hours before protein extraction as described previously. Western blot analysis was performed with antibodies against ICAM-1 and VCAM-1 along with GAPDH for loading control (Figure 3.42).

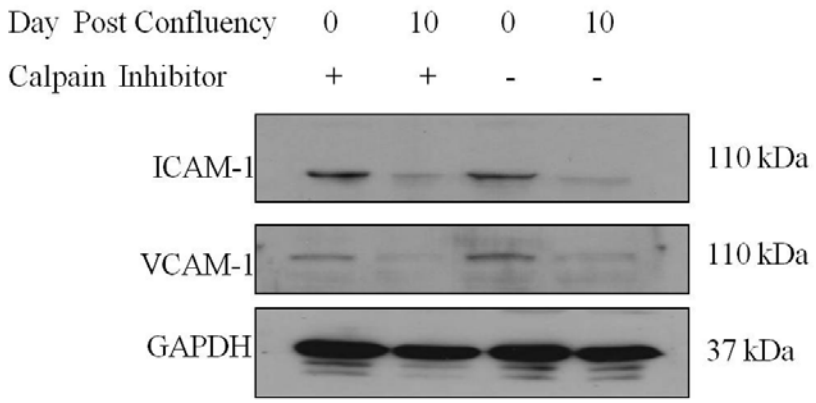

Figure 3.42: Effect of Calpain Induced Degradation on ICAM-1 and VCAM-1 Expression During Spontaneous Differentiation of Caco-2 Cells. Lanes; 0-10 Days after confluency, +: Cells treated with Calpain Inhibitor ALLN, -: Untreated) Day 0 and Day 10 Caco-2 cells were treated with ALLN (100 μM) for 24 hours. 80μg of total proteins from each sample was loaded and transferred on PVDF membrane at 100V for 1 hour 45 minutes, 10% Skim milk in PBST was used as blocking agent. Antibody Dilutions: Anti-ICAM-1 1:500, Anti VCAM-1 1:250, Anti-GAPDH 1:1000, Anti-Rabbit-HRP 1:2000; All primary antibody incubations were carried out at 4°C overnight in the presence of blocking agent except secondary antibodies (room temperature 1h with gentle agitation). GAPDH protein was probed as loading control

Western blot results (Figure 3.42) indicate that the Calpain mediated degradation pathway was not involved in the degradation in ICAM-1 and VCAM-1 protein expression in both differentiated and undifferentiated cells. Therefore, ICAM-1 and VCAM-1 proteins appear to be regulated at the post translational level via degradation mediated by lysosomes as well as the proteasome during the differentiation of Caco-2 cells.

3.7 Functional Significance of the Loss of ICAM-1 and VCAM-1 Proteins in the Differentiated Caco-2 Cells.

ICAM-1 and VCAM-1 are cell adhesion molecules that are known to be involved in the adhesion of cells to the extracellular matrix (ECM) proteins and vascular endothelial cells (Gallicchio *et al.,* 2008). In addition, the expression of these proteins are also associated with more invasive cancers (Kobayashi *et al.,* 2007) and cancer cells expressing ICAM-1 and VCAM-1 can extravasate and mediate metastasis by adhesion to endothelial cells (Dianzani *et al.,* 2008)

3.7.1 Adhesion of Differentiating Caco-2 Cells to Fibronectin and Endothelial Cells

<u>Epithelial cell – extracellular matrix interaction</u>

In order to determine whether the adhesion of Caco-2 cells to the extracellular matrix (ECM) was altered in the course of differentiation, an adhesion assay was carried out with undifferentiated (Day 0) and differentiated (Day 10) confluent Caco-2 cells using fibronectin. The cells were plated in 96 well plates previously coated fibronectin (50μg/ml) and incubated for 2 hours at 37°C. After washing, the attached live cells were detected by an MTT assay (Figure 3.43). In order to determine whether inhibition of the lysosomal degradation of adhesion molecules affected the adhesion of the Caco-2 cells to fibronectin, the cells were preincubated with the lysosomal inhibitors for 24h before processing them for the adhesion assay as above.

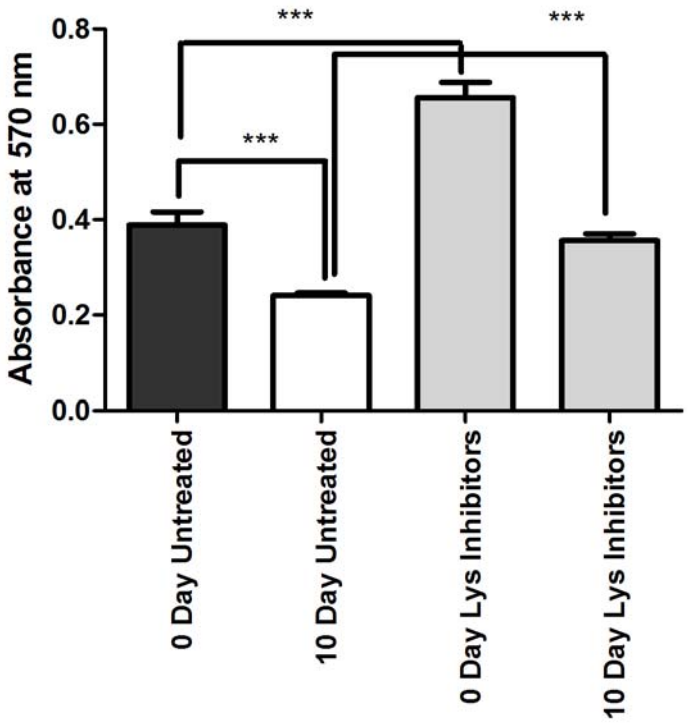

Figure 3.43: Adhesion of Differentiating Caco-2 Cells to Fibronectin. 0-10 Day: Days of confluent Caco-2 Cells, Lys Inhibitors: 0 and 10 day confluent Caco-2 cells were incubated with lysosomal inhibitors Pepstatin A (1µg/ml), Leupeptin (100µM) and E-64 (10µM) for 24 hours before adding on Fibronectin cotated (50µg/ml) 96 well plates. 400.000 treated or untreated 0 and 10 day confluent Caco-2 cells were incubated at 37°C for 2 hours in fibronectin coated plates. Then 10µl MMT (Invitrogen, USA) reagent was added and cells were incubated at 37°C for 4 hours after adding 100µl SDS solution plates were read at 570 nm spectrophotometrically. Only medium containing wells were used as blank. The data are displayed with mean ± standard deviation of seven replicates. Data show that 10 day confluent (white bar) Caco-2 cells showed significantly lower ($p=0.0002$) adhesion compared to 0 day confluent cells (black bar). Treatment with lysosomal inhibitors significantly increased ($p<0.0001$) the adhesion of both 0 and 10 day confluent cells (gray bars).

As can be seen from Figure 3.43 the adhesion of Caco-2 cells decreased significantly in the differentiated cells when compared to the undifferentiated cells (*** $P < 0.002$). Addition of the lysosomal inhibitors significantly increased

the adhesion of the undifferentiated cells (*** $P < 0.002$) and almost restored the adhesion of the differentiated cells close to the values seen for the undifferentiated cells (*** $P < 0.001$).

The data revealed that as the cells undergo differentiation, they lose their adhesiveness to the ECM. Adhesion to fibronectin is mediated by integrins expressed on the membranes of cells and the decreased adhesion indicates that the process of differentiation entails a general loss of contact with the ECM. This phenomenon may also result in the shedding of the differentiated cells as they are pushed up the villi and undergo apoptosis.

Epithelial – endothelial cell interaction

In order to determine whether the process of differentiation specifically affected the cell – cell adhesion mediated by ICAM-1 and VCAM-1, the adhesion of Caco-2 cells to Human Umbilical Vein Endothelial Cells (HUVEC) was assayed in a co-culture model. Caco-2 cells were collected on Day 0 (undifferentiated) or Day 10 (differentiated) after reaching confluency and labeled with Cytotracker Dye (Cytoselect, CellBiolabs, USA) according to the manufacturer's instructions. The cells were then plated in 96 well plates containing a monolayer of HUVEC cells. After removal of non-adherent cells, signals from labeled Caco-2 cells were measured fluorometrically in a Spectramax M5 microplate reader (Molecular Devices, UNAM, Bilkent University, Ankara). In order to confirm whether the adhesion of Caco-2 cells to HUVEC cells was mediated by the cell adhesion molecules, the undifferentiated

(Day 0) Caco-2 cells were preincubated with either increasing amount of the ICAM-1 or with a non-specific IgG. As a control, Caco-2 cells were directly added to the wells of the plate with the ICAM-1 antibody but without a precoating of HUVEC cell monolayer (Figure 3.44).

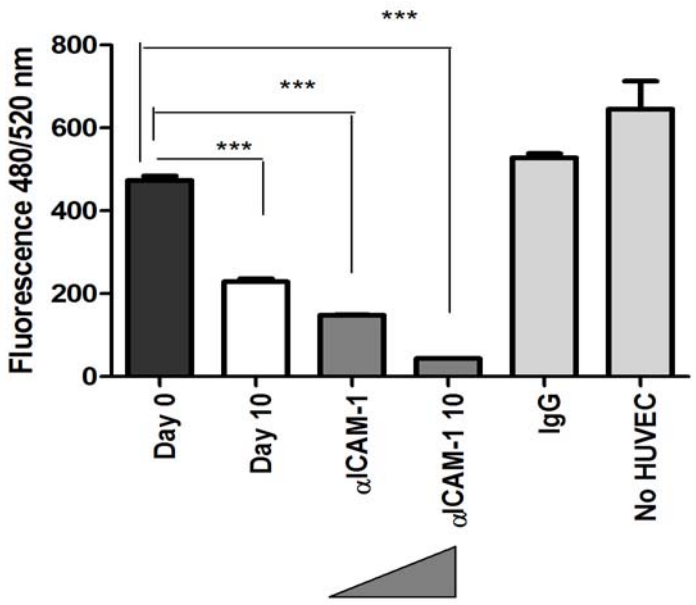

Figure 3.44: Caco-2 Cell Adhesion to HUVEC Cells as a Function of Differentiation. Day 0: Undifferentiated, Day 10: Differentiated Caco-2 Cells, αICAM-1: Undifferentiated Cells + αICAM-1 (5µl), αICAM-1-10: Undifferentiated Cells + αICAM-1 (10µl), IgG: Undifferentiated Cells + αAntirabbit (5µl), No HUVEC: Undifferentiated cells + αICAM-1(5µl) in HUVEC uncoated wells. 0 and 10 day confluent CytoTracker™ labeled Caco-2 cells were (100.000 cells per well) added to gelatin coated monolayer HUVEC containing wells and incubated for 6 hours at 37°C. Data were obtained by fluorescence reader at 480 nm/520 nm. The data are displayed with mean ± standard deviation of 3 replicates of two independent experiments. 10 day differentiated Caco-2 (white bar) cells showed significantly lower ($p<0.0001$) adhesion to HUVEC compared to 0 day confluent cells (black bar). Addition of ICAM-1 antibody to day 0 confluent cells showed significant decrease ($p<0.0001$) in adhesion of Caco-2 cells to HUVECs. HUVEC uncoated cells were used as Caco-2 cells control. Unspecific IgG antibody was used as antibody control.

The data obtained (Figure 3.44) indicate that Caco-2 cell adhesion to endothelial cells was significantly lower in the differentiated cells when compared to the undifferentiated cells (***$P < 0.001$). In the presence of increasing amounts of the ICAM-1 antibody, which could bind to the ICAM-1 protein and thereby prevent its interactions with its ligands on the endothelial cells, the undifferentiated Caco-2 cells could adhere significantly less (***$P < 0.001$) to the HUVEC cells. Furthermore, the specificity of the reaction was confirmed by the addition of an unspecific IgG antibody which did not lead to any decrease in the adhesion. Additionally, both Caco-2 and HUVEC cells were necessary for the interaction, since incubation of the Caco-2 cells with ICAM-1 antibody in wells where there were no HUVEC cells did not lead to any decrease in cell-cell interaction.

Overall, we have shown here that the process of differentiation in Caco-2 cells led to an overall decrease in cell adhesion to fibronectin, a component of the extracellular matrix. The lower levels of ICAM-1 and VCAM-1 proteins in the differentiated cells were also reflected in the decrease in the adhesion of the Caco-2 cells to HUVEC cells. This epithelial-endothelial cell interaction is mediated by ICAM-1 since the interaction was significantly obstructed upon incubation of the Caco-2 cells with the ICAM-1 antibody and not with a non-specific IgG antibody.

SECTION II

MicroRNA 146a and Matrix Metalloproteinase-16

The intestinal epithelium, formed of a single layer of columnar cells, form projections (crypts) into the underlying connective tissue. These crypts house multipotent stem cell niches, which differentiate into absorptive cells, mucus producing goblet cells or endocrine cells as they move upwards towards the villi to be finally expelled into the lumen (Humphries & Wright 2008). As the cells differentiate, they not only lose their ability to proliferate, but also form tight junctions which prevent the paracellular movement of molecules, thereby providing the intestinal barrier function (Beaurepaire *et al.,* 2009). The importance of microRNAs in intestinal differentiation and function was recently demonstrated by knocking out Dicer1, a key enzyme in miRNA biogenesis, in the intestinal epithelium (McKenna *et al.,* 2010). These authors reported that the Dicer1 knockout mice had disorganized crypts with a loss of goblet cells and an increased inflammatory phenotype with greater neutrophil infiltration into the lamina propria and dramatic increases in paracellular permeability, indicating that miRNAs potentially regulate each of these functions in the intestine (McKenna *et al.,* 2010).

Of these miRNAs, *miR-146a*/b was shown to be highly expressed in differentiated cultured colonic epithelial cells, although no targets of the miRNA was reported in that study (Hino *et al.,* 2008). The *miR-146a* and *miR-146b* genes are on chromosomes 5 and 10 respectively, and differ by only 2 bases in the

3' region of their mature sequences (Taganov *et al.,* 2006). They thus may target similar mRNAs for translational repression or destabilization. *miR-146a*/b can be transcriptionally upregulated by NF-κB and targets the TLR4 pathway genes TNF receptor–associated factor 6 (TRAF6) and IL-1 receptor – associated kinase 1 (IRAK1), indicating the presence of a negative feedback loop (Taganov *et al.,* 2006). The importance of *miR-146a* in the intestine was highlighted in a recent study showing that tolerance to intestinal microbes in neonates was dependent on the loss of IRAK1 proteins by degradation in the proteasome and lysosome as well as its translational repression by *miR-146a*.

Interestingly, *miR-146a* and *miR-146b* have both been shown to inhibit the invasive potential in pancreatic cancer cells and brain glioma cells respectively, indicating a tumor suppressive nature (Ali *et al*., 2010; Xia *et al*., 2009). Matrix metalloprotease 16 (MMP16) was implicated as a target of *miR-146b* in mediating loss of invasiveness in the brain glioma cells (Xia *et al*., 2009).

Formation of the polarized cells during epithelial differentiation involves the activity of transcription factors, non-coding RNA mediated regulation, and contact with fibroblast and extracellular matrix proteins (Dalmasso *et al*., 2010; Simon-Assmann *et al*., 2007a). Based on the existing literature, we hypothesized that epithelial differentiation may be associated with altered levels of matrix metalloproteases (MMPs) and that the expression of these molecules may be regulated by miRNAs. MMPs are a large family of Zn dependent endopeptidases

which induce the degradation of extracellular matrix components and are highly implicated in motility of cells (Nelson *et al*., 2000).

3.9.1 *miR-146a* Expression in Spontaneously Differentiating Caco-2 Cells

Caco-2 cells were grown to confluency and the cells were collected at indicated days between Days 0 and 30 to reflect their increasing differentiation. mRNA was isolated from these cells and duplex reverse transcriptase and real time PCR reactions were carried out to determine the expression of *pre-miR-146a* and mature *miR-146a* over the course of differentiation (Figure 3.45).

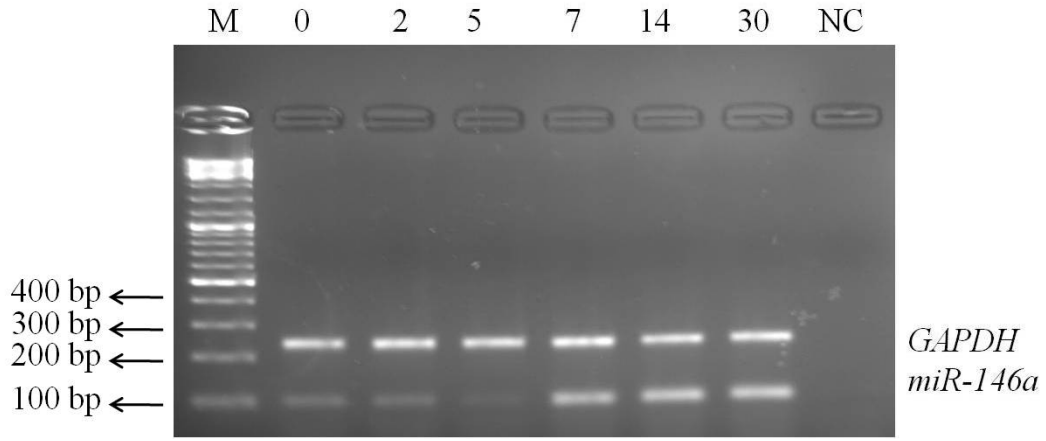

Figure 3.45 *Pre-miR146a* Expression in Spontaneously Differentiating Caco-2 Cells Lanes: M: GeneRuler™ DNA Ladder Mix (Fermentas), 0-30: days of post confluency, NC: Negative control. cDNAs were synthesized from 2µg DNAse I treated RNA by using random hexamer primer

As can be seen from the Figure 3.45, the expression of *pre-miR-146a* was found to increase in the course of spontaneous differentiation.

As *miR146a* and *miR-146b* have similar seed sequences, we wanted to determine whether *miR-146b* was also expressed in the differentiated cells.

5' - **ugagaacugaauuccauggguu** - 3' (length = 22) *miR-146a*

5' - **ugagaacugaauuccauaggcu** - 3' (length = 22) miR-146b

For that purpose, Caco-2 cells were grown to confluency and the cells were collected at indicated days between Days 0 and 30 to reflect their increasing differentiation. mRNA was isolated from these cells and duplex reverse transcriptase and real time PCR reactions were carried out to determine the expression of *pre-miR-146b* and mature *miR-146b* over the course of differentiation (Figure 3.45).

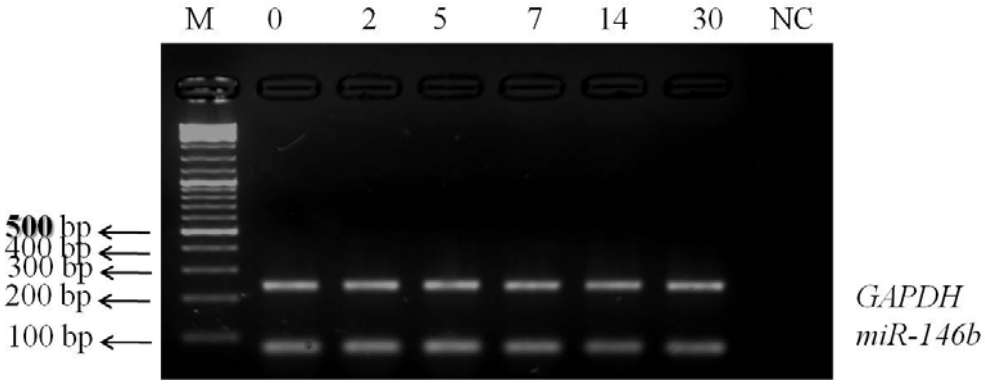

Figure 3.46 *Pre-miR146b* Expression in Spontaneously Differentiating Caco-2 Cells Lanes: M: GeneRuler™ DNA Ladder Mix (Fermentas), 0-30: days of post confluency, NC: Negative control. cDNAs were synthesized from 2µg DNAse I treated RNA by using random hexamer primer

After the PCR analysis, a it can be seen from Figure 3.46 *pre-miR-146b* expression is not changing during differentiation of Caco-2 cells.

The mature levels of *miR-146a* and *miR-146b* were analyzed with the TaqMan® probes, which entail reverse transcription with a miRNA-specific primer, followed by real-time PCR with TaqMan® probes. Using high quality RNA that was collected from Caco-2 cells at days 0, 2, 4, 7, 14, 30 after reaching 100% confluency and measured for purity using a Nanodrop, the expression of mature forms of both *miR-146a* and *miR-146b* were determined (Figure 3.47).

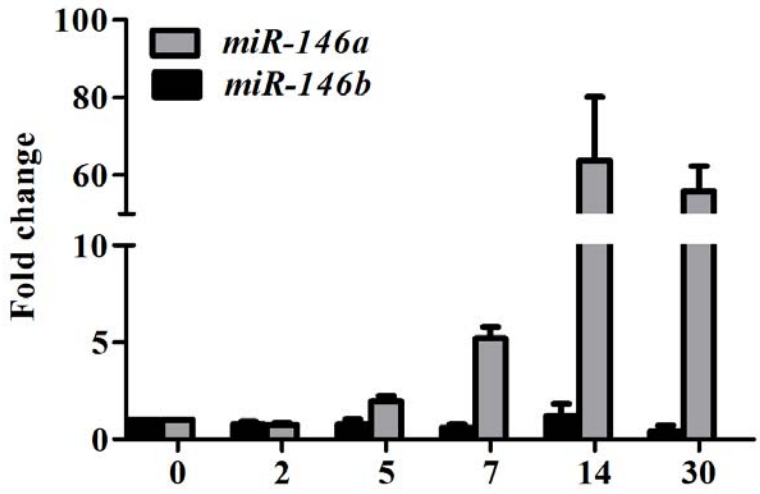

Figure 3.47: Mature *miR-146a* and *miR-146b* Expression in Spontaneously Differentiating Caco-2 Cells. 0-30: days of post confluency, cDNAs were synthesized from 30 ng DNAse I treated RNA by using gene specific primers. The data are displayed with mean ± standard deviation of three replicates. 14 and 30 Day differentiated Caco-2 cells showed significant increase ($p=0.0018$ and $p=0.0004$, respectively) in mature *miR-146a* expression.

The mature levels of *miR-146a* were found to increase dramatically over the course of differentiation, indicating that gene expression changes occurring in the course of differentiation may be regulated by *miR-146a*.

In Caco-2 differentiation Hino *et al.,* showed that *miR-146a* is increasing nearly 50 fold during the differentiation process (Hino *et al.*, 2008).

Our data indicate that although the expression of mature *miR-146b* also changes over the course of differentiation, the fold change in the differentiated cells is very low compared to the fold change in *miR-146a* (50 fold). Therefore, any regulation that we observe is most likely mediated by *miR-146a*.

3.9.2 MMP16 Expression during Spontaneous Differentiation of Caco-2 Cells

In order to determine the expression of *MMP16* in the course of differentiation, RT-PCR experiments were conducted using RNA samples from cells were grown for predesignated days after reaching confluency (Figure 3.48).

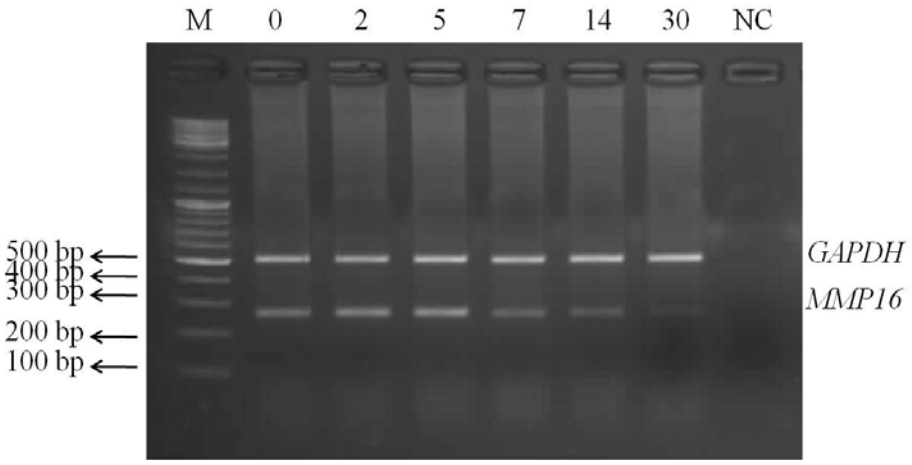

Figure 3.48: *MMP16* Expression in Spontaneous Differentiation of Caco-2 Cells. Lanes; M: GeneRuler™ DNA Ladder Mix (Fermentas), 0-30: Days of post-confluency, NC: Negative control. cDNAs were synthesized from 2µg DNAse I treated RNA by using oligo dT primers

As seen from Figure 3.48, *MMP16* expression decreased during spontaneous differentiation of Caco-2 cells. In order to determine whether the protein expression of MMP16 reflected the genes' mRNA expression, protein samples were collected from the post confluent Caco-2 cells and a Western blot was carried out against the MMP16 antibody. The membrane was stripped and reprobed with the GAPDH antibody to ensure equal protein loading (Figure 3.49).

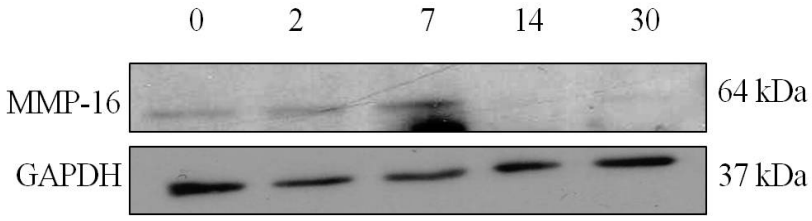

Figure 3.49: MMP16 Protein in Spontaneously Differentiating Caco-2 Cells. 0-30: Days of post-confluency. 80µg of proteins from each sample was loaded and transferred on PVDF membrane at 100V for 1 hour 45 minutes, 5% Skim milk in PBST was used as blocking agent. Antibody Dilutions: Anti-MMP16 1:200, Anti-GAPDH 1:1000, Anti-Rabbit-HRP 1:2000, Anti-mouse-HRP 1:2000; All incubations were carried out at 4°C overnight except secondary antibodies which were carried out at room temperature for 1 hour with gentle agitation in the presence of blocking agent. Proteins were probed against GAPDH as loading control after stripping.

Western blot analysis (Figure 3.49) indicated that MMP16 protein levels decreased in the course of spontaneous differentiation.

Having established that the levels of mature *miR-146a* increased and the mRNA and protein expression of MMP16 decreased in the course of differentiation in Caco-2 cells, we wanted to confirm whether the expression of MMP16 was regulated by *miR-146a*.

3.9.3 3' UTR Analysis *MMP16* Gene in Spontaneously Differentiating Caco-2 Cells

MMP16 is regulated by *miR-146a* during differentiation

Since MMP16 has previously been shown to be regulated by miRNAs by mRNA destabilization (Xia *et al*., 2009), we decided to examine miRNA binding to the 3'UTR of *MMP16* using bioinformatics approaches. TargetScan 5.0 (R. C. Friedman *et al.,* 2009) and Probability of Interaction by Target Accessibility (PITA) (Kertesz *et al.,* 2007) predicted a single binding site of *miR-146a* containing a poorly conserved 7-mer exact seed match at positions 1475-1481 on the 3'UTR of MMP16 (Figure 3.50)

Position 1479-1485 of MMP16 3' UTR	5' ...UUGCAUGUCCACCAUAGUUCUCA...
hsa-*miR-146a*	3' UUGGGUACCUUAAG--UCAAGAGU

Figure 3.50: Bioinformatics Analysis of the Predicted Interactions of *miR-146a* with Their Binding Sites at the 3′UTR of *MMP16* (Targetscan)

In order to confirm whether MMP16 is a target of *miR-146a*, we cloned a 489 bp region from the 3'UTR of MMP16 containing the predicted binding site of *miR-146a* or a mutated sequence into the pMIR-REPORT vector to generate the pMIRMMP16 or the pMIRMMP16_mut constructs. These vectors were

separately transfected into Caco-2 cells that were at Day 0 or Day 10 of differentiation after reaching 100% confluency.

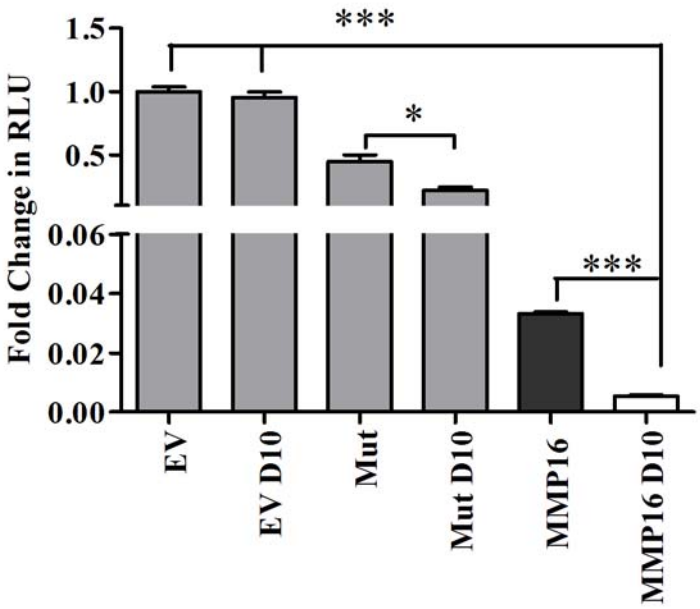

Figure 3.51: *MMP16* 3'UTR Activity in Spontaneously Differentiating Caco-2 Cells. 0 Day (black bar) and 10 day (white bar) confluent Caco-2 cells were transfected with pMIR-REPORT containing 3' UTR Region of *MMP16* gene (MMP16) along with Empty Vector (EV) and Mutated *miR-146a* binding site containing vector (Mut). 24 hours posttransfection, proteins were extracted with 1X CLB buffer and luciferase activities were measured with 20µl of the extracts. Beta–galactosidase activity was used for normalization. The data are displayed with mean ± standard deviation of three replicates. Day 10 confluent cells (white bar) displayed significantly lower (p=0.0001) *MMP16* UTR activity compared to Day 0 confluent cells (black bar)

We have observed a significant decrease in the luciferase signal (***P<0.0001) when the Day 0 or Day 10 cells were transfected with the pMIRMMP16 vector compared to the empty vector (EV) transfected cells (Figure 3.51). More importantly, a significant decrease in luciferase activity was observed in the Day 10 cells compared to the Day 0 cells transfected with the

pMIRMMP16 vector (***P<0.0001), indicating a stronger repression of *MMP16* in the differentiated (Day10) cells when compared to the undifferentiated cells (Day 0). We have also observed a significant decrease in the luciferase activity when the cells were transfected with the pMIRMMP16_mut vector containing the mutated binding site for *miR-146a* (*P=0.0203). This may have been due to the presence of other miRNA binding sites in the cloned region of the 3'UTR of MMP16. For all luciferase reporter gene assays, β-galactosidase activity was measured and used for normalization. Taken together, our data suggest that MMP16 is regulated by miRNAs in spontaneously differentiating Caco-2 cells and that *miR-146a* is a strong candidate for this regulation.

3.9.4 Overexpression of *MiR-146a* in Caco-2 Cells

In order to further verify the regulation of *MMP16* by *miR-146a*, we cloned the *miR-146a* gene (pSPR*miR-146a*) and its mutated counterpart (pSPR*miR-146a*_mut) into a pSUPER vector and overexpressed it in Caco-2 cells at Day 0 of reaching 100% confluency. At this stage of differentiation, the MMP16 expression was found to be high (Figure 3.52).

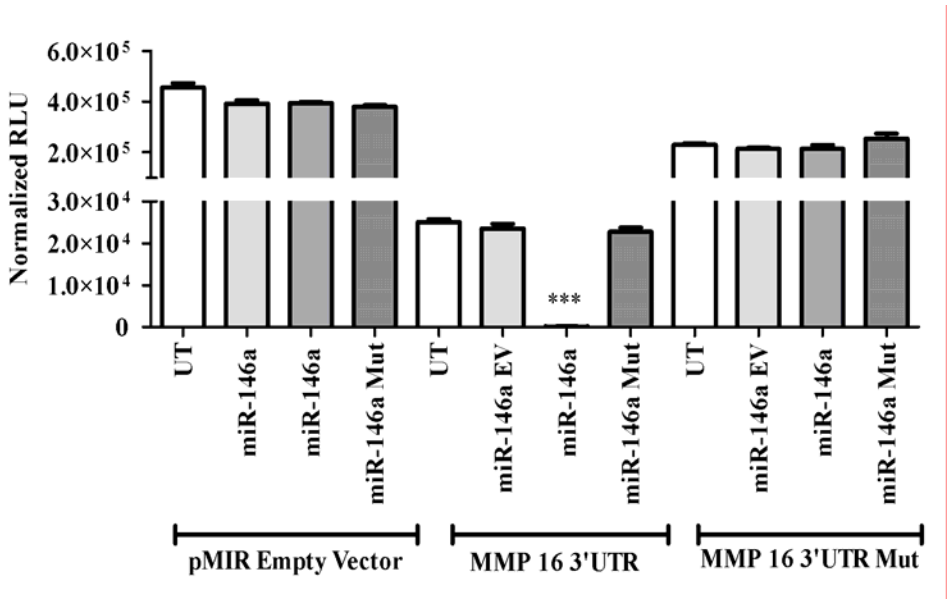

Figure 3.52: *MMP16* 3' UTR Analysis in *miR146a* Overexpressed Caco-2 Cells. Day 0 confluent Caco-2 cells were transfected with pMIR-REPORT containing 3' UTR Region of *MMP16* gene (MMP16 3' UTR) along with pMIR Empty Vector and Mutated *miR-146a* binding site containing vector (MMP 16 3' UTR Mut). Overexpression of *miR-146a* was sustained with transfecting the 0 Day confluent cells with P-SUPER with *miR-146a* (*miR-146a*). As controls mutated and empty vector (*miR-146a* EV, *miR-146a* Mut) counterparts were also transfected. 24 hours post-transfection, proteins were extracted with 1X CLB buffer and luciferase activities were measured with 20µl of the extracts. Beta–galactosidase activity was used for normalization. The data are displayed with mean ± standard deviation of three replicates. *miR146a* transfected cells showed significantly lower (p=0.0001) MMP16 UTR activity compared to untransfected cells (white bar, MMP16 3' UTR).

Our data indicate that when the Caco-2 cells were co-transfected pMIRMMP16 and the pSUPER*miR-146a* vectors, a significant decrease in the luciferase activity was observed (***P<0.0001) (Figure 3.52). No significant change was observed when the cells were co-transfected with the pMIRMMP16 and pSUPER*miR-146a*_mut vectors, indicating that it was necessary to

overexpress the intact miRNA in order to regulate MMP16. Additionally, when the cells were transfected with the empty pMIR-REPORT vector, or the pMIRMMP16_mut vector in cells overexpressing (or not) *miR-146a* or its mutated version, no change in the luciferase activity was observed, further emphasizing the necessity for intact binding between *miR-146a* and the 3'UTR of MMP16 for successful regulation. For all luciferase reporter gene assays, β-galactosidase activity was measured and used for normalization.

We next wanted to determine whether the overexpression of *miR-146a* affected the expression of MMP16 in Caco-2 cells. We first confirmed the overexpression of *pre-miR-146a* and its mutated counterpart in Day 0 postconfluent Caco-2 cells by coamplifying pre-*miR-146a* and GAPDH in a duplex RT-PCR (Figure 3.53).

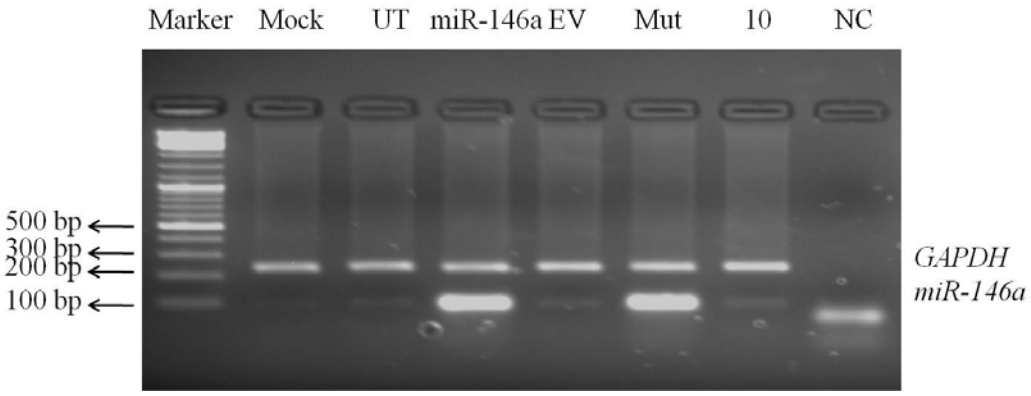

Figure 3.53: Forced Expression of *pre-miR-146a* in Undifferentiated Caco-2 Cells. Lanes: Marker: GeneRuler™ DNA Ladder Mix (Fermentas) , UT: Untransfected, *miR-146a*: Cells transfected with P-SUPER with *miR-146a*, EV: Empty Vector (P-SUPER), Mut: Mutated *miR-146a*, 10: Day 10 post confluent Caco-2 cells, NC: Negative control. cDNAs were synthesized from 2µg DNAse I treated RNA by using random hexamer primer

As can be seen from Figure 3.53, *pre-miR-146a* as well as its mutated form could be successfully overexpressed in Caco-2 cells. We further confirmed that the mature *miR-146a* was also overexpressed using the TaqMan probe based assay in real time PCR.

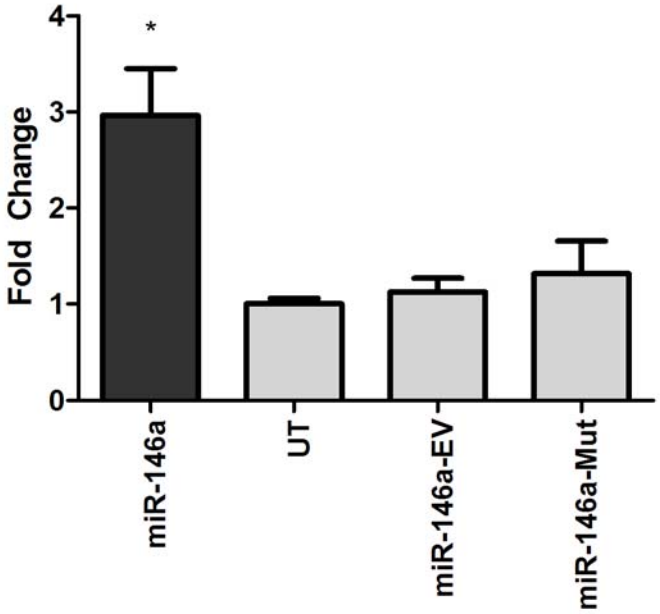

Figure 3.54: Mature *miR-146a* Overexpression in Undifferentiated Caco-2 Cells. UT: Untransfected, *MiR-146a*: Cells transfected with P-SUPER with *miR-146a*, EV: Empty Vector (P-SUPER), Mut: Cells transfected with mutated *miR-146a* vector. Cells were transfected for 24 hours and RNA samples were collected. cDNAs were synthesized from 30 ng DNAse I treated RNA with gene specific primers. Normalization was done with RNU6 amplification. The data are displayed with mean ± standard deviation of three replicates. *miR-146a* transfected cells (black bar) showed significantly higher (p=0.0163) Mature *miR-146a* expression compared to untransfected cells.

Figure 3.54 indicates that mature *miR-146a* levels were significantly (*$p<0.01$) higher in the Caco-2 cells transfected with the *miR-146a* expression vector.

Having established a *miR-146a* overexpressing cell line, we next determined whether the microRNA would regulate MMP16 expression (Figure 3.55).

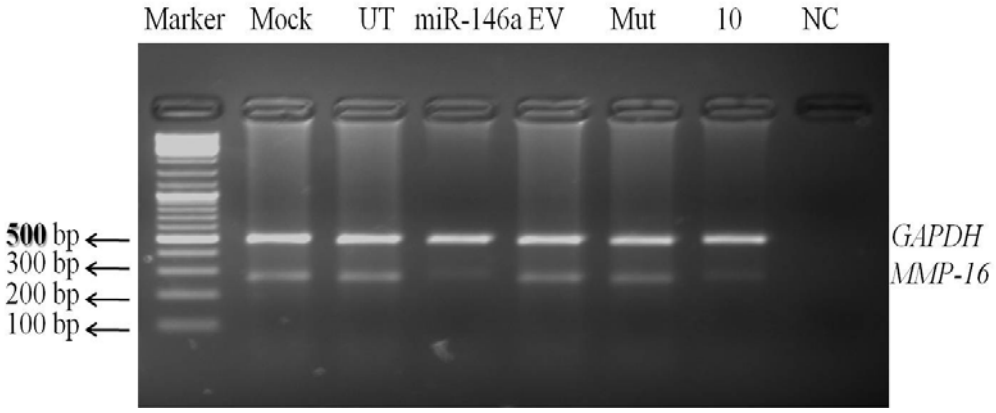

Figure 3.55: *MMP16* Expression in *miR-146a* Overexpressed Caco-2 Cells. Lanes; Marker: GeneRuler™ DNA Ladder Mix (Fermentas), Mock: Cells treated with transfection agent only, UT: Untransfected, *miR-146a*: *miR-146a*: Cells transfected with P-SUPER with *miR-146a*, EV: Empty Vector (P-SUPER), Mut: Mutated *miR-146a*,10: Day 10 post confluent Caco-2 cells, NC: Negative control. cDNAs were synthesized from 2µg DNAse I treated RNA by using random hexamer primer

The overexpression of *miR-146a* was observed to accompany a decrease in the expression of *MMP16* mRNA (Figure 3.55). However, no such decrease in *MMP16* expression was observed when the Caco-2 cells were overexpressed with the mutated *miR-146a* counterpart further confirming the specificity of the regulation. No change in expression of *MMP16* was observed in the pSUPER empty vector transfected, untransfected or mock transfected control cells. We next determined the protein levels of MMP16 in *miR-146a* overexpressing Caco-2 cells.

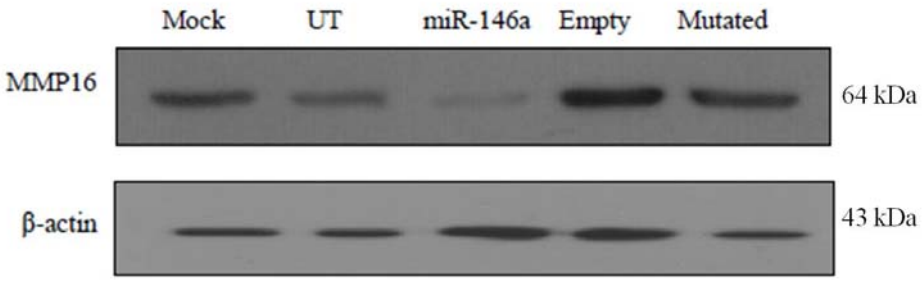

Figure 3.56: MMP16 Protein Expression in *miR146a* Overexpressing Caco-2 Cells. Mock: Cells treated with transfection agent only, UT: Untransfected, *miR-146a*: Cells transfected with P-SUPER with *miR-146a*, Empty: Empty Vector (P-SUPER), Mutated: Mutated *miR-146a*. 80µg of proteins from each sample was loaded and transferred on PVDF membrane at 100V for 1 hour 45 minutes, 3% Skim milk in PBST was used as blocking agent. Antibody Dilutions: Anti-MMP16 1:200, Anti-β-Actin 1:1000, Anti-Rabbit-HRP 1:2000, Anti-Mouse HRP 1:2000; All incubations were carried out at 4°C overnight except Anti-rabbit-HRP and Anti-Mouse-HRP which were carried out at room temperature for 1 hour with gentle agitation in the presence of blocking agent. Proteins were probed against β-actin as loading control after stripping.

In order to determine the expression of MMP16 at the protein level, Caco-2 cells were separately transfected with the *miR-146a* overexpression vector (pSPR*miR-146a*), its mutated counterpart (pSPR*miR-146a*_mut) or the pSUPER empty vector and collected for protein isolation. Western blot of these proteins with an anti-MMP16 antibody indicated a loss of MMP16 protein level in the *miR-146a* overexpressing cells, but not in the control cells transfected with the mutated *miR-146a* overexpressing vector or the empty pSUPER vector (Figure 3.56).

Taken together we have established that *miR-146a* expression could decrease the expression of MMP16 at both mRNA and protein levels.

3.9.5 *miR-146a* expressing cells show an inhibition of MMP16 activity

MMP16 (MT3-MMP) is a membrane type metalloprotease that functions in activating proMMP-2 (gelatinase A) into its active form as the zymogen is excreted out of the cell (Nakada *et al*., 1999). Therefore, a zymogram depicting the gelatinase activity of activated MMP-2 would be an indirect mechanism of determining the activity of MMP16. We therefore transfected the *miR-146a* overexpression vector or its mutated counterpart in Day 0 postconfluent Caco-2 cells for 48h and collected the conditioned medium. The medium was then concentrated and prepared zymography as described in Materials and methods. Our data (Figure 3.57) indicate that the *miR-146a* overexpressing cells exhibited lower gelatinase activity (lane 3) with respect to the cells transfected with the mutated plasmid, the mock transfected or the untransfected counterparts. Additionally, we have also shown that the gelatinase activity was considerably low on the Day 10 differentiated postconfluent cells, which corroborates to a loss of MMP16 owing to an increase in *miR-146a* levels.

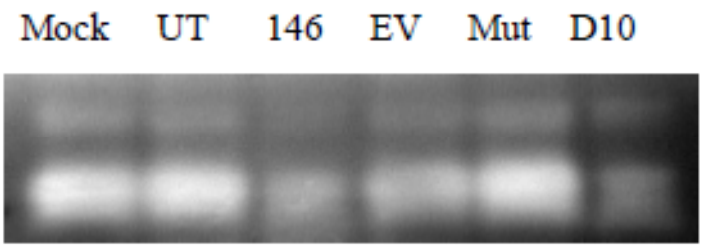

Figure 3.57: Zymography Analysis of *miR-146a* Overexpressing Caco-2 Cells. Lanes: Mock: Transfection agent only, UT: Untransfected, 146: p-Super with *miR-146a*, EV: P-super empty vector, Mut: P-super carrying mutated *miR-146a*, D10: Untransfected 10 day confluent Caco-2 cells. 96 hours after transfection conditioned media were collected and concentrated with acetone precipitation. Samples were run in native conditions in 10% SDS-PAGE which was co-polymerized with gelatin (0.15%). Gels were treated with Triton-X-100 to remove the SDS, then developed for 48 hours in developing buffer. After washing, gels were stained in (0.5% Coomassie Brilliant Blue) and destained.

Zymography analysis showed a remarkable decrease in the gelatinase activity of Caco-2 cells transfected with *miR-146a* overexpression vector with respect to mock, untransfected, empty vector and mutated vector-transfected cells (Figure 3.57). In the differentiated cells, the gelatinase activity also seemed to be decreasing which was regarded as a natural consequence of differentiation. Membrane type metalloproteases such as MMP16 (MT3-MMP) are known to activate the zymogen of MMP-2 as it is extruded out of the cell. MMP-2, along with MMP-9 are the two main proteases that can cleave collagen IV of the basement membrane and are therefore implicated in tissue migration associated with development and diseases states such as cancer metastasis (Rowe and Weiss, 2008). It is therefore not surprising that MMP16 expression has been associated with increasing invasiveness in gastric cancer (Lowy *et al*., 2006), hepatocellular

carcinoma (Arai *et al*., 2007), prostate cancer (Daja *et al*., 2003) as well as melanoma cells (Ohnishi *et al*., 2001).

To examine whether *miR-146a* could affect the invasion of cancer cells, we ectopically expressed *miR-146a* in HT-29 cells and carried out a Transwell invasion assay through Matrigel. Caco-2 cells, although isolated from a colorectal cancer, do not have the ability to invade and migrate through Transwells (data not shown). We therefore selected the HT-29 cell line which can also differentiate, but does not show any increase in *miR-146a* expression in the differentiated cells. After having confirmed the *miR-146a* overexpression and MMP16 repression in *miR-146a* transfected HT-29 cells (Figure 3.58 and 3.59), results obtained showed that overexpression of *miR-146a* inhibited HT-29 cell invasion *in-vitro* (Figure 3.60).

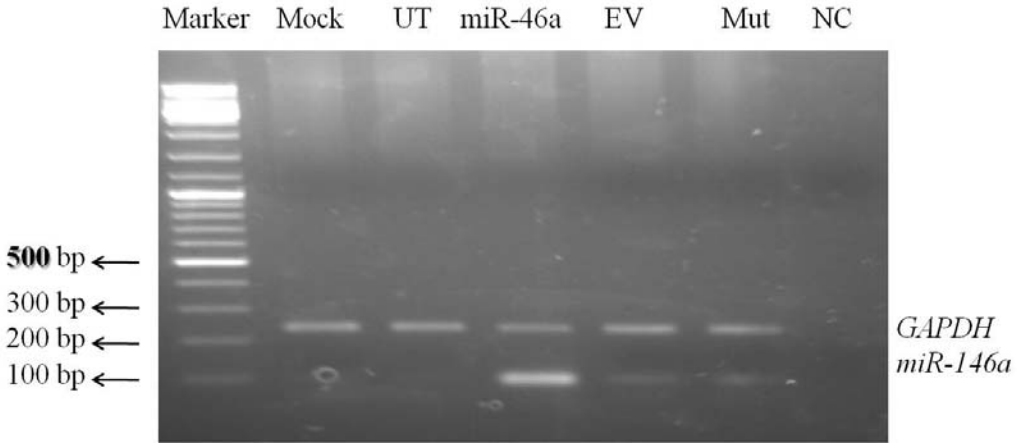

Figure 3.58 Confirmation of Overexpression of *pre-miR-146a* in Undifferentiated (Day 0) Confluent HT-29 Cells. Lanes: Marker: GeneRuler™ DNA Ladder Mix (Fermentas), Mock: Transfection agent only, UT: Untransfected, *MiR-146a*: Cells transfected with P-SUPER with *miR-146a*, EV: Empty Vector (P-SUPER), Mut: Mutated *miR-146a*, NC: Negative control. cDNAs were synthesized from 2µg DNAse I treated RNA by using random hexamer primer

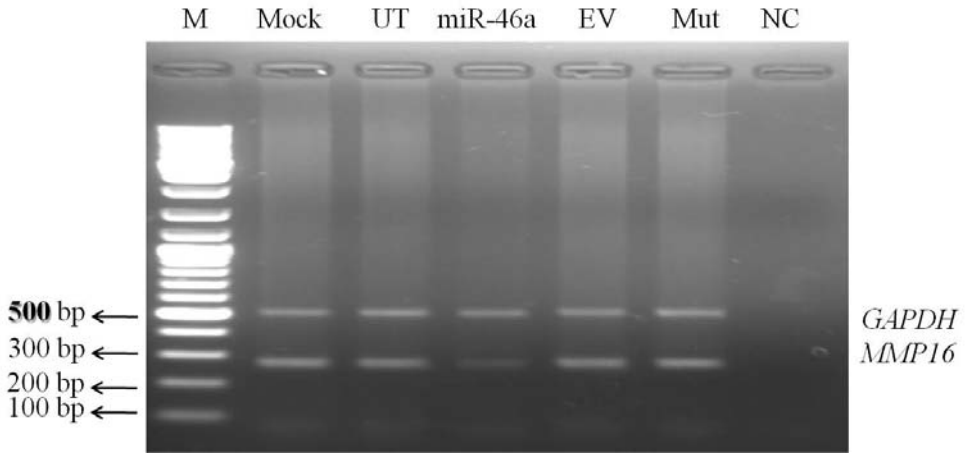

Figure 3.59 *MMP16* Expression in *miR-146a* Transfected HT-29 Cells. Lanes: M: GeneRuler™ DNA Ladder Mix (Fermentas), Mock: Transfection agent only, UT: Untransfected, *MiR-146a*: Cells transfected with P-SUPER with *miR-146a*, EV: Empty Vector (P-SUPER), Mut: Mutated *miR-146a*, NC: Negative control. cDNAs were synthesized from 2µg DNAse I treated RNA by using random hexamer primer

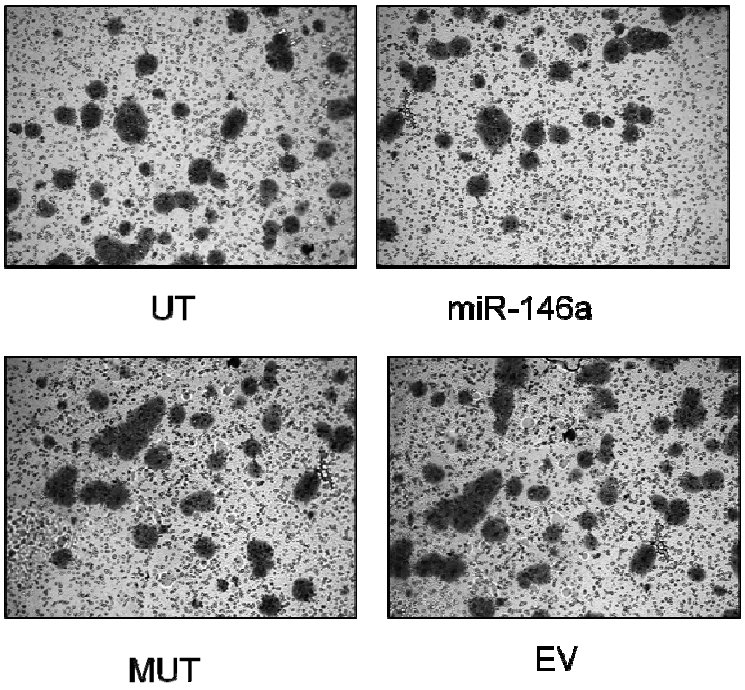

Figure 3.60: Matrigel Invasion Assay of *miR-146a* Overexpressing HT-29 Cells. Cells were transfected with *miR-146a* Overexpression vector (*miR-146a*), Mutated (Mut) or Empty Vector (EV). 24 hours after transfection cells were moved into the transwells with matrigel. After incubation for 96 hours, membranes were cleaned, cut, fixed and stained and counted under microscope. Picture shows the representative images of three independent experiments.

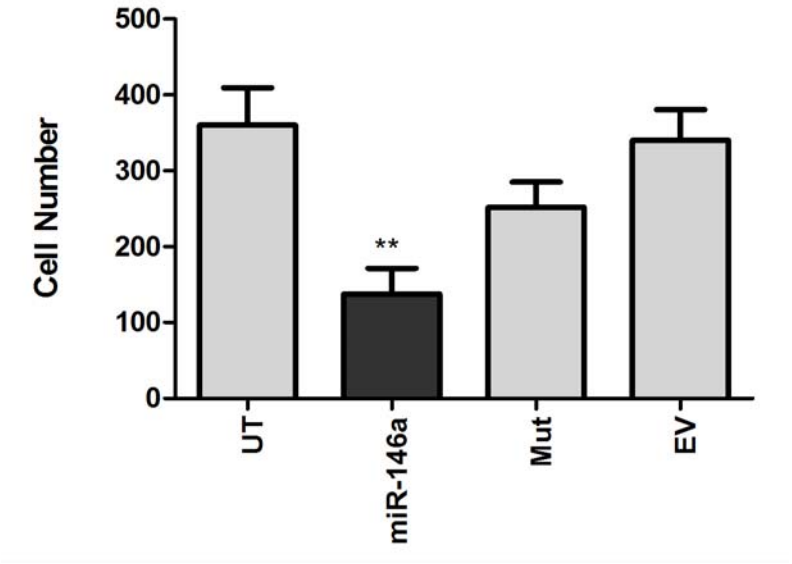

Figure 3.61: Quantitative Analysis of Matrigel Invasion Assays. Cells were transfected with *miR-146a* Overexpression vector (*miR-146a*), Mutated (Mut) or Empty Vector (EV). 24 hours after transfection cells were moved into the transwells with matrigel. After incubation for 96 hours, membranes were cleaned, cut, fixed and stained and counted under microscope. The data are displayed with mean ± standard deviation of three independent experiments. *miR146a* transfected cells (black bar) showed significantly lower (p=0.003) invasion compared to untransfected cells.

Matrigel assays showed a significant decrease in HT-29 cells transfected with *miR-146a* overexpression vector with respect to the empty and mutated vector counterparts (Figure 3.60, 3.61). Since *MMP16* is one of the three membrane type matrix metalloproteinase which can activate the zymogen form of the MMPs involved in the invasion and metastasis such as MMP-2 and MMP-9 (Nakada *et al.,* 1999) it is not surprising that decrease in the *MMP16* levels via overexpression of *miR-146a* resulted in a significant decrease in the invasion of HT-29 cells. Taken together with the zymogram analysis *miR-146a* inhibits the invasion of HT-29 cells in vitro.

Differentiated Caco-2 cells lack MMP16 expression, which could be due to the candidate regulator *miR-146a*. This data illustrates the mechanism underlying the loss of the mobility in differentiated cells compared to transformed cells and may provide an insight about designing the potential therapeutics by non-coding RNA mediated silencing of MMP16 in metastatic tumors.

In conclusion, we have shown here for the first time that differentiated Caco-2 cells, that closely resemble enterocytic cells, lack the expression of MMP16, a critical matrix metalloprotease, and that one of candidates for this regulation is *miR-146a*. This data not only highlights a mechanism behind the loss of motility and migration of differentiated cells compared to transformed cells, but also provides potential opportunities for therapeutic intervention by non-coding RNA mediated silencing of *MMP16* in metastatic tumors.

SECTION III

Activation of PPAR gamma by 15-Lipoxygenase I Inhibits Nuclear Factor Kappa B

15-lipoxygenase-1 (15-LOX-1) belongs to eicosanoid pathway and in colorectal cancer its expression is lost (Cuendet & Pezzuto 2000; Jones *et al.,* 2003; Pidgeon *et al.,* 2007). We have hypothesized that NF-κB may be inhibited by the anti-tumorigenic actions of 15-LOX-1. As the 15-LOX-1 enzymatic product 13(S)-HODE is known to be one of the PPARgamma (PPARγ) ligands (Bull *et al.,* 2003; J. B. Nixon *et al.,* 2003), and NF-κB can be inhibited by PPARγ, we examined whether activation of PPARγ was necessary for the abrogation of NF-κB activity.

We examined the phosphorylation of IκBα protein in 15-LOX-1 expressing HT-29 cells (Figure 3.62).

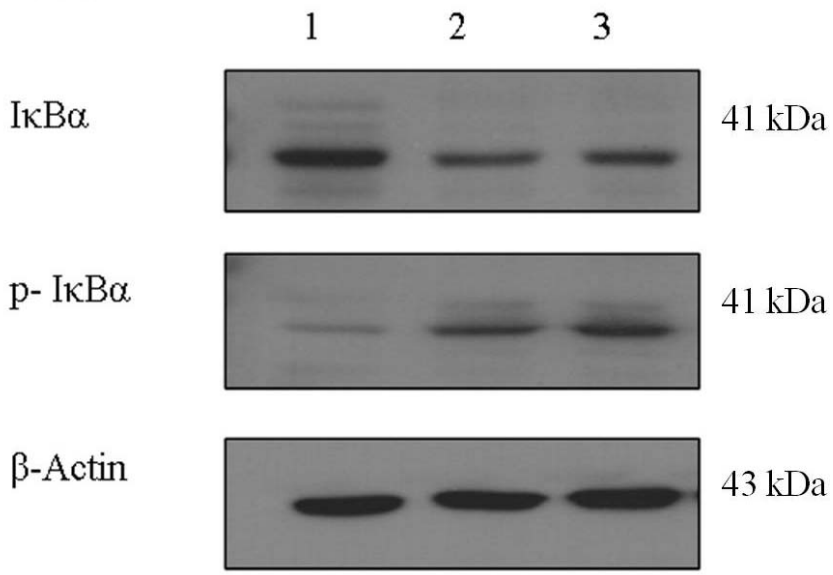

Figure 3.62: Phospho-IκBα in 15-LOX-1 Expressing HT-29 Cells. Lanes; 1: 15LOX1 transfected cells, 2: Empty Vector, 3: 15LOX1 Transfected and 15LOX1 inhibitor PD146176 (1μM) treated cells. 80μg of proteins from each sample was loaded and transferred on PVDF membrane at 100V for 1 hour 45 minutes, 10% Skim milk in PBST was used as blocking agent. Antibody Dilutions: Anti-p-IκBα 1:500, Anti-IκBα 1:500, Anti-β-Actin 1:1000 Anti-Mouse-HRP 1:2000, Anti-Rabbit-HRP 1:2000; All primary antibody incubations were carried out at 4°C overnight in the presence of blocking agent except secondary antibodies (room temperature 1h with gentle agitation).

Our data indicate a higher level of IκBα in 15LOX1 expressing HT-29 cells when compared to empty vector transfected cells. Additionally, the phosphorylated form of IκBα was found to be much lower in the 15LOX1 expressing cells when compared to the control cells, indicating that degradation of IκBα and release of active NF-κB was inhibited when 15LOX1 was expressed. When the 15LOX1 expressing cells were treated with 1μM PD146176 and probed

for the expression of IκBα and its phosphorylated form, we observed a reduction of IκBα level along with an increase in its phosphorylated form compared to EV and inhibitor treated cells. This further confirms that the retention of the NF-κB subunits by IκBα in the cytoplasm most likely resulted from the expression of 15LOX1 (Figure 3.62).

Additionally, we carried out a non-radioactive EMSA to determine binding of the NF-κB subunits to the κB consensus oligonucleotides (Figure 3.63). For this purpose, nuclear extracts were isolated from cells transfected either stably (HCT-116) or transiently (HT-29) with the 15LOX1vector. The proteins were then incubated with the biotin labeled κB consensus oligonucleotides and processed for EMSA as described in the Materials and Methods.

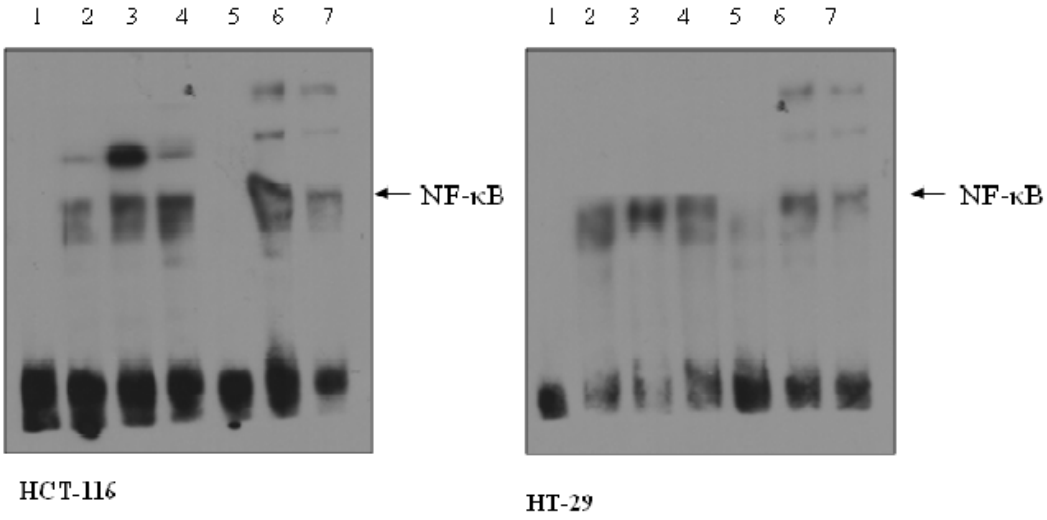

Figure 3.63: EMSA of Stable (HCT-116) and Transiently (HT-29) 15LOX1 Transfected Cells. Lanes; 1: free probe, 2: 15LOX1 expressing cells, 3: 15LOX1 expressing cells treated with PD146176, 4: Empty vector transfected cells, 5: reaction mixture incubated with 200 fold excess cold probe, 6: Supershift with p65 antibody, 7: supershift with p50 antibody. For all binding reactions 5µg of the nuclear extracts obtained cells were used. Binding reactions were prepared and incubated on ice for 10 minutes and at room temperature for 20 min after which the oligos and Anti-p50 (3µl) or Anti-p65 antibody was added and incubated for a further 10 min at room temperature. Samples were separated in 8% polyacrylamide gel prepared with TBE transferred on to a nylon membrane (Biodyne, precut B Nylon membrane, Pierce, USA) for 45 minutes at 4°C. After crosslinking, membranes were treated according to the instructions of the manufacturer

The data (Figure 3.63) indicate that expression of 15LOX1 resulted in reduced mobility shift and thereby reduced κB consensus DNA binding *in-vitro* when compared to empty vector transfected or 15LOX1 expressing cells treated with specific inhibitor PD146176. Additionally, for both cell lines, the specificity of the reaction was confirmed by incubating the reaction mixture with 200 fold

excess of the cold probe which resulted in a loss of mobility shift (Figure 3.63, Lane 5 Left and Right Panels), as well as by incubating with 2µl of p65 and p50 antibodies which resulted in a supershift (lanes 7 and 8 respectively, left and right panels).

In order to determine whether PPARγ is involved in the inhibition of NF-κB DNA binding in the 15LOX1 expressing cells, we conducted EMSA to determine nuclear DNA binding.

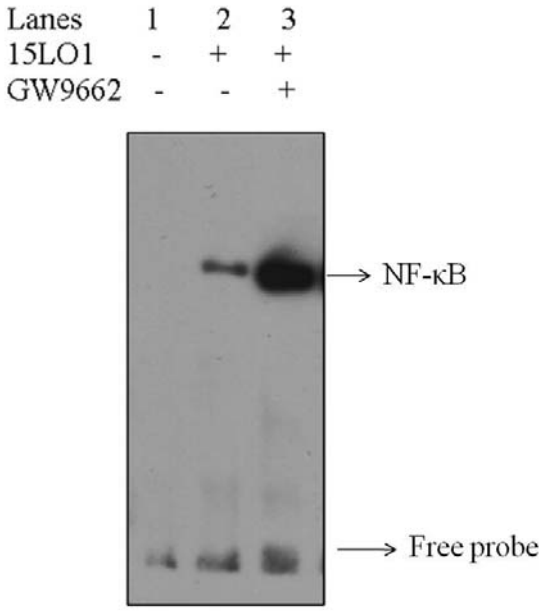

Figure 3.64: NF-κB EMSA of 15LOX1 Transfected Cells Treated with PPARγ Inhibitor GW 9662. Lanes; 1: Free probe, 2: 15LOX1 expressing cells, 3: 15LOX1 expressing cells treated with 1μM GW9662. For all binding reactions 5μg of the nuclear extracts obtained cells were used. Binding reactions were prepared and incubated on ice for 10 minutes and at room temperature for 20 min after which the oligos were added and incubated for a further 10 min at room temperature. Samples were separated in 8% polyacrylamide gel prepared with TBE transferred on to a nylon membrane (Biodyne, precut B Nylon membrane, Pierce, USA) for 45 minutes at 4°C. After crosslinking, membranes were treated according to the instructions of the manufacturer

Data (Figure 3.64) indicated that pretreatment of the cells with 1μM of the PPARγ antagonist GW9662 (lane 3) could revert the inhibition in DNA binding observed with the expression of 15LOX1

Previous reports have indicated that treatment of HCT-116 CRC cells and PC3 prostate cancer cells with 13(S)-HODE could increase PPARγ

phosphorylation and that this phosphorylation was mediated by extracellular signal regulated kinase (ERK) 1/2 (L C Hsi *et al.,* 2001; Linda C Hsi *et al.,* 2002). Additionally, phosphorylated PPARγ has been shown to inhibit NF-κB (F. Chen *et al.,* 2003). We therefore examined the phosphorylation status of PPARγ and ERK1/2 in HCT-116 cells stably expressing 15LOX1 (Figure 3.65). As the HCT-116 cell line has a mutation in *Ras*, the MAPK pathway is constitutively active in these cells.

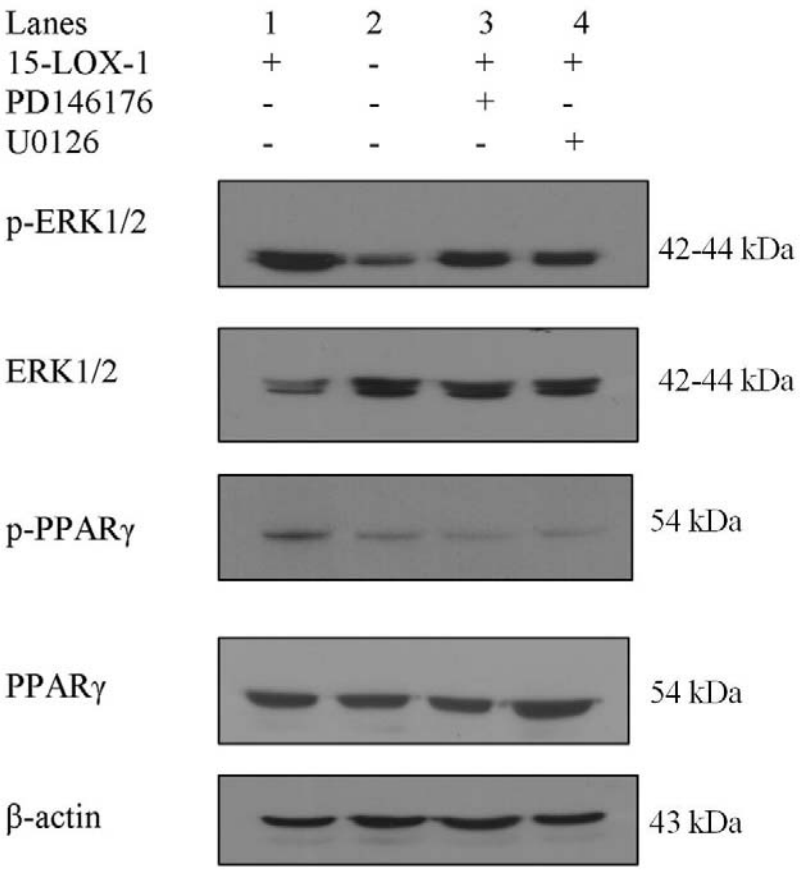

Figure 3.65: 15LOX1 Expression Results in Phosphorylation of ERK1/2 and PPARγ. Lanes; 1: 15LOX1 Expressing Cells, 2: Empty Vector Cells, 3: 15LOX1 expressing cells with PD146176 (1μM), 4: 15LOX1 expressing cells with ERK1/2 inhibitor U0126 (10μM). 80μg of proteins from each sample was loaded and transferred on PVDF membrane at 100V for 1 hour 45 minutes, 10% Skim milk in PBST was used as blocking agent. Antibody Dilutions: Anti-pERK1/2 1:500, Anti-ERK1/2 1:500, Anti-PPARγ: 1/500, Anti-p-PPARγ 1:500, Anti-β-Actin 1:1000 Anti-Mouse-HRP 1:2000, Anti-Rabbit-HRP 1:2000; All primary antibody incubations were carried out at 4°C overnight in the presence of blocking agent except secondary antibodies (room temperature 1h with gentle agitation).

Whole cell extracts were probed with the ERK1/2, p-ERK1/2, PPARγ and p-PPARγ antibodies. Increased phosphorylation of ERK1/2 and PPARγ was

observed in 15LOX1 expressing cells (Figure 3.65, lane 1) when compared to the control empty vector transfected cells (lane 2). Treatment of 15LOX1 expressing cells with PD146176 (1μM, lane 3) or with the ERK1/2 inhibitor U0126 (10μM, lane 4) reversed the phosphorylation of both proteins. Total ERK1/2 was seen to decrease in the 15LOX1 expressing cells (lane 1) when compared to the control cells (lane 2). No change in total PPARγ expression was observed with 15LOX1 expression

Western blot using an antibody against phosphorylated ERK1/2 indicated increased phosphorylation in cells that express 15LOX1 (lane 1) compared to empty vector transfected cells (lane 2).This phosphorylation was decreased when the 1E7 cells were treated with the 15LOX1 specific inhibitor PD146176 (lane 3). Additionally, treatment of 15LOX1 expressing cells with the ERK1/2 inhibitor U0126 decreased the phosphorylation of ERK1/2. When the proteins were probed with an antibody against p-PPARγ, the phosphorylation of PPARγ was seen to be higher in the 15LOX1 expressing cells (lane 1) when compared to the empty vector transfected cells (lane 2). Treatment with both PD146176 and U0126 could reduce the phosphorylation of PPARγ, indicating that the phosphorylation was a specific effect of 15LOX1 expression and that it was via the kinase activity of ERK1/2. The levels of total PPARγ were stable in 15LOX1 expressing and control cells. Interestingly, the levels of total ERK1/2 were seen to be lower in the 15LOX1 expressing cells when compared to the empty vector transfected cells.

Thus, although overall ERK1/2 levels are seen to decrease in 15LOX1 expressing cells, this ERK1/2 appears to be more active, with PPARγ as one of its targets.

Taken together, we have shown in this study that: (i) 15LOX1 expression increases the cytoplasmic levels of IκBα and decreases its phosphorylation reversed by incubation with the 15LOX1 specific inhibitor PD146176 and the PPARγ antagonist GW9662. 15LOX1 expression results in decreased binding of NF-κB subunits p50 and p65 to their consensus DNA binding sequences, which could be reversed by GW9662. Cells expressing 15LOX1 show increased phosphorylation of PPARγ via ERK1/2. Based on previous reports, this phosphorylated PPARγ may associate with p65 and inhibit NF-κB. These properties of 15LOX1 further emphasize the importance of this protein as a possible therapeutic option in colorectal carcinogenesis.

CONCLUSIONS

The intestinal epithelial layer consists of several cell types with distinct functions and arranged in a crypt-villus axis. In the small intestine, the bottom of the crypt contains Paneth cells and intestinal stem cells, whereas the remainder of the crypt consists of rapidly proliferating cells that are keys to the rapid renewal of the epithelium. As the cells reach the top of the crypt, they cease to proliferate and the cells differentiate into either secretory (goblet, Paneth and entero-endocrine) cells or enterocytes. The colon has a similar arrangement, differing by the lack of villi and the absence of Paneth cells in addition to the differentiated cells occupying a large part of the crypt (Medema and Vermeulen 2011).

PART I: Regulation of ICAM-1 and VCAM-1 in the course of differentiation

Using the Caco-2 colon cancer cell line that spontaneously undergoes differentiation upon reaching confluency to resemble enterocyte like cells (Simon-Assmann *et al.,* 2007); the expression and regulation of the inflammatory cell adhesion molecules ICAM-1 and VCAM-1 were examined in this study. Cell adhesion molecules are crucial in mediating cell-cell and cell to matrix interaction. As the cellular microenvironment is crucial in influencing cell fate, whether it is the ability of a cell to proliferate, differentiate, die, or undergo neoplastic transformation, understanding the regulation of cell adhesion

molecules during the process of cellular differentiation is of considerable significance.

The major outcomes of the study are as follows:

1- The mRNA expression of *ICAM1* was found to remain steady in the course of 30 days of spontaneous differentiation of Caco-2 cells, whereas *VCAM1* mRNA levels were seen to decrease over the same time interval. When the protein expression of these genes was studied, the protein levels of both ICAM-1 and VCAM-1 were seen to decrease in the course of spontaneous differentiation.
2- The regulation of *ICAM1* and *VCAM1* was determined at the
    a. Transcriptional levels – role of transcription factors NF-κB and C/EBPβ
    b. Post transcriptional level – role of microRNAs
    c. Post translational level – role of protein degradation pathways

Transcriptional regulation:

a) Regulation by NF-κB:

As both *ICAM1* and *VCAM1* are known to be transcriptionally regulated by NF-κB, a master regulation of inflammation and inflammatory cancers, NF-κB activation was determined during spontaneous differentiation

of Caco-2 cells. In the differentiated cells, NF-κB nuclear translocation, DNA binding and specific recruitment to the promoter of *ICAM1* and *VCAM1* and transcriptional activity were lower.

b) Cross-talk with PKC:

Incubation of the undifferentiated Caco-2 cells with an intracellular Ca^{++} inhibitor, TMB-8, resulted in the inhibition of NF-κB. A link with Protein Kinase C was therefore hypothesized. Several lines of evidence indicated that in the undifferentiated cells, Protein Kinase Cα (PKCα) activated PKCθ, which in turn activated IKK leading to the inhibition of IκBα and the activation of NF-κB. This entire axis was inhibited in the differentiated cells. This loss of NF-κB activity could explain the reduced expression of *VCAM1*. To explain the stable mRNA expression of *ICAM1* we explored the activation of other transcription factors.

c) Regulation by C/EBPβ

ICAM1 promoter was found to recruit C/EBPβ more in the differentiated cells, with a concurrent increase in the DNA binding and transcriptional activation of C/EBPβ. This indicated that the stable levels of ICAM-1 in the course of differentiation possible resulted from the increased transcriptional activity of C/EBPβ.

Posttranscriptional regulation:

As *ICAM1* showed stable mRNA expression over the course of differentiation with a decrease in its protein levels, we hypothesized microRNA mediated regulation. However, no miRNA regulation could be observed for the entire 3'UTR of the *ICAM1* gene in the course of differentiation of Caco-2 cells.

Posttranslational regulation:

Protein degradation pathway analyses indicated that both *ICAM1* and VCAM-1 were degraded in the lysosomes and by the proteasome, but not by a calpain mediated mechanism. Therefore, the protein levels of both ICAM-1 and VCAM-1 were decreased in the course of differentiation owing to post translational degradation mechanisms.

3- Functionally, a significant decrease in adhesion of differentiated Caco-2 cells to endothelial cells was observed. Co incubation with an ICAM-1 antibody, but not a non specific IgG resulted in a decrease in the adhesion, indicating that the interaction between Caco-2 cells and endothelial cells was mediated by ICAM-1.

PART II: Regulation of *MMP16* by *miR-146a* in the course of differentiation

MicroRNAs (miRNAs) are known to play a critical role in the regulation of gene expression of several thousand genes. We determined the regulation of MMP16 by *miR-146a* in the course of differentiation of Caco-2 cells.

The major findings were as follows:

a) The mRNA and protein expression of MMP16 was inversely correlated with the expression of mature *miR-146a*, but not *miR-146b* over 30 days of post confluent differentiation in Caco-2 cells.

b) Luciferase assays revealed that the intact *miR-146a* binding sequence but not the mutated one in the 3'UTR of *MMP16* could reduce luciferase gene transcription and translation, leading to reduced luciferase activity. This confirmed that *MMP16* was regulated by miRNAs and that *miR-146a* was a likely candidate.

c) Ectopic expression of *miR-146a*, but not a mutated construct, resulted in a decreased mRNA and protein expression of MMP16 in the undifferentiated confluent Caco-2 and HT-29 cells.

d) Ectopic expression of *miR-146a* decreased gelatinase activity of Caco-2 cells as determined by gelatin zymography. As MMP16 activates

the zymogens MMP-2 and MMP-9 both of which have gelatinase activity, this was an indirect indication of the functional significance of *miR-146a* mediated regulation of MMP16.

e) Transwell assays conducted in the presence or absence of Matrigel indicated that ectopic expression of *miR-146a* in HT-29 cells could reduce the invasion and migration of HT-29 cells.

PART III: 15-Lipoxygenase-1 inhibits NF-κB via PPARγ

15-lipoxygenase-1 (15LOX1) has been shown to have a tumor suppressive nature in colorectal cancer and the enzymatic products via oxygenation of linoleic acid, 13(S)-HODE, has been implicated as an agonist for PPARγ in colorectal cancer cell lines (Bull *et al.,* 2003; J. B. Nixon *et al.,* 2003). PPARγ has been shown to transrepress the NF-κB activity (Pascual *et al.,* 2005). We investigated whether 15LOX1 is involved in inactivation of NF-κB mediated by PPARγ.

The major findings are as follows:

a) 15LOX1 expressing cells had higher IκBα but lower phospho-IκBα which is reversed with the 15LOX1 inhibitor.
b) 15LOX1 expressing cells had lower NF-κB DNA binding activity, which is reversed with the 15LOX1 inhibitor and also PPARγ antagonist which proves the NF-κB DNA binding activity is PPARγ dependent.

c) 15LOX1 expressing cells had higher p-ERK 1/2, and p-PPARγ with and lower ERK 1/2 .Phosphorlyation of PPARγ and ERK 1/2 is decreasing with ERK 1/2 and PPARγ inhibitors suggesting the phosphorlyation of PPARγ is ERK 1/2 dependent.

REFERENCES

Ali, S., K. Almhanna, W. Chen, P. A. Philip, and F. H. Sarkar, 2010, Differentially expressed miRNAs in the plasma may provide a molecular signature for aggressive pancreatic cancer: Am J Transl Res, v. 3, p. 28-47.

Ambros, V., 2004, The functions of animal microRNAs, Nature, v. 431: England, p. 350-5.

Arai, I., H. Nagano, M. Kondo, H. Yamamoto, N. Hiraoka, Y. Sugita, H. Ota, S. Yoshioka, M. Nakamura, H. Wada, B. Damdinsuren, H. Kato, S. Marubashi, A. Miyamoto, Y. Takeda, K. Dono, K. Umeshita, S. Nakamori, K. Wakasa, M. Sakon, and M. Monden, 2007, Overexpression of MT3-MMP in hepatocellular carcinoma correlates with capsular invasion: Hepatogastroenterology, v. 54, p. 167-71.

Barmina, O. Y., H. W. Walling, G. J. Fiacco, J. M. Freije, C. Lopez-Otin, J. J. Jeffrey, and N. C. Partridge, 1999, Collagenase-3 binds to a specific receptor and requires the low density lipoprotein receptor-related protein for internalization: J Biol Chem, v. 274, p. 30087-93.

Bartel, D. P., 2004, MicroRNAs: genomics, biogenesis, mechanism, and function, Cell, v. 116: United States, p. 281-97.

Basson, M. D., G. Turowski, and N. J. Emenaker, 1996, Regulation of human (Caco-2) intestinal epithelial cell differentiation by extracellular matrix proteins.: Exp Cell Res, v. 225, p. 301-5.

Bassères, D. S., and A. S. Baldwin, 2006, Nuclear factor-kappaB and inhibitor of kappaB kinase pathways in oncogenic initiation and progression.: Oncogene, v. 25, p. 6817-30.

Bernstein, C. N., M. Sargent, W. M. Gallatin, and J. Wilkins, 1996, Beta 2-integrin/intercellular adhesion molecule (ICAM) expression in the normal human intestine.: Clin Exp Immunol, v. 106, p. 160-9.

Binion, D. G., G. A. West, E. E. Volk, J. A. Drazba, N. P. Ziats, R. E. Petras, and C. Fiocchi, 1998, Acquired increase in leucocyte binding by intestinal microvascular endothelium in inflammatory bowel disease.: Lancet, v. 352, p. 1742-6.

Birkedal-Hansen, H., 1995, Proteolytic remodeling of extracellular matrix, Curr Opin Cell Biol, v. 7: United States, p. 728-35.

Birkenmeier, E. H., B. Gwynn, S. Howard, J. Jerry, J. I. Gordon, W. H. Landschulz, and S. L. McKnight, 1989, Tissue-specific expression, developmental regulation, and genetic mapping of the gene encoding CCAAT/enhancer binding protein.: Genes Dev, v. 3, p. 1146-56.

Briscoe, D. M., R. S. Cotran, and J. S. Pober, 1992, Effects of tumor necrosis factor, lipopolysaccharide, and IL-4 on the expression of vascular cell adhesion molecule-1 in vivo. Correlation with CD3+ T cell infiltration.: J Immunol, v. 149, p. 2954-60.

Cai, X., C. H. Hagedorn, and B. R. Cullen, 2004, Human microRNAs are processed from capped, polyadenylated transcripts that can also function as mRNAs, RNA, v. 10: United States, p. 1957-66.

Cambien, B., and D. D. Wagner, 2004, A new role in hemostasis for the adhesion receptor P-selectin.: Trends Mol Med, v. 10, p. 179-86.

Cao, Z., R. M. Umek, and S. L. McKnight, 1991, Regulated expression of three C/EBP isoforms during adipose conversion of 3T3-L1 cells.: Genes Dev, v. 5, p. 1538-52.

Chantret, I., A. Barbat, E. Dussaulx, M. Brattain, and A. Zweibaum, 1988, Epithelial polarity, villin expression, and enterocytic differentiation of cultured human colon carcinoma cells: a survey of twenty cell lines.: Cancer Res, v. 48, p. 1936-42.

Chen, C. Z., L. Li, H. F. Lodish, and D. P. Bartel, 2004, MicroRNAs modulate hematopoietic lineage differentiation, Science, v. 303: United States, p. 83-6.

Chen, F., and V. Castranova, 2007, Nuclear factor-kappaB, an unappreciated tumor suppressor.: Cancer Res, v. 67, p. 11093-8.

Christy, R. J., V. W. Yang, J. M. Ntambi, D. E. Geiman, W. H. Landschulz, A. D. Friedman, Y. Nakabeppu, T. J. Kelly, and M. D. Lane, 1989, Differentiation-induced gene expression in 3T3-L1 preadipocytes: CCAAT/enhancer binding protein interacts with and activates the promoters of two adipocyte-specific genes.: Genes Dev, v. 3, p. 1323-35.

Coussens, L. M., and Z. Werb, 2002, Inflammation and cancer: Nature, v. 420, p. 860-867.

Daja, M. M., X. Niu, Z. Zhao, J. M. Brown, and P. J. Russell, 2003, Characterization of expression of matrix metalloproteinases and tissue inhibitors of metalloproteinases in prostate cancer cell lines, Prostate Cancer Prostatic Dis, v. 6: England, p. 15-26.

Dalmasso, G., H. T. Nguyen, Y. Yan, H. Laroui, S. Srinivasan, S. V. Sitaraman, and D. Merlin, 2010, MicroRNAs determine human intestinal epithelial cell fate, Differentiation, v. 80: England, 2010 International Society of Differentiation. Published by Elsevier B.V, p. 147-54.

De Lott, L. B., C. Morrison, S. Suster, D. E. Cohn, and W. L. Frankel, 2005, CDX2 is a useful marker of intestinal-type differentiation: a tissue microarray-based study of 629 tumors from various sites.: Arch Pathol Lab Med, v. 129, p. 1100-5.

Ding, Q., Q. Wang, Z. Dong, and B. M. Evers, 2000, Characterization and regulation of E2F activity during Caco-2 cell differentiation.: Am J Physiol Cell Physiol, v. 278, p. C110-7.

Dippold, W., B. Wittig, W. Schwaeble, W. Mayet, and K. Meyer zum Büschenfelde, 1993, Expression of intercellular adhesion molecule 1 (ICAM-1, CD54) in colonic epithelial cells.: Gut, v. 34, p. 1593-7.

Dolcet, X., D. Llobet, J. Pallares, and X. Matias-Guiu, 2005, NF-kB in development and progression of human cancer.: Virchows Arch, v. 446, p. 475-82.

Doyle, S. L., and L. A. O'Neill, 2006, Toll-like receptors: from the discovery of NFkappaB to new insights into transcriptional regulations in innate immunity.: Biochem Pharmacol, v. 72, p. 1102-13.

Esau, C., X. Kang, E. Peralta, E. Hanson, E. G. Marcusson, L. V. Ravichandran, Y. Sun, S. Koo, R. J. Perera, R. Jain, N. M. Dean, S. M. Freier, C. F. Bennett, B. Lollo, and R. Griffey, 2004, MicroRNA-143 regulates adipocyte differentiation, J Biol Chem, v. 279: United States, p. 52361-5.

Fiocchi, C., 1998, Inflammatory bowel disease: etiology and pathogenesis.: Gastroenterology, v. 115, p. 182-205.

Fogh, J., J. M. Fogh, and T. Orfeo, 1977, One hundred and twenty-seven cultured human tumor cell lines producing tumors in nude mice.: J Natl Cancer Inst, v. 59, p. 221-6.

Gagna, C. E., H. R. Kuo, E. Florea, W. Shami, R. Taormina, N. Vaswani, M. Gupta, R. Vijh, and W. C. Lambert, 2001, Comparison of apoptosis and terminal differentiation: the mammalian aging process.: J Histochem Cytochem, v. 49, p. 929-30.

Ghosh, S., and M. Karin, 2002, Missing pieces in the NF-kappaB puzzle.: Cell, v. 109 Suppl, p. S81-96.

Ghosh, S., M. J. May, and E. B. Kopp, 1998, NF-kappa B and Rel proteins: evolutionarily conserved mediators of immune responses.: Annu Rev Immunol, v. 16, p. 225-60.

Granger, D. N., and P. Kubes, 1994, The microcirculation and inflammation: modulation of leukocyte-endothelial cell adhesion.: J Leukoc Biol, v. 55, p. 662-75.

Gregory, R. I., T. P. Chendrimada, and R. Shiekhattar, 2006, MicroRNA biogenesis: isolation and characterization of the microprocessor complex.: Methods Mol Biol, v. 342, p. 33-47.

Guarner, F., and J. R. Malagelada, 2003, Gut flora in health and disease.: Lancet, v. 361, p. 512-9.

Guttridge, D., C. Albanese, J. Reuther, R. Pestell, and A. J. Baldwin, 1999, NF-kappaB controls cell growth and differentiation through transcriptional regulation of cyclin D1.: Mol Cell Biol, v. 19, p. 5785-99.

Hino, K., K. Tsuchiya, T. Fukao, K. Kiga, R. Okamoto, T. Kanai, and M. Watanabe, 2008, Inducible expression of microRNA-194 is regulated by HNF-1alpha during intestinal epithelial cell differentiation, RNA, v. 14: United States, p. 1433-42.

Hinz, M., D. Krappmann, A. Eichten, A. Heder, C. Scheidereit, and M. Strauss, 1999, NF-kappaB function in growth control: regulation of cyclin D1 expression and G0/G1-to-S-phase transition.: Mol Cell Biol, v. 19, p. 2690-8.

Hinz, M., P. Löser, S. Mathas, D. Krappmann, B. Dörken, and C. Scheidereit, 2001, Constitutive NF-kappaB maintains high expression of a characteristic gene network, including CD40, CD86, and a set of antiapoptotic genes in Hodgkin/Reed-Sternberg cells.: Blood, v. 97, p. 2798-807.

Hsia, C., S. Cheng, A. Owyang, S. Dowdy, and H. Liou, 2002, c-Rel regulation of the cell cycle in primary mouse B lymphocytes.: Int Immunol, v. 14, p. 905-16.

Inuzuka, K., Y. Ogata, H. Nagase, and K. Shirouzu, 2000, Significance of coexpression of urokinase-type plasminogen activator, and matrix metalloproteinase 3 (stromelysin) and 9 (gelatinase B) in colorectal carcinoma, J Surg Res, v. 93: United States, 2000 Academic Press., p. 211-8.

Kajita, M., Y. Itoh, T. Chiba, H. Mori, A. Okada, H. Kinoh, and M. Seiki, 2001, Membrane-type 1 matrix metalloproteinase cleaves CD44 and promotes cell migration: J Cell Biol, v. 153, p. 893-904.

Karin, M., 2006, Nuclear factor-kappaB in cancer development and progression.: Nature, v. 441, p. 431-6.

Karin, M., and Y. Ben-Neriah, 2000, Phosphorylation meets ubiquitination: the control of NF-[kappa]B activity.: Annu Rev Immunol, v. 18, p. 621-63.

Khan, A. I., R. C. Landis, and R. Malhotra, 2003, L-Selectin ligands in lymphoid tissues and models of inflammation.: Inflammation, v. 27, p. 265-80.

Kobayashi, H., K. C. Boelte, and P. C. Lin, 2007, Endothelial cell adhesion molecules and cancer progression: Curr Med Chem, v. 14, p. 377-86.

Koizumi, M., N. King, R. Lobb, C. Benjamin, and D. K. Podolsky, 1992, Expression of vascular adhesion molecules in inflammatory bowel disease.: Gastroenterology, v. 103, p. 840-7.

Kosik, K. S., 2006, The neuronal microRNA system.: Nat Rev Neurosci, v. 7, p. 911-20.

Kruh, J., 1982, Effects of sodium butyrate, a new pharmacological agent, on cells in culture.: Mol Cell Biochem, v. 42, p. 65-82.

Lawson, C., and S. Wolf, 2009, ICAM-1 signaling in endothelial cells: Pharmacol Rep, v. 61, p. 22-32.

Lelandais-Brière, C., C. Sorin, M. Declerck, A. Benslimane, M. Crespi, and C. Hartmann, 2010, Small RNA diversity in plants and its impact in development.: Curr Genomics, v. 11, p. 14-23.

Lowy, A. M., W. M. Clements, J. Bishop, L. Kong, T. Bonney, K. Sisco, B. Aronow, C. Fenoglio-Preiser, and J. Groden, 2006, beta-Catenin/Wnt signaling regulates expression of the membrane type 3 matrix metalloproteinase in gastric cancer, Cancer Res, v. 66: United States, p. 4734-41.

Lund, L. R., J. Romer, T. H. Bugge, B. S. Nielsen, T. L. Frandsen, J. L. Degen, R. W. Stephens, and K. Dano, 1999, Functional overlap between two classes of matrix-degrading proteases in wound healing: EMBO J, v. 18, p. 4645-56.

Maaser, C., S. Schoeppner, T. Kucharzik, M. Kraft, E. Schoenherr, W. Domschke, and N. Luegering, 2001, Colonic epithelial cells induce endothelial cell expression of ICAM-1 and VCAM-1 by a NF-kappaB-dependent mechanism.: Clin Exp Immunol, v. 124, p. 208-13.

Malizia, G., A. Calabrese, M. Cottone, M. Raimondo, L. K. Trejdosiewicz, C. J. Smart, L. Oliva, and L. Pagliaro, 1991, Expression of leukocyte adhesion molecules by mucosal mononuclear phagocytes in inflammatory bowel disease.: Gastroenterology, v. 100, p. 150-9.

Mariadason, J. M., D. Arango, G. A. Corner, M. J. Aranes, K. A. Hotchkiss, W. Yang, and L. H. Augenlicht, 2002, A gene expression profile that defines colon cell maturation in vitro: Cancer Res, v. 62, p. 4791-804.

Nakada, M., H. Nakamura, E. Ikeda, N. Fujimoto, J. Yamashita, H. Sato, M. Seiki, and Y. Okada, 1999, Expression and tissue localization of membrane-type 1, 2, and 3 matrix metalloproteinases in human astrocytic tumors.: Am J Pathol, v. 154, p. 417-28.

Nakamura, H., H. Ueno, K. Yamashita, T. Shimada, E. Yamamoto, M. Noguchi, N. Fujimoto, H. Sato, M. Seiki, and Y. Okada, 1999, Enhanced production and activation of progelatinase A mediated by membrane-type 1 matrix metalloproteinase in human papillary thyroid carcinomas.: Cancer Res, v. 59, p. 467-73.

Nelson, A., B. Fingleton, M. Rothenberg, and L. Matrisian, 2000, Matrix metalloproteinases: biologic activity and clinical implications.: J Clin Oncol, v. 18, p. 1135-49.

Neutra M, L. D., 1989, Differentiation of intestinal cells *in vitro*. In:Functional epithelial cells in culture: New York: Alan R. Liss: NewYork, 35 p.

Nortamo, P., R. Li, R. Renkonen, T. Timonen, J. Prieto, M. Patarroyo, and C. G. Gahmberg, 1991, The expression of human intercellular adhesion molecule-2 is refractory to inflammatory cytokines.: Eur J Immunol, v. 21, p. 2629-32.

Ohnishi, Y., S. Tajima, and A. Ishibashi, 2001, Coordinate expression of membrane type-matrix metalloproteinases-2 and 3 (MT2-MMP and MT3-MMP) and matrix metalloproteinase-2 (MMP-2) in primary and metastatic melanoma cells: Eur J Dermatol, v. 11, p. 420-3.

Olsen, P. H., and V. Ambros, 1999, The lin-4 regulatory RNA controls developmental timing in Caenorhabditis elegans by blocking LIN-14 protein synthesis after the initiation of translation, Dev Biol, v. 216: United States, p. 671-80.

Papa, S., C. Bubici, F. Zazzeroni, C. G. Pham, C. Kuntzen, J. R. Knabb, K. Dean, and G. Franzoso, 2006, The NF-kappaB-mediated control of the JNK cascade in the antagonism of programmed cell death in health and disease.: Cell Death Differ, v. 13, p. 712-29.

Parkos, C., S. Colgan, M. Diamond, A. Nusrat, T. Liang, T. Springer, and J. Madara, 1996, Expression and polarization of intercellular adhesion molecule-1 on human intestinal epithelia: consequences for CD11b/CD18-mediated interactions with neutrophils.: Mol Med, v. 2, p. 489-505.

Pinto, M., 1983, Enterocyte like differentiation and polarization of the human colon carcioma cell line Caco-2, *in* S. Robine-Leon, ed., Biol Cell, p. 323-30.

Poulsom, R., M. Pignatelli, W. G. Stetler-Stevenson, L. A. Liotta, P. A. Wright, R. E. Jeffery, J. M. Longcroft, L. Rogers, and G. W. Stamp, 1992, Stromal expression of 72 kda type IV collagenase (MMP-2) and TIMP-2 mRNAs in colorectal neoplasia: Am J Pathol, v. 141, p. 389-96.

Ramji, D. P., and P. Foka, 2002, CCAAT/enhancer-binding proteins: structure, function and regulation.: Biochem J, v. 365, p. 561-75.

Roebuck, K. A., and A. Finnegan, 1999, Regulation of intercellular adhesion molecule-1 (CD54) gene expression.: J Leukoc Biol, v. 66, p. 876-88.

Rowe, R. G., and S. J. Weiss, 2008, Breaching the basement membrane: who, when and how?, Trends Cell Biol, v. 18: England, p. 560-74.

Salmi, M., K. Granfors, R. MacDermott, and S. Jalkanen, 1994, Aberrant binding of lamina propria lymphocytes to vascular endothelium in inflammatory bowel diseases.: Gastroenterology, v. 106, p. 596-605.

Sambuy, Y., I. De Angelis, G. Ranaldi, M. L. Scarino, A. Stammati, and F. Zucco, 2005, The Caco-2 cell line as a model of the intestinal barrier: influence of cell and culture-related factors on Caco-2 cell functional characteristics.: Cell Biol Toxicol, v. 21, p. 1-26.

Sancho, E., E. Batlle, and H. Clevers, 2004, Signaling pathways in intestinal development and cancer.: Annu Rev Cell Dev Biol, v. 20, p. 695-723.

Sandoval, I. V., and O. Bakke, 1994, Targeting of membrane proteins to endosomes and lysosomes.: Trends Cell Biol, v. 4, p. 292-7.

Sato, H., T. Takino, Y. Okada, J. Cao, A. Shinagawa, E. Yamamoto, and M. Seiki, 1994, A matrix metalloproteinase expressed on the surface of invasive tumour cells: Nature, v. 370, p. 61-5.

Semba, S., Y. Kodama, K. Ohnuma, E. Mizuuchi, R. Masuda, M. Yashiro, K. Hirakawa, and H. Yokozaki, 2009, Direct cancer-stromal interaction increases fibroblast proliferation and enhances invasive properties of scirrhous-type gastric carcinoma cells: Br J Cancer, v. 101, p. 1365-73.

Shen, H. M., and V. Tergaonkar, 2009, NFkappaB signaling in carcinogenesis and as a potential molecular target for cancer therapy.: Apoptosis, v. 14, p. 348-63.

Shiozawa, J., M. Ito, T. Nakayama, M. Nakashima, S. Kohno, and I. Sekine, 2000, Expression of matrix metalloproteinase-1 in human colorectal carcinoma: Mod Pathol, v. 13, p. 925-33.

Simon-Assmann, P., N. Turck, M. Sidhoum-Jenny, G. Gradwohl, and M. Kedinger, 2007a, In vitro models of intestinal epithelial cell differentiation: Cell Biol Toxicol, v. 23, p. 241-56.

Simon-Assmann, P., N. Turck, M. Sidhoum-Jenny, G. Gradwohl, and M. Kedinger, 2007b, In vitro models of intestinal epithelial cell differentiation.: Cell Biol Toxicol, v. 23, p. 241-56.

Song, Y. A., Y. L. Park, S. H. Yoon, K. Y. Kim, S. B. Cho, W. S. Lee, I. J. Chung, and Y. E. Joo, 2010, Black tea polyphenol theaflavin suppresses LPS-induced ICAM-1 and VCAM-1 expression via blockage of NF-κB and JNK activation in intestinal epithelial cells.: Inflamm Res.

Staunton, D. E., M. L. Dustin, and T. A. Springer, 1989, Functional cloning of ICAM-2, a cell adhesion ligand for LFA-1 homologous to ICAM-1.: Nature, v. 339, p. 61-4.

Teller, I. C., and J. F. Beaulieu, 2001, Interactions between laminin and epithelial cells in intestinal health and disease.: Expert Rev Mol Med, v. 3, p. 1-18.

Turck, N., O. Lefebvre, I. Gross, P. Gendry, M. Kedinger, P. Simon-Assmann, and J. F. Launay, 2006, Effect of laminin-1 on intestinal cell differentiation involves inhibition of nuclear nucleolin.: J Cell Physiol, v. 206, p. 545-55.

Turck, N., S. Richert, P. Gendry, J. Stutzmann, M. Kedinger, E. Leize, P. Simon-Assmann, A. Van Dorsselaer, and J. F. Launay, 2004, Proteomic analysis of nuclear proteins from proliferative and differentiated human colonic intestinal epithelial cells.: Proteomics, v. 4, p. 93-105.

Umek, R. M., A. D. Friedman, and S. L. McKnight, 1991, CCAAT-enhancer binding protein: a component of a differentiation switch.: Science, v. 251, p. 288-92.

Vainer, B., 2005, Intercellular adhesion molecule-1 (ICAM-1) in ulcerative colitis: presence, visualization, and significance.: Inflamm Res, v. 54, p. 313-27.

Vainer, B., T. Horn, and O. Nielsen, 2006a, Colonic epithelial cell expression of ICAM-1 relates to loss of surface continuity: a comparative study of inflammatory bowel disease and colonic neoplasms.: Scand J Gastroenterol, v. 41, p. 318-25.

Vainer, B., T. Horn, and O. H. Nielsen, 2006b, Colonic epithelial cell expression of ICAM-1 relates to loss of surface continuity: a comparative study of inflammatory bowel disease and colonic neoplasms: Scand J Gastroenterol, v. 41, p. 318-25.

Vogelstein, B., and K. W. Kinzler, 2004, Cancer genes and the pathways they control: Nat Med, v. 10, p. 789-799.

Wightman, B., I. Ha, and G. Ruvkun, 1993, Posttranscriptional regulation of the heterochronic gene lin-14 by lin-4 mediates temporal pattern formation in C. elegans, Cell, v. 75: United States, p. 855-62.

Xia, H., Y. Qi, S. S. Ng, X. Chen, D. Li, S. Chen, R. Ge, S. Jiang, G. Li, Y. Chen, M. L. He, H. F. Kung, L. Lai, and M. C. Lin, 2009, microRNA-146b

inhibits glioma cell migration and invasion by targeting MMPs.: Brain Res, v. 1269, p. 158-65.

Yoshida, M., and M. A. Gimbrone, 1997, Novel roles for E-selectin in endothelial-leukocyte adhesion.: Ann N Y Acad Sci, v. 811, p. 493-7.

Zamore, P. D., and B. Haley, 2005, Ribo-gnome: the big world of small RNAs, Science, v. 309: United States, p. 1519-24.

Zen, K., and C. Parkos, 2003, Leukocyte-epithelial interactions.: Curr Opin Cell Biol, v. 15, p. 557-64.

Zeng, Z. S., Y. Huang, A. M. Cohen, and J. G. Guillem, 1996, Prediction of colorectal cancer relapse and survival via tissue RNA levels of matrix metalloproteinase-9: J Clin Oncol, v. 14, p. 3133-40.

Zhang, S., B. Zhao, H. Jiang, B. Wang, and B. Ma, 2007, Cationic lipids and polymers mediated vectors for delivery of siRNA.: J Control Release, v. 123, p. 1-10.

Ziprin, P., P. F. Ridgway, K. L. Pfistermuller, D. H. Peck, and A. W. Darzi, 2003, ICAM-1 mediated tumor-mesothelial cell adhesion is modulated by IL-6 and TNF-alpha: a potential mechanism by which surgical trauma increases peritoneal metastases: Cell Commun Adhes, v. 10, p. 141-54.

Zucker, S., 1988, A critical appraisal of the role of proteolytic enzymes in cancer invasion: emphasis on tumor surface proteinases: Cancer Invest, v. 6, p. 219-31.

Zucker, S., J. Cao, and W. T. Chen, 2000, Critical appraisal of the use of matrix metalloproteinase inhibitors in cancer treatment: Oncogene, v. 19, p. 6642-50.

APPENDICES

Appendix A: Vector Maps

A.1 pMIR-Report™ Luciferase Plasmid (Promega, USA)

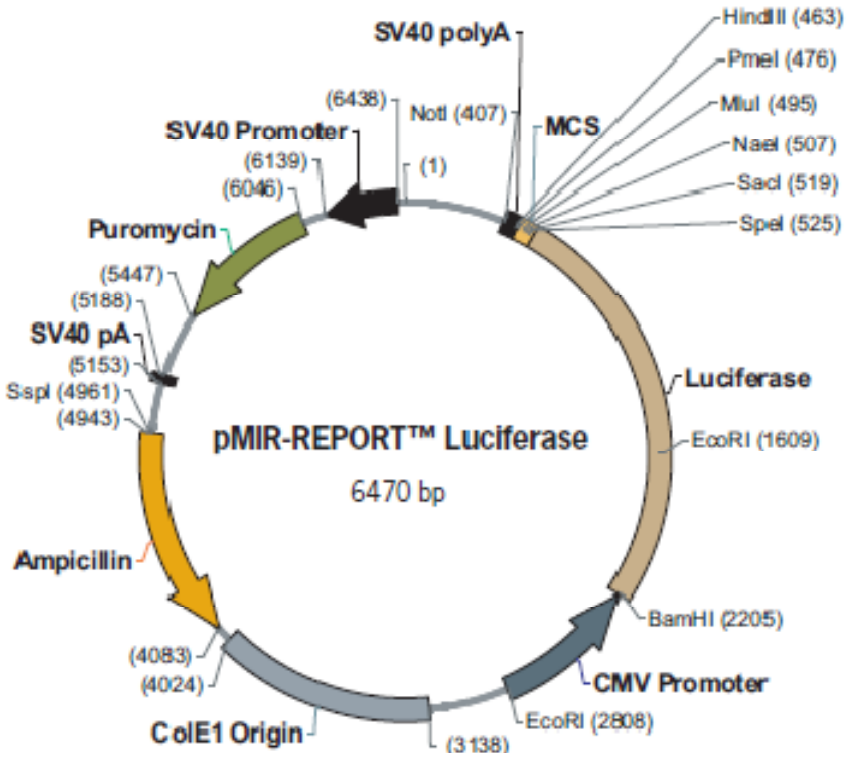

Figure 5.1 pMIR-REPORT Luciferase Vector Map

A.2 pGL3™ Basic Plasmid (Promega, USA)

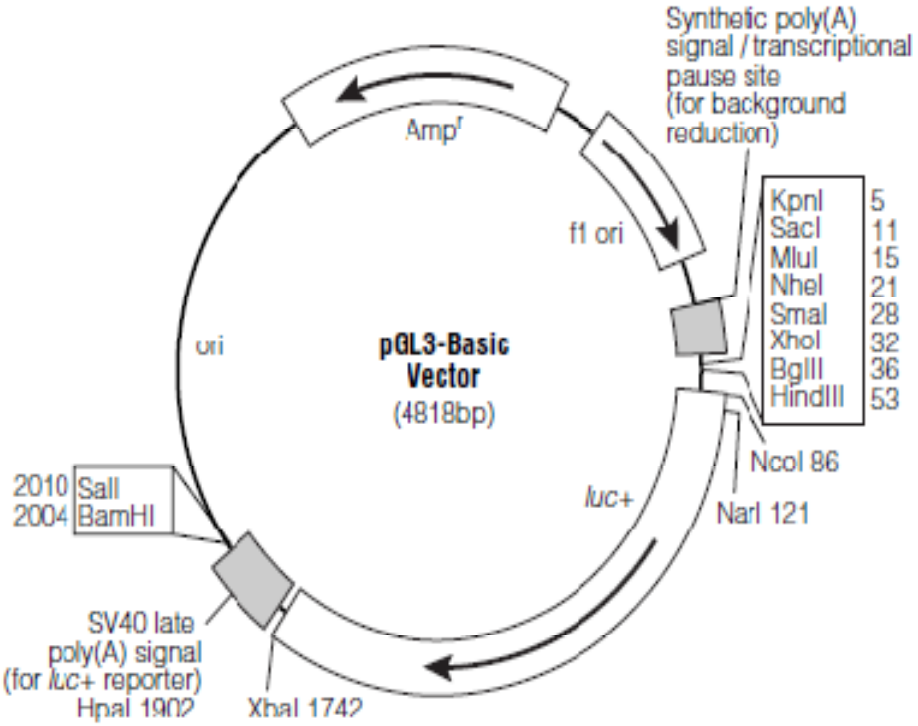

Figure 5.2: pGL3- Basic Vector Map

A.3 Psuper.Gfp/Neo Plasmid (OligoEngine, USA)

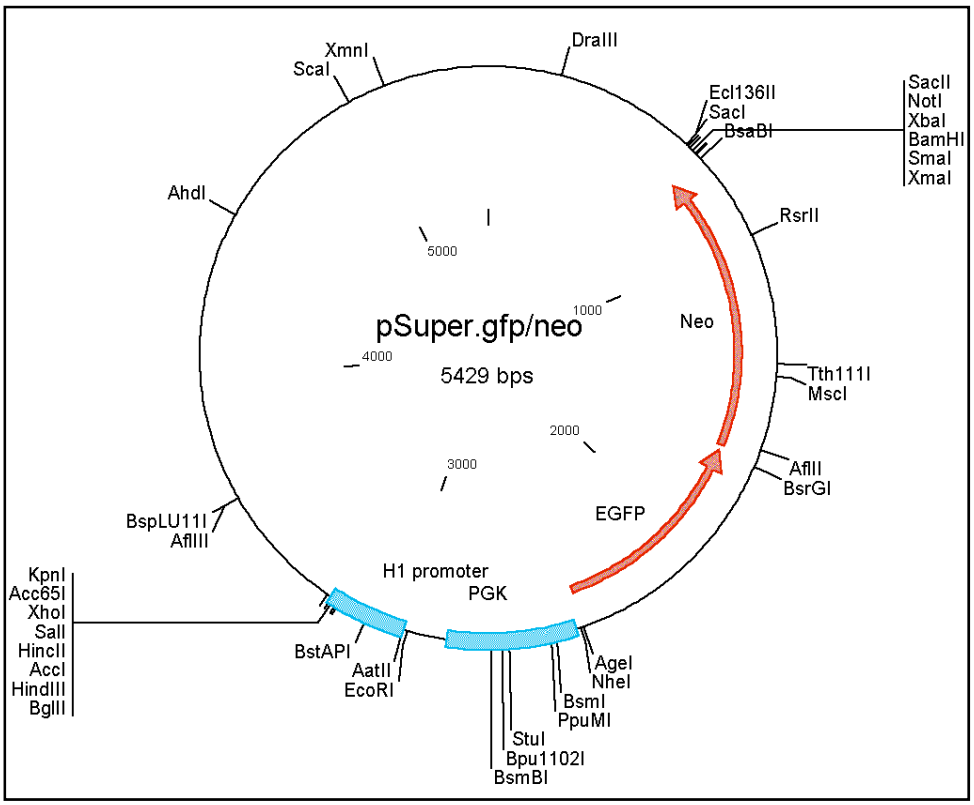

Figure 5.3 pSuper.gfp/neo Plasmid Map

A.4 pSV-β-Galactosidase Control Vector (Promega, USA)

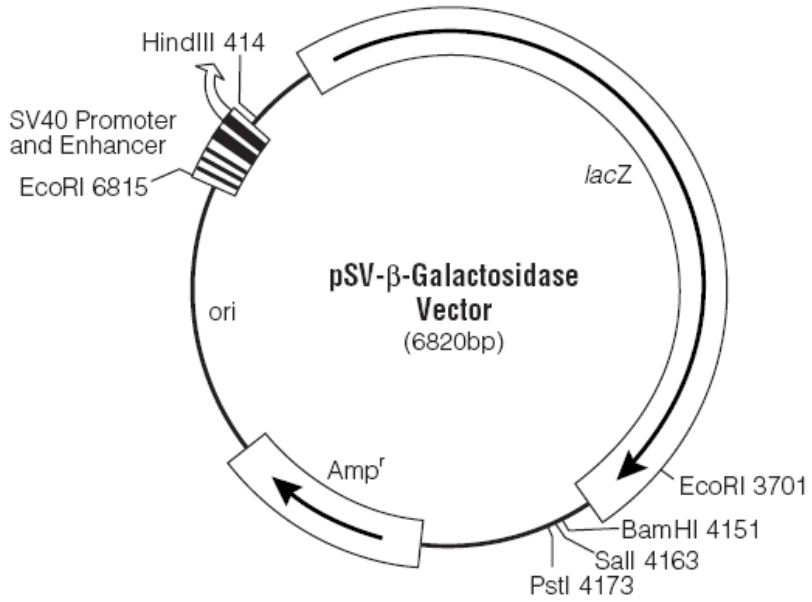

Figure 5.4: pSV-β-Galactosidase Plasmid Map

Appendix B: Buffers And Solutions

B.1 Chromatin Immunoprecipitation Buffers

Buffer C

20 mM HEPES pH7.9
25% glycerol
420 mM NaCl
1.5 mM Mg Cl2
0.2 mM EDTA

Breaking Buffer

50 mM Tris-HCl pH8.0
1 mM EDTA
150 mM NaCl
1% SDS
2% Triton X-100

Triton Buffer

50 mM Tris-HCl pH8.0
1 mM EDTA
150 mM NaCl
0.1% Triton X-100

SDS-NaCl-DTT Buffer

62.5 mM Tris HCl pH6.8
200 mM NaCl
2% SDS
10 mM DTT

B.1.2 SDS-PAGE Buffers

40% Acrylamide 65.4ml

2% Bisacrylamide 34.6ml

Final 100ml

4X Stacking Gel mix 0.5ml Tris-HCl pH 6.8 0.1% SDS

4X Separating Gel mix 1.5 ml Tris-HCl pH 8.8, 0.1%SDS

	Stack Gel		Resolving Gel			
	4%		7,00%	10%	12%	x%
26.9% PAA Mix	1.2ml		3.9ml	5.6ml	6.7ml	(%26.9) 15=A
4X Stacking gel mix	2.0ml		N/A	N/A	N/A	N/A
4X Separating Gel mix	N/A		3.8ml	3.8ml	3.8ml	3.8ml
ddH_2O	4.7ml		7.1ml	5.4ml	4.3ml	(11-A)
10% APS	50 ul		150ul	150ul	150ul	150ul
TEMED	10 ul		20ul	20ul	20ul	20ul
Final VOLUME	8 ml		15ml	15ml	15ml	15ml

B.1.3 Western Blotting Buffers

10 X Blotting buffer (1 L)

30.3 g Trizma Base (0.25M)

144 g Glycine (1.92 M)

pH Should be 8.3 DO NOT ADJUST

Transfer Buffer (2L)

400 ml Methanol

200 ml 10 X Blotting buffer

1400 ml water

PBS-T Washing Buffer

8 g NaCl

0.27 g KH_2PO_4

3.58 g Na_2HPO_4 12 H_2O

Add 500 ml dH_2O stir and complete to 1 L

Adjust pH to 7.4 with HCl

Autoclave

Add 0.1% Tween 20 prior to use

Harsh Stripping Buffer

100 mM β-meOH

2% SDS,

62.5 mM Tris-HCl pH: 6.8

Procedure

Pre-warm the stripping buffer at 55-60°C for 10 minutes

Incubate the membranes for 30 minutes at 55-60°C with shaking

Wash 3 times with PBS-Tween using large volumes

Reblock and probe it

Mild Stripping Buffer

15g glycine

1 g SDS

10 ml Tween 20

Adjust the pH to 2,2

Make uo to 1L with distilled water

Procedure

Use a volume that will cover the membrane. Incubate at room temperature for 5-10 minutes with agitation.

Discard buffer

5-10 minutes fresh stripping buffer

Appendix C: Cloning Studies

C.1 Cloning of *ICAM1* 3' UTR Region in p-MIR-REPORT Luciferase Vector

ICAM1 3' UTR region (1331bp) was cloned in two pieces in sizes of 672 bp (1.1) and 731 bp (1.2) with 72 bp overlapping region. In order to sustain the right orientation first and second halves of the *ICAM1* 3' UTR region was cloned into HindIII/SpeI and SacI/SpeI restriction sites, respectively. For that purpose PCR was performed from genomic DNA obtained by Caco-2 cells.

PCR reaction conditions were as follows;

Table 5.1 PCR Conditions for *ICAM1* 3' UTR Amplification

Chemical	Amount (µl)		PCR Reaction Conditions		
10X Taq buffer	5		94°C	3:00	
25 mM MgCl2	5		94°C	0:30	30 cycles
2 mM dntp	5		59°C	0:30	
Fwd Primer (5µM)	5		72°C	0:30	
Reverse Primer (5µM)	5		72°C	10:00	
Taq DNA polymerase (5 U/µl)	0,5		4°C	HOLD	
Pfu DNA ploymerase (5 U/µl)	0,03				
Genomic DNA	3				
Water	50				

Afterwards the products obtained were pooled separated in 1% Agarose prepared for preparative purpose and then purified from gel by using Agarose Gel DNA Extraction Kit (Roche) by following the instructions. Protocol was mentioned in Appendix F. Afterwards concentrations of obtained fragments were measured spectrophotometrically at 260 nm and samples obtained were subjected to restriction enzyme digestion conditions of which were given below.

Table 5.2 Restriction Digestion Conditions for Cloning of *ICAM1* 3' UTR (1.1) Region

Chemical	Amount (µl)	Reaction Conditions	
1X Buffer Tango	6	Temperature	Time
Vector (100ng/µl) OR insert (300 ng/µl)	50 µl	37°C	16 hours
HindIII (10U/µl)	1,2	80°C	15 minutes
SpeI (10U/µl)	0,6		

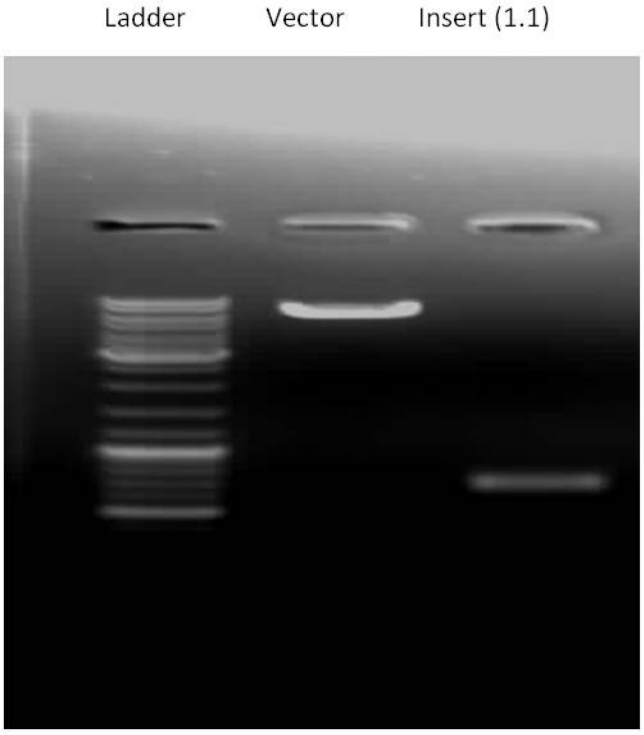

Figure 5.5 Gel Analysis of HindIII/SpeI Digested p-MIR-REPORT and *ICAM1* 3'UTR Region. Lanes; Ladder: GeneRuler™ DNA Ladder Mix (Fermentas), Vector: p-MIR-REPORT vector, Insert: ICAM1 3' UTR Region

Then ligation reactions were performed in 10µl reaction volumes sustaining 1:10 vector: insert molar ratio, reaction conditions were given below.

Table 5.3 Ligation Reaction Conditions for Cloning *ICAM1* 1.1 UTR Region to p-MIR-REPORT Vector

Conc.	Chemical	Amount (µl)
5X	5x Ligation buffer	2
(70ng/µl)	Vector	1,47
(40 ng /µl)	Insert	2,5
5U/µl	Ligase	1
	Water	3,59
16°C 17 hour incubation		

Followingly 5µl of ligation reaction was used to transform previously prepared competent Top10 *E.Coli* cells. Transformation protocol was given in Appendix F. Followingly 100 µl of the transformation reactions were plated in LB-Agar plates containing 100µg/ml Ampicillin overnight at 37°C. Afterwards colonies were selected, inoculated in 1 ml liquid LB containing ampicillin and grown overnight at 37°C at 200 rpm and then centrifuged at 4000 rpm for 5 minutes. Supernatant was removed and a small sterile toothpick was used to touch the precipitated colony to sample enough amounts to sustain colony PCR and the rest was frozen in fresh LB containing 15% glycerol.

Colony PCR was performed with the empty vector P-super primers and conditions were mentioned below.

Table 5.4 Colony PCR Conditions for Amplification of *ICAM1* 1.1 UTR Region

Chemical	Amount (µl)		PCR Reaction Conditions		
10X Taq buffer	3		94°C	3:00	
25 mM MgCl2	3		94°C	0:30	34 cycles
2 mM dntp	3		50°C	0:30	
Fwd Primer (5µM)	3		72°C	0:30	
Reverse Primer (5µM)	3		72°C	10:00	
Taq DNA polymerase (5 U/µl)	0,2		4°C	HOLD	
Colony	N/A				
Water	To 30				

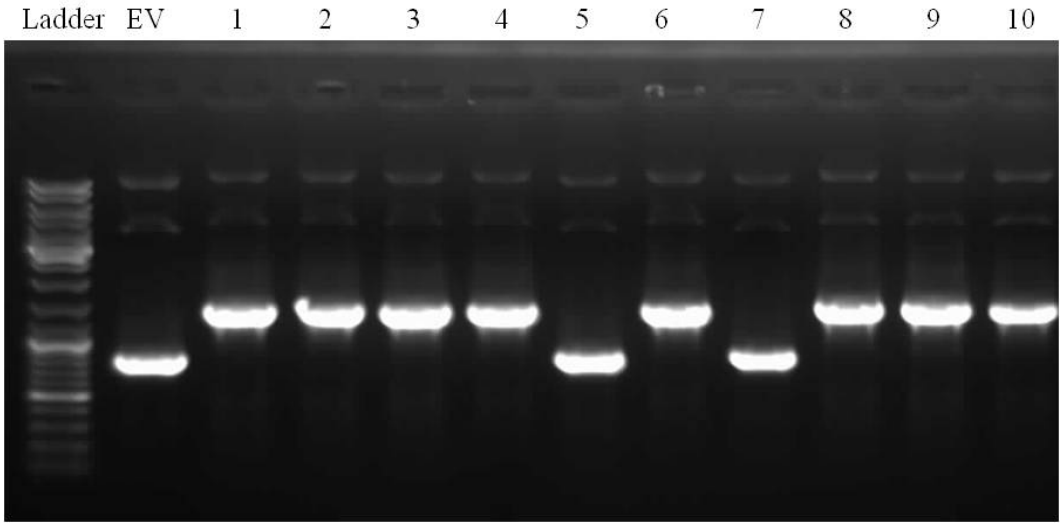

Figure 5.6 Colony PCR for Identification of *ICAM1* 1.1 UTR Region Cloned Plasmids (Lanes: Ladder: GeneRuler™ DNA Ladder Mix (Fermentas), EV: p-MIR-REPORT Empty Vector, 1-10 Selected Colony Number)

After wards colonies which seemed to be accommodating the inserts were selected and grown overnight at 200 rpm at 37°C in 5 ml LB-ampicllin medium

and further plasmids were isolated by using Qiagen Miniprep Plasmid isolation Kit by following the instructions. Plasmids purification protocol was given in Appendix J.

After plasmids were isolated from the selected colonies (1-4) they were subjected to restriction digestion in order to confirm the results with the same restriction digestion reaction used for the preparation of the inserts.

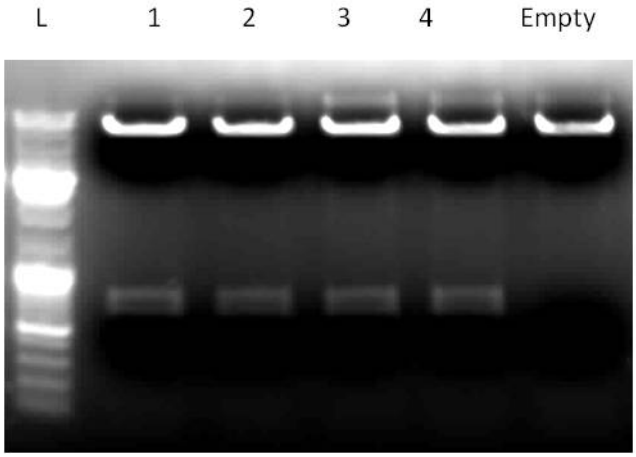

Figure 5.7 Restriction Digestion of *ICAM1* 1.1 UTR Region of p-MIR-REPORT Plasmids from Selected Colonies. Lanes; L: GeneRuler™ DNA Ladder Mix (Fermentas), 1-4: Selected Colonies, Empty: Empty Vector

Afterwards plasmids were sent for sequencing for confirmation of the sequence in the cloned plasmids.

C.2 Cloning of the *ICAM1* 3' UTR Region Second Half (1.2)

For the second half of the ICAR region SacI/SpeI restriction sites were used for the directional cloning of this fragment in p-MIR-REPORT plasmid. For that purpose PCR was performed from genomic DNA obtained from Caco-2 cells.

PCR reaction conditions were as follows;

Table 5.5 PCR Conditions for *ICAM1* (1.2) 3' UTR Amplification

Chemical	Amount (µl)		PCR Reaction Conditions		
10X Taq buffer	5		94°C	3:00	
25 mM MgCl2	5		94°C	0:30	30 cycles
2 mM dntp	5		59°C	0:30	
Fwd Primer (5µM)	5		72°C	0:30	
Reverse Primer (5µM)	5		72°C	10:00	
Taq DNA polymerase (5 U/µl)	0,5		4°C	HOLD	
Pfu DNA ploymerase (5 U/µl)	0,03				
Genomic DNA	3				
Water	50				

Afterwards the products obtained were pooled separated in 1% Agarose prepared for preparative purpose and then purified from gel by using Agarose Gel DNA Extraction Kit (Roche) according to the manufacturer's instructions. Protocol was mentioned in Appendix E. Afterwards concentrations of obtained fragments were measured spectrophotometrically at 260 nm and samples

obtained were subjected to restriction enzyme digestion conditions of which were given below.

Then ligation reactions were performed in 10µl reaction volumes sustaining 1:10 vector: insert molar ratio, reaction conditions were given below.

Table 5.6 Ligation Reaction Conditions for Cloning *ICAM1* 1.2 UTR Region to p-MIR-REPORT Vector

Conc.	Chemical	Amount (µl)
5X	5x Ligation buffer	2
(50ng/µl)	Vector	2
(40 ng /µl)	Insert	2,5
5U/µl	Ligase	1
	Water	2,5
16°C 17 hour incubation		

Followingly 5µl of ligation reaction was used to transform previously prepared competent Top10 *E.Coli* cells. Transformation protocol was given in Appendix F. Followingly 100 µl of the transformation reactions were plated in LB-Agar plates containing 100µg/ml Ampicillin overnight at 37°C. Afterwards colonies were selected, inoculated in 1 ml liquid LB containing ampicillin and grown overnight at 37°C at 200 rpm and then centrifuged at 4000 rpm for 5 minutes. Supernatant was removed and a small sterile toothpick was used to touch

the precipitated colony to sample enough amounts to sustain colony PCR and the rest was frozen in fresh LB containing 15% glycerol.

Colony PCR was performed with the empty vector P-super primers and conditions were mentioned below.

Table 5.7 Colony PCR Conditions for Amplification of *ICAM1* 1.1 UTR

Chemical	Amount (µl)		PCR Reaction Conditions		
10X Taq buffer	3		94°C	3:00	
25 mM MgCl2	3		94°C	0:30	34 cycles
2 mM dntp	3		50°C	0:30	
Fwd Primer (5µM)	3		72°C	0:30	
Reverse Primer (5µM)	3		72°C	10:00	
Taq DNA polymerase (5 U/µl)	0,2		4°C	HOLD	
Colony	N/A				
Water	To 30				

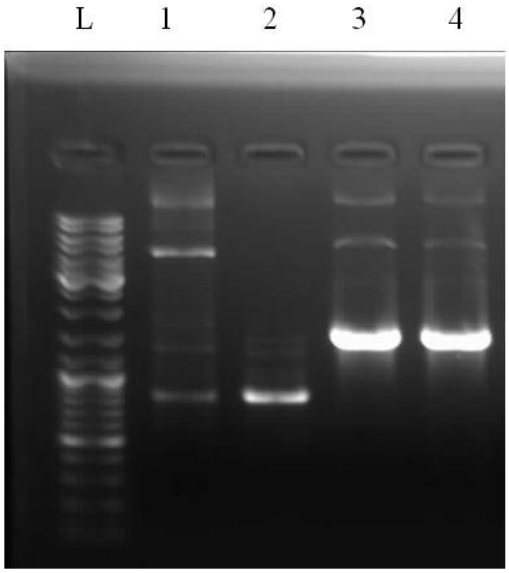

Figure 5.8 Colony PCR for Identification of *ICAM1* 1.2 3'UTR Region Cloned Plasmids. Lanes: L: GeneRuler™ DNA Ladder Mix (Fermentas), 1-4 Colony Number

After wards colonies which seemed to be accommodating the inserts were selected and grown overnight at 200 rpm at 37°C in 5 ml LB-ampicllin medium and further plasmids were isolated by using Qiagen Miniprep Plasmid isolation Kit according to the manufacturer's instructions. Plasmids purification protocol was given in Appendix J.

After plasmids were isolated from the selected colonies (3-4) they were subjected to restriction digestion in order to confirm the results with the same restriction digestion reaction used for the preparation of the inserts.

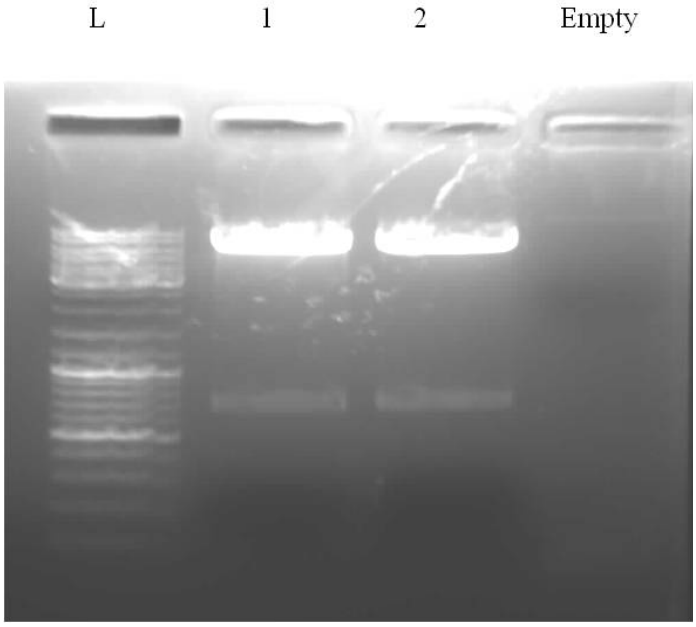

Figure 5.9 Restriction Digestion of *ICAM1* 1.2 UTR Region of p-MIR-REPORT Plasmids from Selected Colonies. Lanes; L: GeneRuler™ DNA Ladder Mix (Fermentas), 1-2: Selected colony number, Empty: p-MIR-REPORT empty vector

Afterwards plasmids were sent for sequencing for confirmation of the sequence in the cloned plasmids.

C.3 Cloning of *MMP16* 3' UTR Region in p-MIR-REPORT Vector

490 bp region (bases between1250-1740) of MMP16 3' UTR was cloned into the Hind III/Sac I sites of the p-MIR-REPORT luciferase vector. For that purpose first the fragment to be cloned was obtained via PCR amplification conditions of which was given below

Table 5.8 PCR Conditions for Amplification of *MMP16* UTR Region

Chemical	Amount (µl)		PCR Reaction Conditions		
10X Taq buffer	3		94°C	3:00	
25 mM MgCl2	3		94°C	0:30	34 cycles
2 mM dNTP	3		55°C	0:30	
Fwd Primer (5µM)	3		72°C	0:30	
Reverse Primer (5µM)	3		72°C	10:00	
Taq DNA polymerase (5 U/µl)	0,2		4°C	HOLD	
Colony	N/A				
Water	To 30				

Then amplified samples were pooled and purified from agarose gel and subjected to restriction digestion reaction.

Table 5.9 Restriction Digestion Reaction of *MMP16* UTR and p-MIR-REPORT Vector

	Amount (µl)	Reaction Conditions	
1X Buffer Tango	6	Temperature	Time
Vector (100ng/µl) OR insert (300 ng/µl)	50 µl	37°C	16 hours
HindIII (10U/µl)	1	80°C	15 minutes
SacI (10U/µl)	1		
Water	To 60µl		

Afterwards the products obtained were pooled separated in 1% Agarose prepared for preparative purpose and then purified from gel by using Agarose Gel DNA Extraction Kit (Roche) according to the manufacturer's instructions. Protocol was mentioned in Appendix E. Afterwards concentrations of obtained fragments were measured spectrophotometrically at 260 nm and samples obtained were subjected to restriction enzyme digestion conditions of which were given below.

Then ligation reactions were performed in 10µl reaction volumes sustaining 1:10 vector: insert molar ratio, reaction conditions were given below.

Table 5.10 Ligation Conditions of *MMP16* UTR and p-MIR-REPORT Vector

Conc.	Chemical	Amount (µl)
5X	5x Ligation buffer	2
(20ng/µl)	Vector	5,9
(20 ng /µl)	Insert	9,1
5U/µl	Ligase	1
	Water	To 10µl
16°C 17 hour incubation		

Afterwards colonies which seemed to be accommodating the inserts were selected and grown overnight at 200 rpm at 37°C in 5 ml LB-ampicllin medium and further plasmids were isolated by using Qiagen Miniprep Plasmid isolation Kit according to the manufacturer's instructions. Plasmid purification protocol was given in Appendix J.

After plasmids were isolated from the selected colonies (1-2), they were first subjected to the PCR reaction with p-MIR-REPORT Empty vector primers with the same conditions described elsewhere.

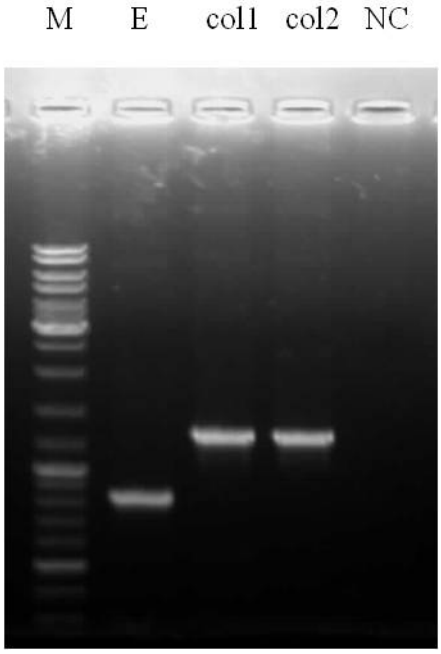

Figure 5.10 PCR Amplification of Selected Colonies for Confirmation of Cloned Inserts. Lanes: M: GeneRuler™ DNA Ladder Mix (Fermentas), E: Empty Vector, col1-2: Selected Colonies, NC: Negative Control

Afterwards colonies were subjected to restriction digestion with the same enzymes used for cloning

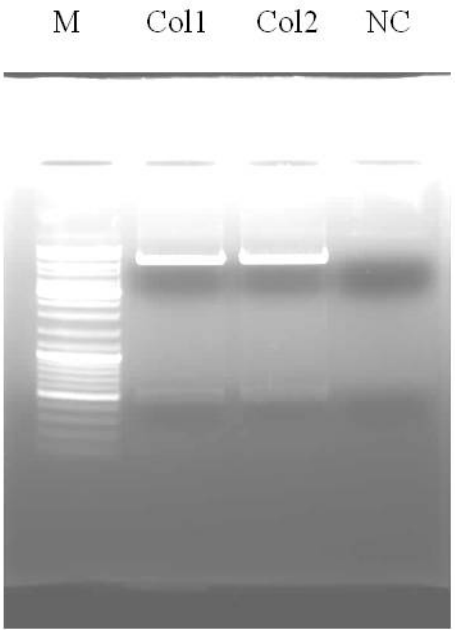

Figure 5.11 Restriction Digestion of selected Colonies Accommodating 3' UTR Region of *MMP16*. Lanes; M: GeneRuler™ DNA Ladder Mix (Fermentas), Col1-2: selected colonies, NC: Negative Control

Then Colonies were sent for sequencing in order to determine whether the cloned products were the faithful copies of the interested fragment.

C.4 Cloning of NF-κB Binding Site In PGL3 Vector

In order to determine the transcriptional activity of the NF-κB PGL3 vector was employed. For that purpose NF-κB element exists in the *ICAM1* promoter was cloned into the PGL3 vector in SacI/XhoI sites. For that purpose PCR was performed from genomic DNA obtained from Caco-2 cells. PCR reaction conditions were as follows

Table 5.11 PCR Conditions for Amplification of NF-κB Binding Site

Chemical	Amount (µl)		PCR Reaction Conditions		
10X Taq buffer	5		94°C	3:00	
25 mM MgCl2	5		94°C	0:30	30 cycles
2 mM dntp	5		59°C	0:30	
Fwd Primer (5µM)	5		72°C	0:30	
Reverse Primer (5µM)	5		72°C	10:00	
Taq DNA polymerase (5 U/µl)	0,5		4°C	HOLD	
Pfu DNA ploymerase (5 U/µl)	0,03				
Genomic DNA	3				
Water	50				

Afterwards the products obtained were pooled separated in 1% Agarose prepared for preparative purpose and then purified from gel by using Agarose Gel DNA Extraction Kit (Roche) according to the manufacturer's instructions. Protocol was mentioned in Appendix E. Afterwards concentrations of obtained fragments were measured spectrophotometrically at 260 nm and samples obtained were subjected to restriction enzyme digestion.

Then ligation reactions were performed in 10µl reaction volumes sustaining 1:10 vector: insert molar ratio, by using 100 ng of vector and appropriate amount of vector to sustain the 1:10 molar ratio.

Table 5.12 PCR conditions for Amplification of NF-κB Element from PGL3 Plasmids

Chemical	Amount (µl)		PCR Reaction Conditions		
10X Taq buffer	3		94°C	3:00	
25 mM $MgCl_2$	3		94°C	0:30	
2 mM dntp	3		54°C	0:30	40 cycles
Fwd Primer (5µM)	3		72°C	0:30	
Reverse Primer (5µM)	3		72°C	10:00	
Taq DNA polymerase (5 U/µl)	0,2		4°C	HOLD	
Colony	N/A				
Water	To 30				

Following 5µl of ligation reaction was used to transform previously prepared competent Top10 *E.Coli* cells. Transformation protocol was given in Appendix F. Followingly 100 µl of the transformation reactions were plated in LB-Agar plates containing 100µg/ml Ampicillin overnight at 37°C. Afterwards colonies were selected, inoculated in 1 ml liquid LB containing ampicillin and grown overnight at 37°C at 200 rpm and then centrifuged at 4000 rpm for 5 minutes. Supernatant was removed and a small sterile toothpick was used to touch the precipitated colony to sample enough amount to sustain colony PCR and the rest was frozen in fresh LB containing 15% glycerol.

Then plasmids were isolated from selected with Qiagen Miniprep Plasmid isolation kit (Qiagen) according to the manufacturer's instructions.

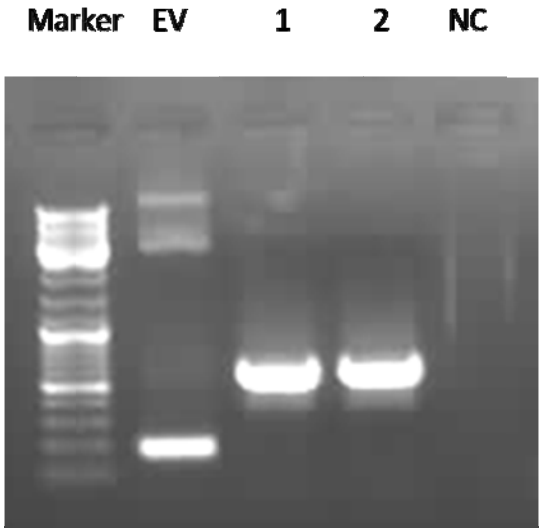

Figure 5.12: Amplification for NF-κB Binding Site from PGL3 Plasmids with PGL3 Empty Vector Primers. Lanes; Marker: GeneRuler™ DNA Ladder Mix (Fermentas), EV: Empty Vector, 1-2: Selected Colonies, NC: Negative control

After wards colonies which seemed to be accommodating the inserts were selected and grown overnight at 200 rpm at 37°C in 5 ml LB-ampicllin medium and further plasmids were isolated by using Qiagen Miniprep Plasmid isolation Kit according to the manufacturer's instructions

Afterwards plasmids were sent for sequencing for confirmation of the sequence in the cloned plasmids

As control, a mutated sequence was obtained in the form of synthetic oligos which contains cytosine residues instead of the consensus sequence of NF-κB to be cloned in Hind III/Sac I sites of PGL3 vector . Oligos were first annealed by mixing in equal amounts in 30 µl reaction conditions and then heating up to 95°C for 5 minutes and cooling to ambient temperature with a cooling rate of 1°C /min. Afterwards annealed oligos were separated in 1% agarose gel and purified by using Agarose Gel DNA Extraction Kit (Roche) according to the manufacturer's instructions. Protocol was mentioned in Appendix F. Vector was also prepared with the same enzyme and ligation was performed sustaining 1:10 vector: insert molar ratio in 10 µl reaction conditions with 100 ng vector and appropriate amount of vector accordingly. Followingly 5µl of ligation reaction was used to transform previously prepared competent Top10 *E.Coli* cells. Transformation protocol was given in Appendix F. Followingly 100 µl of the transformation reactions were plated in LB-Agar plates containing 100µg/ml Ampicillin overnight at 37°C. Afterwards colonies were selected, inoculated in 1ml liquid LB containing ampicillin and grown overnight at 37°C at 200 rpm and

then centrifuged at 4000 rpm for 5 minutes. Supernatant was removed and a small sterile toothpick was used to touch the precipitated colony to sample enough amount to sustain colony PCR and the rest was frozen in fresh LB containing 15% glycerol. Afterwards plasmids were isolated from the selected colonies and directly sent to sequencing with the empty PGL3 primers

C.5 Cloning of *C/EBPβ* in PGL3 Vector

C/EBPβ element on the *ICAM1* promoter was cloned into the PGL3 vector in HindIII/SacI sites in order to determine the transcriptional activity of C/EBPβ. For that purpose three copies of the *C/EBPβ* element was obtained as synthetic oligos. Oligos were annealed by mixing in equal amounts in 30µl reaction conditions and then heating up to 95°C for 5 minutes and cooling to ambient temperature with a cooling rate of 1°C /min. Afterwards annealed oligos were separated in 1% agarose gel and purified by using Agarose Gel DNA Extraction Kit (Roche) according to the manufacturer's instructions. Protocol was mentioned in Appendix F. Vector was also prepared with the same enzyme and ligation was performed sustaining 1:10 vector: insert molar ratio in 10 µl reaction conditions with 100 ng vector and appropriate amount of vector accordingly. Followingly 5µl of ligation reaction was used to transform previously prepared competent Top10 *E.Coli* cells. Transformation protocol was given in Appendix F. Followingly 100 µl of the transformation reactions were plated in LB-Agar plates containing 100µg/ml Ampicillin overnight at 37°C. Afterwards colonies were selected, inoculated in 1 ml liquid LB containing ampicillin and grown overnight at 37°C at 200 rpm and then centrifuged at 4000 rpm for 5 minutes. Supernatant was removed and a small sterile toothpick was used to touch the precipitated colony to sample enough amount to sustain colony PCR and the rest was frozen in fresh LB containing 15% glycerol. Afterwards plasmids were isolated from the selected colonies and directly sent to sequencing with the empty PGL3 primers.

Mutated element of this vector was also prepared by using the same protocols in which the in which the C/EBP consensus site was changed to cytosine.

C.6 Cloning of *miR-146a* in P-SUPER Vector

Premature full length *miR-146a* was cloned into P_SUPER in Hind III/SalI sites for overexpression of *miR-146a*. For that purpose firs miR_146a was amplified with PCR with extensions of the indicated restriction sites. PCR conditions were mentioned below.

Table 5. 13 PCR Conditions for Amplification of *pre-miR-146a*

Chemical	Amount (µl)	PCR Reaction Conditions		
10X Taq buffer	3	94°C	3:00	
25 mM MgCl2	3	94°C	0:30	34 cycles
2 mM dNTP	3	56°C	0:30	
Fwd Primer (5µM)	3	72°C	0:30	
Reverse Primer (5µM)	3	72°C	10:00	
Taq DNA polymerase (5 U/µl)	0,2	4°C	HOLD	
Genomic DNA	3µl			
Water	To 30			

Then amplified samples were pooled and purified from agarose gel and subjected to restriction digestion reaction.

Then 100 ng of vector was subjected to ligation reaction in 10µl reaction conditions with required amount of insert sustaining the 1:10 vector: insert molar ratio at 16°C for 17 hours. Afterwards 5µl of the ligation reaction was transformed in *E.Coli* Top 10 cells and grown overnight in the presence of ampicillin 100µg/µl. Afterward plasmids were isolated from the selected colonies

and *pre-miR-146a* was tried to be amplified from the plasmids with the same PCR conditions as mentioned before.

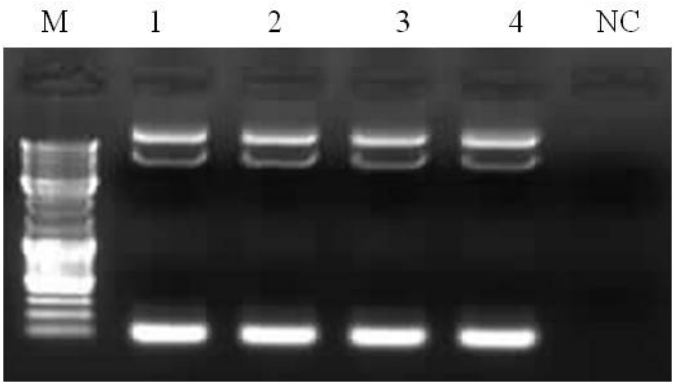

Figure 5.13 *pre-miR-146a* Amplification from Selected p-SUPER Plasmids. Lanes; M: GeneRuler™ DNA Ladder Mix (Fermentas), 1-4: Selected colonies, NC: Negative control

Then plasmids were sent to sequencing with empty P-SUPER primers.

Appendix D: Site Directed Mutagenesis (SDM) Studies

D.1 Site Directed Mutagenesis of the *miR-146a* Binding Site of *MMP16* 3' UTR Region

In order to evaluate the effect of miR146a on 3'UTR of MMP16, *miR-146a* binding region of *MMP16* was changed to thymidine residues. For that purpose plasmids harboring the UTR region of *MMP16* gene was subjected to PCR amplification with the primers carrying the intended mutation.

Table 5.14 PCR Conditions of SDM for *miR-146a* Binding Site of *MMP16* 3' UTR

Chemical	Amount (µl)		PCR Reaction Conditions		
10X Pfu Buffer	5		95°C	0:30	
2 mM dntp	5		95°C	1:00	
Fwd Primer (0.1µg/µl)	1.25		55°C	0:40	20 cycles
Reverse Primer (0.1 µg/µl))	1.25		68°C	13:00	
Pfu DNA Polymerase (2.5U/µl)	1				
Template Plasmid (50g/µl)	1				
Water	To 50				

After the reaction 1 µl DpnI (10U/µl) was directly added to the reaction and incubated at 37°C overnight. In the following day 2µl from the reaction product was transformed into the competent *E.Coli* Top10 cells and grown overnight in the presence of selective antibiotic. Then colonies were selected and sent for sequencing to confirm the desired mutation.

D.2 Site Directed Mutagenesis of *miR146a* in P-SUPER Vector

Mature sequence of the *miR-146a* was mutated with complete thymidines in the P-super vector containing the premature full length sequence of *miR-146a*. For that purpose plasmids containing the full length pre-*miR-146a* sequence were subjected to PCR amplification with the primers carrying the intended mutation.

PCR condition for the Mutated Plasmid amplification was as follows:

Table 5.15 PCR Conditions for SDM of *miR-146a* Binding Site

Chemical	Amount (µl)		PCR Reaction Conditions		
10X Pfu Buffer	5		95°C	0:30	
2 mM dntp	5		95°C	1:00	20 cycles
Fwd Primer (0.1µg/µl)	1.25		55°C	0:40	
Reverse Primer (0.1 µg/µl))	1.25		68°C	13:00	
Pfu DNA Polymerase (2.5U/µl)	1				
Template Plasmid (50g/µl)	1				
Water	To 50				

After the reaction 1 µl DpnI (10U/µl) was directly added to the reaction and incubated at 37°C overnight. In the following day 2µl from the reaction product was transformed into the competent *E.Coli* Top10 cells and grown overnight in the presence of selective antibiotic. Then colonies were selected and sent for sequencing to confirm the desired mutation.

Appendix E: Extraction of DNA From Agarose Gels

1- After separating the band of interest cut DNA band with clean scalpel.

2- Add 300µl of the solubilization buffer per 100 mg

3- Vortex silica matrix add 10 µl to the sample

4- Incubate at 60°C for 10 minutes. Vortex every 2-3 minutes.

5- Centrifuge for 30 seconds at maximum speed.

6- Add 500 µl binding buffer for resuspending. Centrifuge and remove supernatant.

7- Add 500µl Wash Buffer. Centrifuge and remove the supernatant.

8- Dry the pellet for 15 minutes.

9- Add 50µl water to elute samples incubate 10 minutes at 56-60°C to improve the recovery.

Appendix F: Transformation Protocol

1- Thaw competent cells on ice (100µl aliquot)

2- Mix with 50ng plasmid (1µl from 50µl)

3- Place on ice for 30 minutes

4- Shock at 42°C in water bath for 30 seconds

5- Place on ice for 2 minutes

6- Add 1 ml LB at 42°C (or 500µl SOC)

7- Shake at 37°C (400 rpm) for 1 hour

8- Plate 200 µl (50µl at least) on LB medium containing the appropriate antibiotic (Ampicillin in most cases)

Appendix G: RNA Isolation Protocol

1- Aspirate the cell-culture medium

2- Trypsinize the cells. Pellet at 500 x g

3. Add 350 µl RLT- Buffer.

4. Add same amount of 70% ethanol to the homogenized lysate mix with pipette.

5. Transfer 700 µl to the column centrifuge for 15 seconds at 8000 x g.

6. 700 µl RW1 to the column. Centrifuge for 15 seconds at 8000 x g.

7. 500 µl RPE to the column. Centrifuge for 15 seconds at 8000 x g.

8. Repeat the previous step with 2 minutes of centrifuging

9. Place column in a new tube. Add approximately 50 µl water directly to the membrane. Centrifuge for 15 seconds at 8000 x g.

Appendix H: Dnase I Treatment

1- Add 1µg RNA, 1µl 10X, water to 9 µl then add 1µl Dnase I

2- Incubate at 30 minutes at 37°C.

3- Add 1 µl 25 mM EDTA and incubate at 10 minutes at 65°C.

Appendix I: cDNA Synthesis Protocol

1- Add the following in indicated order:

Template RNA	total RNA	100 ng - 5 µg
	or poly(A) RNA	10 - 500 ng
	or specific RNA	0.01 pg - 0.5 µg
Primer	$oligo(dT)_{18}$	0.5 µg (100 pmol)
	or random hexamer	0.2 µg (100 pmol)
	or gene-specific	15-20 pmol
	DEPC-treated Water	to 12.5 µl

2- Add the following components in the indicated order:

5X reaction buffer	4 µl
RNAse Inhibitor	0.5 µl (20 u)
dNTP Mix, 10 mM each	2 µl (1 mM final concentration)
Reverse Transcriptase	1 µl (200 u)
Total volume:	20 µl

3- Mix gently and centrifuge briefly.

4- Incubate for 60 minutes at 42°C.

5- Terminate the reaction at 70°C 10 minutes.

Appendix J: Plasmid Isolation Protocol

1- Pelleted bacterial cells and suspend in 250 µl P1 Buffer and transfer to an eppendorf tube. Buffer P1 should be RNase added. Avoid cell clumps after suspension of the pellet. Ensure there is no left Lyse-Blue particles in P1 buffer.

2- Add 250µl Buffer-P2 mix by inversion 4 to 6 times.

3- Add 350µl Buffer-N3 and mix by inversion 4 to 6 times.

4- Centrifuge at 14000 x g for 10 minutes.

5- Take the supernatant and apply it to the spin column.

6- Centrifuge briefly (30-60 sec).

7- Add 500 µl Buffer-PB and centrifuge briefly.

8- Wash with 750µl PE Buffer and centrifuge briefly.

9- Centrifuge for 1 minute to remove the ethanol.

10- Elute DNA in a clean eppendorf tube.

Appendix K: Cytoselect Standard Curve

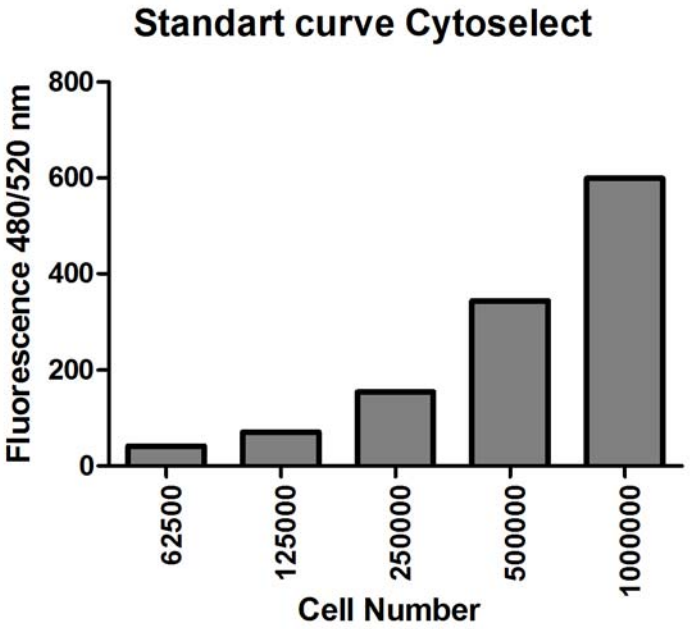

Appendix L: PKC Activity Standard Curve

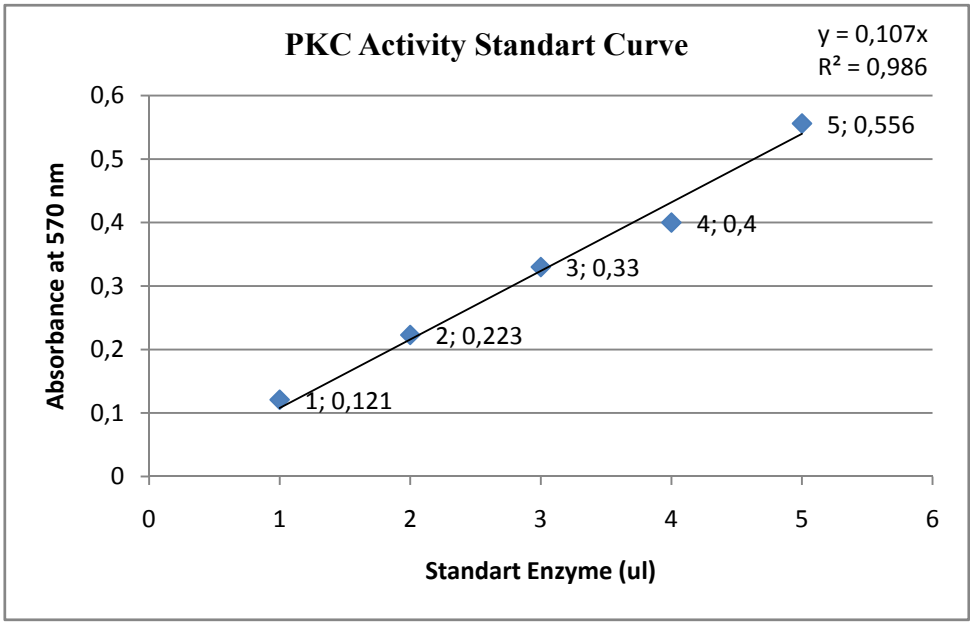

Appendix M: Protein Degradation Pathway Inhibitors

Inhibitor	Inhibiton	Working Concentration	Preparation
Pepstatin A	Lysosome	0.5-1µg/ml	Add 5 ml Methanol/Acetic Acid for 1.45 mM (1mg/ml) stock
Leupeptin	Lysosome	10-100 µM	Add 1ml waterfor 10mM
Z-Leu-Leu-Phe-CHO MG132	Proteasome	10µM	Add 1ml DMSO for1.96 mM
Calpain inhibitor I ALLN	Calpain	100µM	Add 1.3ml DMSO for 10 mM
Trans-Epoxysuccinyl-L-leucylamido(4-guanidino)butane E64	Lysosome	10µM	Add 400 ul water + 100 ul DMSO to give for 28 mM

Appendix N: Synthetic Oigos Used as Casettes

Number	Oligo	Sequence	Application
1	CEBP MUT_HIND_SAC_ SENSE	CCGAGCTCGGGGGGGGGG GGGGGGGGGGGGGAAGC TTGGG	Synthetic oligo used as cassette for mutated C/EBPβ consensus sequence in PGL3
	CEBP MUT HIND SAC ANTISENSE	CCCAAGCTTCCCCCCCCCC CCCCCCCCCCCCCCCCGA GCTCGG	
2	INF_KB_MUT SENSE_HIND_SAC	CCGAGCTCGGGGGGGGGG GGGGGGGGGGGGGGGGG GGGAAGCTTGGG	Synthetic oligo used as cassette for mutated NF-κB consensus sequence in PGL3
	NF_KB MUT__ HIND_SAC_ANTIS ENSE	CCCAAGCTTCCCCCCCCCC CCCCCCCCCCCCCCCCCCC CGAGCTCGG	

Appendix O: Quantitative PCR Standards

O.1 Standard and Amplification Curves for NF-κB on *ICAM1* Promoter

First, different dilutions of (1/10-1/1000 of the original) day 0 immunoprecipitated sample were used to construct a standard curve (Figures 5.14, 5.15 and 5.16).

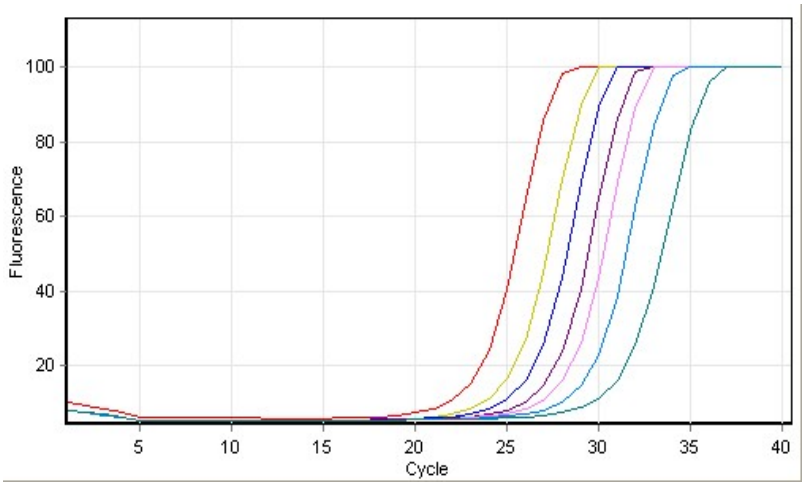

Figure 5.14 *ICAM1* Promoter NF-κB Element Amplification Standard Curve. Different dilutions of input control samples were used to construct a standard curve.

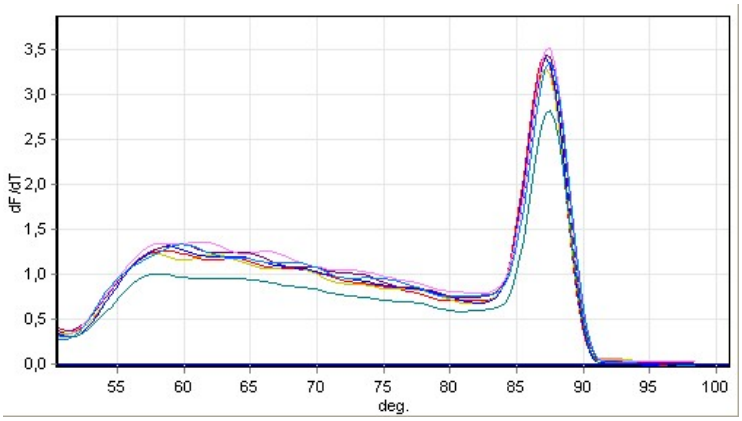

Figure 5.15 *ICAM1* Promoter NF-κB Element Standard Melt Curve

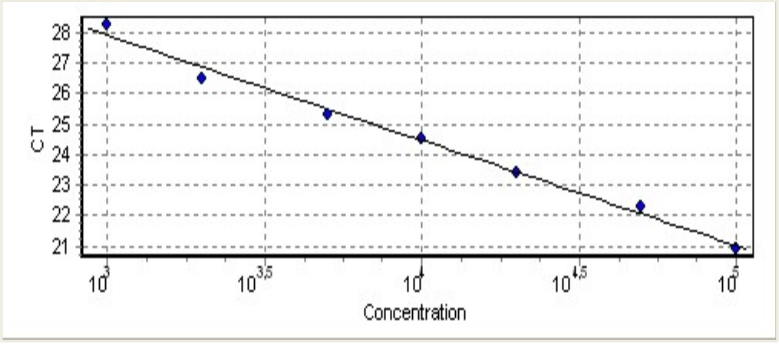

Figure 5.16 *ICAM1* Promoter NF-κB Element Standard Curve. (Blues dots are different dilutions of Caco-2 Day 0 input control DNA)

Table 5.16 Reaction Parameters of NF-κB Element Amplification

Threshold	0,4162
Left Threshold	1,000
Standard Curve Imported	Yes
Standard Curve (1)	conc= 10^(-0,277*CT + 9,777)
Standard Curve (2)	CT = -3,604*log(conc) + 35,234
Reaction efficiency (*)	0,8945 (* = 10^(-1/m) - 1)
Start normalising from cycle	1
Noise Slope Correction	No
No Template Control Threshold	0%
Reaction Efficiency Threshold	Disabled
Normalisation Method	Dynamic Tube Normalisation
Digital Filter	Light
Sample Page	Page 1
Imported Analysis Settings	

After the standard curve was obtained, real time PCR was performed using immunoprecipitated samples from the post-confluent Day0 and Day10 Caco-2 cells and their input counterparts. Every sample was studied in triplicate and deltadeltaCt values were obtained by normalizing the Ct values of samples to its input counterparts.

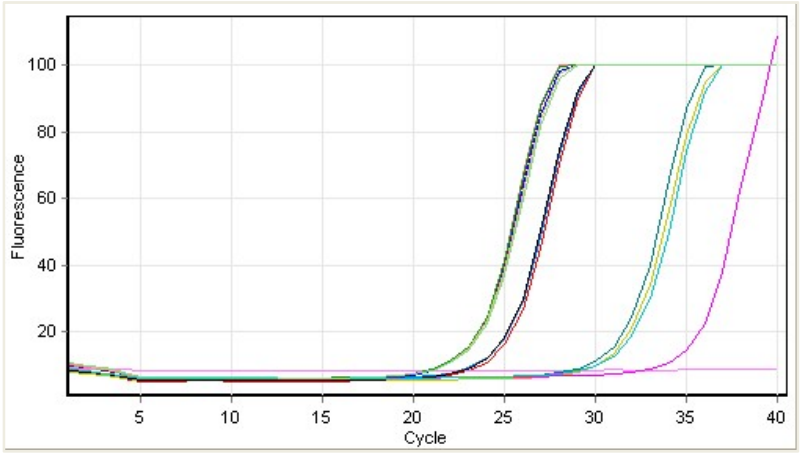

Figure 5.17 Amplification of the NF-κB Element in the *ICAM1* Promoter using αp65 Immunoprecipitated Caco-2 Cells

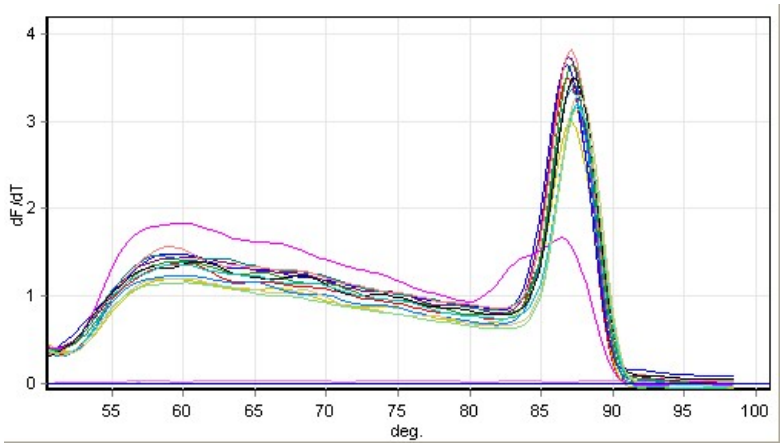

Figure 5.18 Melt curve of the NF-κB Element in the *ICAM1* Promoter using αp65 Immunoprecipitated Caco-2 Cells

O.2 Standard and Amplification Curves for NF-κB on *VCAM1* Promoter

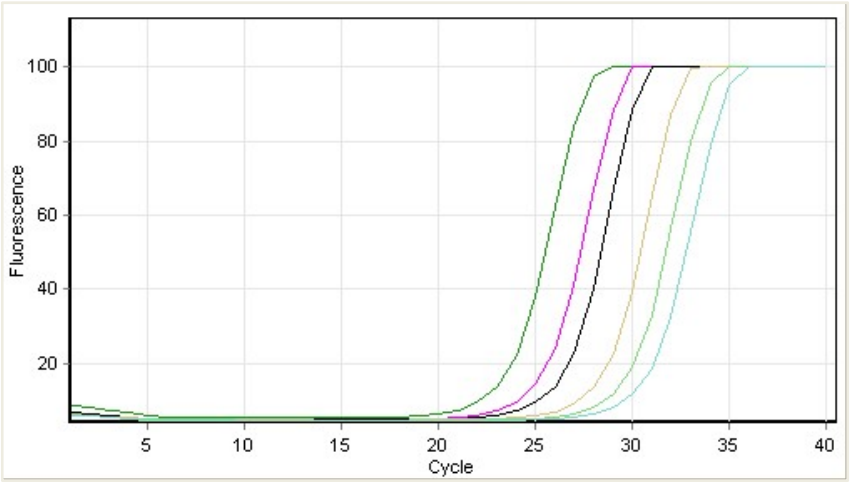

Figure 5.19 Standard Amplification Curve for the NF-κB Element in the *VCAM1* Promoter

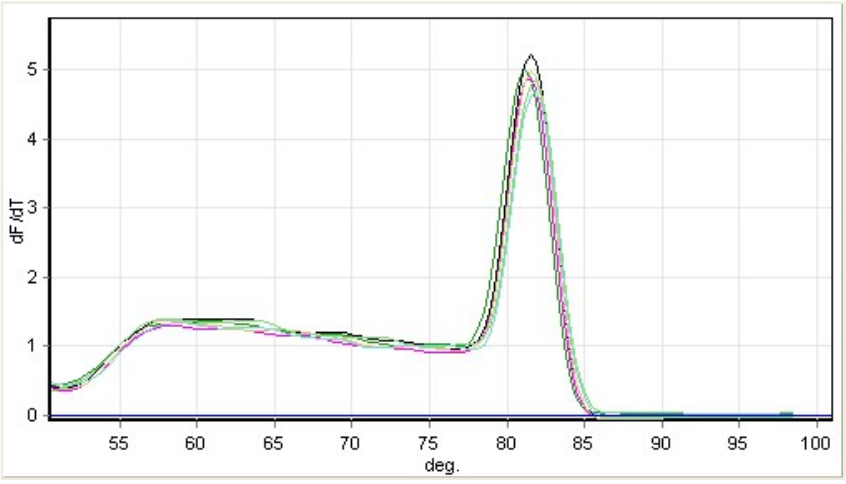

Figure 5.20 Standard Melt Curve for the NF-κB Element in the *VCAM1* Promoter

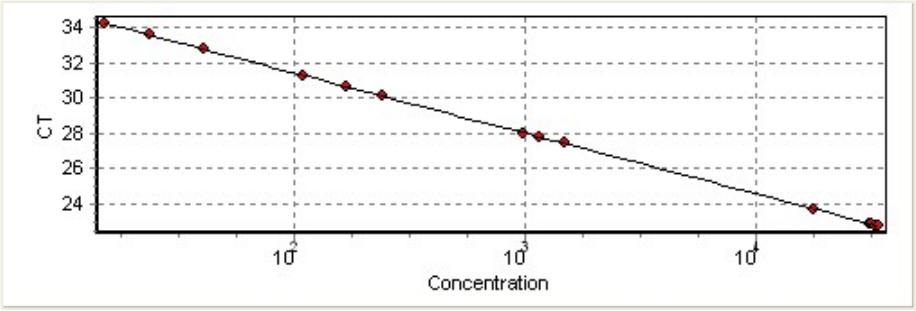

Figure 5.21 Standard Curve for the Amplification of the NF-κB Element in the *VCAM1* Promoter.

Table 5.17 Reaction Parameters of NF-κB Element Amplification

Threshold	0,4162
Left Threshold	1,000
Standard Curve Imported	Yes
Standard Curve (1)	conc= 10^(-0,277*CT + 9,777)
Standard Curve (2)	CT = -3,604*log(conc) + 35,234
Reaction efficiency (*)	0,8945 (* = 10^(-1/m) - 1)
Start normalising from cycle	1
Noise Slope Correction	No
No Template Control Threshold	0%
Reaction Efficiency Threshold	Disabled
Normalisation Method	Dynamic Tube Normalisation
Digital Filter	Light
Sample Page	Page 1
Imported Analysis Settings	

After obtaining a standard curve for the NF-κB element located in the VCAM-1 promoter, ChIP was performed from the samples obtained by the immunoprecipitation of the post confluent Day 0 and Day 10 day Caco-2 cells with p65 antibody. The data obtained from the samples were normalized against the input controls.

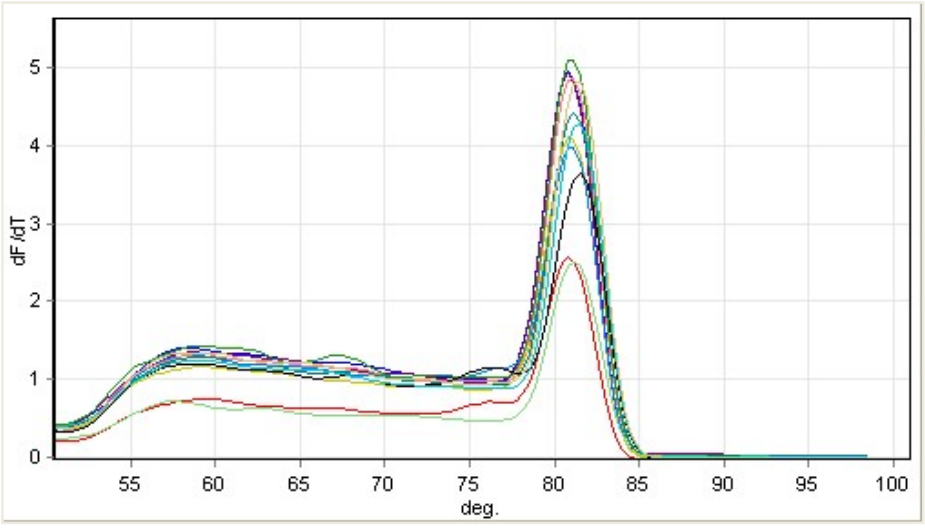

Figure 5.22 Amplification Melt Curve of the NF-κB Element from *VCAM1* Promoter in the Differentiating Caco-2 Cells

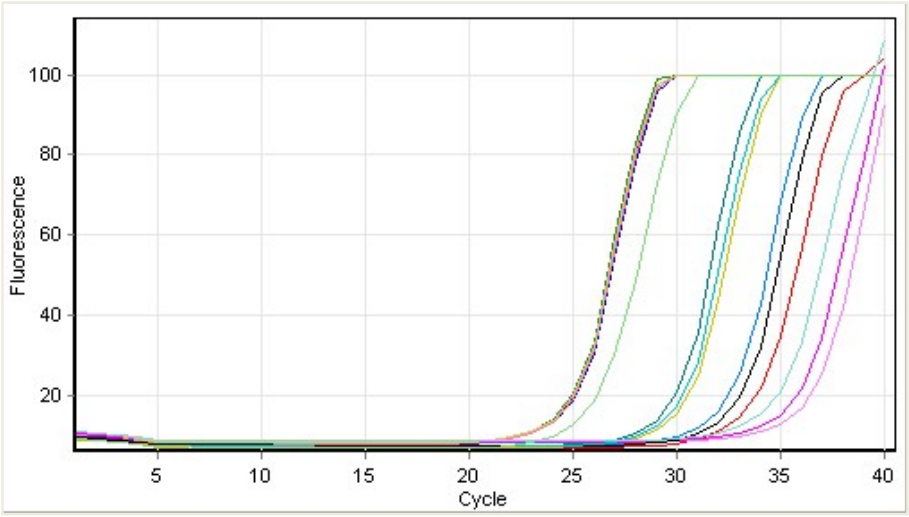

Figure 5.23 Amplification of the NF-κB Element in the *VCAM1* Promoter using αp65 Immunoprecipitated Caco-2 Cells

O.3 Standard and Amplification Curves for C/EBPβ in *ICAM1* Promoter

First, a standard curve was constructed using different dilutions of (1/10-1/1000 of the original) day 0 immunoprecipitated sample).

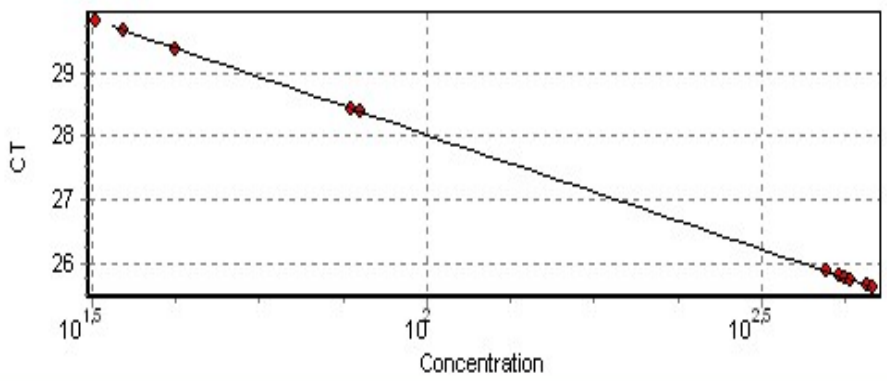

Figure 5.24 C/EBPβ Element in the *ICAM1* Promoter Standard Curve (Dots represent different dilutions of input control)

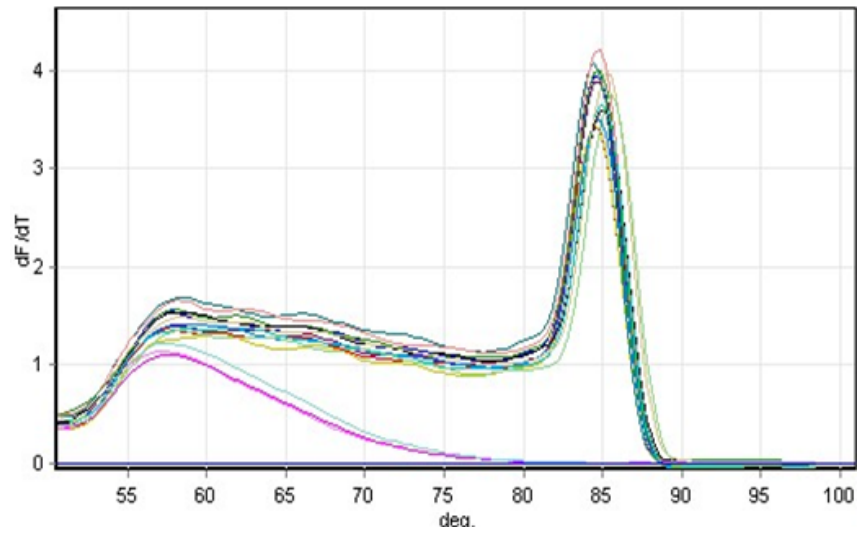

Figure 5.25 C/EBPβ Element Amplification Melt Curve

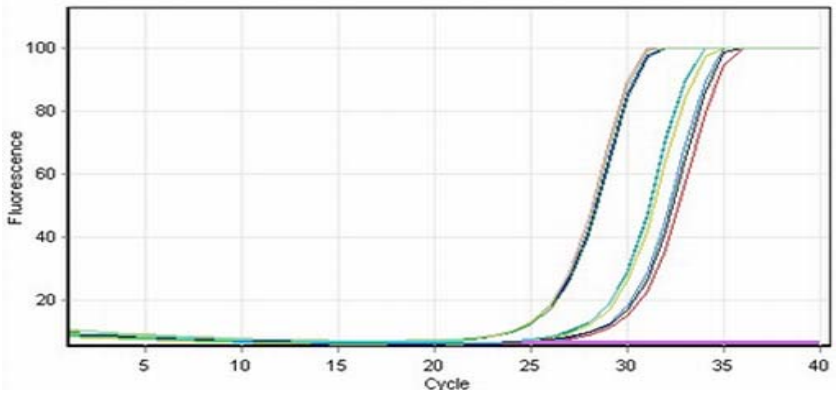

Figure 5.26 C/EBPβ Element Amplification Curve

Appendix P: RNA Quality for Taqman MicroRNA Assays

P.1 RNA Measurement

Table 5.18 Nanodrop Values for RNAs

Sample ID	Conc.	Unit	A260	A280	260/280	260/230
Day 0	263	ng/µl	6,576	3,289	2	0,66
Day 2	474,1	ng/µl	11,852	5,76	2,06	1,31
Day 5	277,8	ng/µl	6,945	3,38	2,05	0,78
Day 7	320,9	ng/µl	8,021	3,901	2,06	1,25
Day 14	224	ng/µl	5,599	2,751	2,04	1,48
Day 30	153,5	ng/µl	3,838	1,908	2,01	1,53

P.2 Absorbance Spectra of the RNA Samples

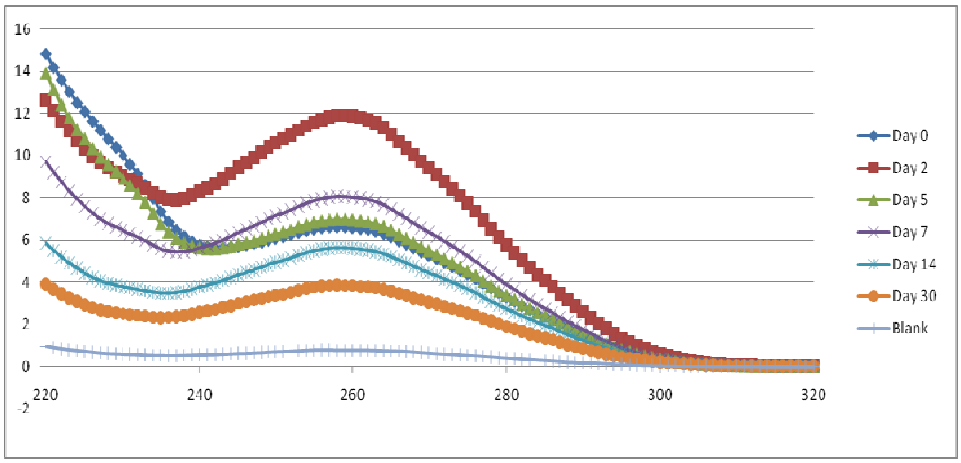

Figure 5.27 Absorbance Spectra of the RNA Samples

P.3 Agarose Gel Analysis of the RNA Samples

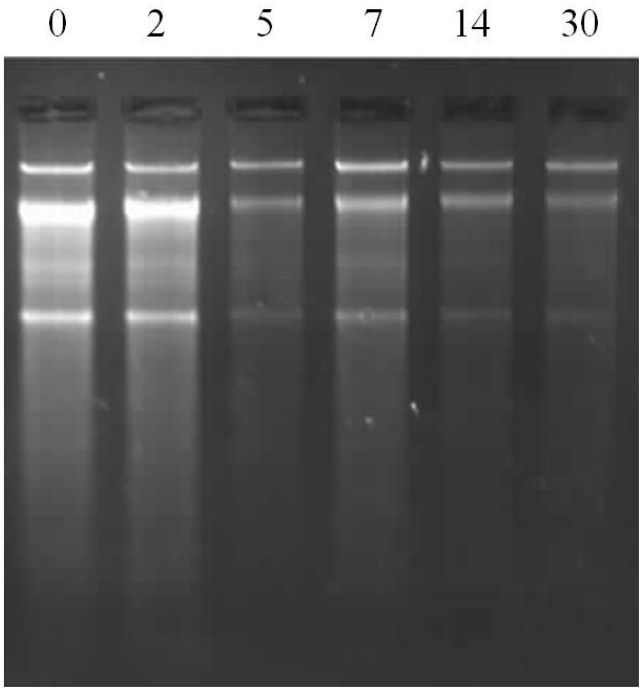

Figure 5.28 Agarose Gel Analysis of the RNA Samples. Lanes; 0-30: RNA samples obtained from spontaneously differentiating Caco-2 cells.

Appendix R: Curriculum Vitae

PERSONAL INFORMATION

Surname, Name: Astarcı, Erhan
Nationality: Turkish (TC)
Date and Place of Birth: 17 December1978, Ankara
Marital Status: Single
Phone: +90 312 210 64 82
Fax: +90 312 210 17 19
Email: erhanastarci@yahoo.com

EDUCATION

Degree	Institution	Year of Graduation
MSc	METU Biotechnology	2003
BS	Ankara University Biology	2000
High School	Özel Yükseliş Koleji	1995

WORK EXPERIENCE

Year	Place	Enrollment
2008-	METU, Biochemistry	Research Assistant
2006-2007	Medicor Advanced Technologies	Product Manager
2005-2006	Koç-Fen Preparatory Course	Biology Teacher
2004-2005	Spektralab Laboratuvar Cihazları	Product Manager

FOREIGN LANGUAGES

Advanced English, Intermediate German

PUBLICATIONS

1- Çimen I, Astarci, E and Banerjee S. 15-Lipoxygenase-1 exerts its tumor suppressive role by inhibiting nuclear factor-kappa B via activation of PPAR gamma. J. Cellular Biochemistry. Accepted April 2011. DOI: 10.1002/jcb.23174

2- Astarci E, Banerjee S. PPARD (peroxisome proliferator-activated receptor delta). Atlas Genet Cytogenet Oncol Haematol. June 2009.

3- Astarci E**,** Banerjee S**.** PPARG (peroxisome proliferator-activated receptor gamma). Atlas Genet Cytogenet Oncol Haematol. July 2008.

HOBBIES

Electric Guitar, Swimming, Movies